ROLES OF BONE MORPHOGENETIC PROTEIN 4 IN LIVER FIBROGENESIS

by

Jianghong Fan

A Thesis Submitted to the Faculty of Graduate Studies

In Partial Fulfillment of the Requirements for the

Degree of Doctor of Philosophy

Faculty of Pharmacy

University of Manitoba

Winnipeg, Manitoba

THE UNIVERSITY OF MANITOBA

FACULTY OF GRADUATE STUDIES

*****

COPYRIGHT PERMISSION

ROLES OF BONE MORPHOGENETIC PROTEIN 4 IN LIVER FIBROGENESIS

BY

Jianghong Fan

A Thesis/Practicum submitted to the Faculty of Graduate Studies of The University of Manitoba in partial fulfillment of the requirement of the degree

DOCTOR OF PHILOSOPHY

ABSTRACT

Bone morphogenetic proteins (BMPs) are important cytokines involved in cell proliferation and differentiation. Hepatic stellate cells (HSCs) undergo trans-differentiation during their activation after liver injury. Activated HSCs could migrate to areas that are close to oval cells. The aim of this study is to investigate the roles of BMP4 during liver fibrogenesis. Expression of BMP4 was significantly elevated in the liver of BDL rats and activated HSCs. The expression and phosphorylation of Smad1, ERK1/2 and p38 were also elevated after BDL. BMP4 stimulated phosphorylation of Smad1, p38 and ERK1/2 in HSCs. BMP4 treated WB-F344 cells showed an increase in the mRNA abundance of albumin, TAT and glucose-6-phosphate but not β4-integin and CK-19. Similar results were obtained from WB-F344 cells after they were transfected with adenovirus containing BMP4 cDNA. We also found that BMP4 secreted from HSCs could promote the differentiation of WB-F344 cells toward hepatocytes. Smad1 and ERK1/2 may, therefore, be important signaling molecules involved in the differentiation of WB-F344 cells. Moreover, the expression and DNA binding activity of transcriptional factor-C/EBPα were increased after treatment with BMP4 in WB-F344 cells. Furthermore, we employed the heterogeneous population of hepatic stellate cells (CFSC-8B, 2G, 3H and 5H) to investigate the susceptibility of HSCs to apoptosis. The results showed that CFSC-3H and CFSC-5H cells are more resistant to apoptosis induced by staurosporine than CFSC-8B and CFSC-2G cells. The different levels of α-SMA and phospho-ERK1/2 may contribute to susceptibility of HSCs to apoptosis. In conclusion, BMP4 and its signaling play a crucial role in trans-differentiation and apoptosis of hepatic stellate cells as well as differentiation of hepatic stem cells.

ACKNOWLEDGEMENTS

I wish to express my deepest gratitude to my supervisor, Dr. Yuewen Gong. He provided me with an excellent training environment and guiding support and taught me so much about science, problem solving and research. He always encouraged me to discover and explain the scientific phenomena on my own. Dr. Gong's passion and enthusiasm for science are contagious. He gave me the freedom to do as much as I could and any successes I have had are directly resulting from Dr. Gong's supervise and vast knowledge.

Thanks to all the members of Dr. Gong's lab for their excellent technical assistance, support and helpful discussion. It was a pleasure to collaborate with all of these people and I was truly thankful to work along side such gifted individuals.

I was very luck in that I was able to interact with brilliant individuals. They are Dr. Patrick Choy, Dr. Gerald Minuk and Dr. Frank Burczynski, who are members of my Advisory Committee and are among the top faculty members at the University of Manitoba. They were always willing to share their insight and knowledge as well as ask the really hard questions to stimulate my thinking. Because of the critical assessment and advice offered by this group, my work became better. I thank them for their key contribution to my training and development as a scientist.

A very special thank to my family. They always gave me their full support throughout my Ph. D study. Even though they may not have always understood what I was studying, they were always interested and encouraging.

Thanks to Dr. Gong and University of Manitoba Graduate Studies for providing financial support during my Ph.D study.

TABLE OF CONTENTS

ABSTRACT.....i

ACKNOWLEDGEMENTS.....ii

TABLE OF CONTENTS.....iii

LIST OF TABLES.....x

LIST OF FIGURES.....xi

LIST OF ABBREVIATIONS.....xiv

I. INTRODUCTION

Background.....1

Bone Morphogenetic Protein 4

1. General introduction to BMPs

1.1 History of bone morphogenetic proteins.....3

1.2 Classification and molecular structure of BMPs.....4

1.3 BMPs signaling transduction pathways.....5

1.3.1 Smad-dependent signaling pathway.....5

1.3.2 Smad-independent signaling through MAPK pathway.....6

1.4 Negative regulation of BMPs signaling.....7

1.4.1 BMPs antagonists.....7

1.4.2 Inhibitory Smads proteins.....8

1.4.3 Tob.....8

1.4.4 Smurf1.....9

1.4.5 CRIM1.....9

1.5 Biological functions of BMPs.....11

2. Bone morphogenetic protein 4.....15

2.1 Gene and protein structure of BMP4.....15

2.2 BMP4 signaling transduction pathways.....17

2.3 Biological functions of BMP4.....17

3. BMPs and liver.....18

Liver Fibrosis and Hepatic Stellate Cells

1. Introduction to liver fibrosis.....21

1.1 Liver structure.....21

1.2 Hepatic cell types and functions.....21

1.3 Roles of different hepatic cell types in liver fibrosis.....26

1.4 Changes during fibrogenesis.....26

1.5 Stimuli for liver fibrosis.....27

1.5.1 Alcohol abuse.....27

1.5.2 NASH.....28

1.5.3 HCV.....28

2. Hepatic stellate cells.....29

2.1 General introduction.....29

2.1.1 Basic cell biology.....29

2.1.2 Heterogeneous population of HSCs.....30

2.1.3 HSCs in pathological conditions.....30

2.2 Factors involved in the activation of HSCs.....31

2.3 Intracellular events during hepatic stellate cells activation.....32

2.3.1 MAPK signaling pathway..... 32

2.3.2 Smad signaling pathway.....35

2.3.3 Intracellular Ca^{2+} signaling pathway..... 35

2.3.4 Wnt signaling pathway.....36

3. Signaling pathways contribute to the initiation of HSCs apoptosis..... 36

3.1 Fas/Fas-ligand..... 37

3.2 TRAIL Receptors..... 38

3.3 Nerve Growth Factor Receptor p75..... 38

3.4 Bcl-2 family proteins.....39

4. Animal models of cholestatic liver fibrosis.....40

Oval Cells

1. General introduction..... 42

2. Oval cells: stem cells..... 43

3. Oval cells niche.....44

4. Hepatic and biliary markers for oval cells..... 46

HYPOTHESIS AND OBJECTIVES..... 48

II. MATERIALS AND METHODS

1. Materials..... 50

2. Methods..... 53

2.1 Animal model of liver fibrosis.....53

2.2 Isolation of rat hepatic stellate cells..... 54

2.3 Cell line and culture conditions.....55

2.3.1 Rat hepatic stellate cell line-T6 cells..... 55

2.3.2 Rat hepatic stellate cell lines-CFSC-8B, 2G, 3H and 5H.....55

2.3.3 Rat hepatic stem cells-WB-F344 cells.....56

2.3.4 Human kidney cells-293A cells.....57

2.4 Cell co-culture..... 57

2.5 Microphotography..... 58

2.6 RNA isolation.....58

2.7 Reverse transcription polymerase chain reaction (RT-PCR).....58

2.8 Protein isolation.....60

2.8.1 Nuclear protein.....60

2.8.2 Whole cellular protein.....62

2.9 Western blot analysis.....62

2.10 Electrophoretic Mobility Shift Assay (EMSA)..... 64

2.11 Cell proliferation..... 69

2.11.1 ^{3}H Thymidine incorporation assay..... 70

2.11.2 WST-1..... 70

2.11.3 Cell counting.....71

2.12 Cell apoptosis detection..... 71

2.13 Construction of recombinant adenovirus (short hairpin RNA (shRNA))... 73

2.13.1 Structural features of shRNA and oligonucletide encoding shRNA. 73

2.13.2 Generation of double-stranded oligonucleotide..... 75

2.13.3 Ligation reaction..... 76

2.13.4 Bacterial transformation.....76

2.13.5 Plasmid DNA isolation.....77

2.13.6 Recombination of *pAd/BLOCK-iT™-DEST and pENTR™/U6* vector.....79

2.13.7 Preparation of the expression clone..... 80

2.13.8 Package of adenovirus in 293A cells..... 81

2.13.9 Amplification of adenoviral stock..... 83

2.13.10 Titration of adenoviral stock..... 83

2.14 Construction of recombinant adenovirus containing BMP4 cDNA..... 84

2.15 Statistical analysis..... 85

III. RESULTS AND DISCUSSION

1. The Effect of Bone Morphogenetic Protein 4 on Rat Hepatic Stellate Cells Proliferation and Differentiation

1.1 Introduction..... 86

1.2 Results

1.2.1 BMP4 expression in the liver of BDL rats.....87

1.2.2 Expression of BMP4 downstream signaling molecules after BDL.. 93

1.2.3 BMP4 expression in rat hepatic stellate cells..... 97

1.2.4 Effects of BMP4 on T6 cells.....100

1.3 Discussion.....107

2. The Effect of Bone Morphogenetic Protein 4 on Rat Hepatic Stem Cell Proliferation and Differentiation

2.1 Introduction.....110

2.2 Results

2.2.1 BMP4 and its receptors expression in WB-F344 cells and CFSC-8B cells..... 112

2.2.2 Effect of BMP4 on differentiation of WB-F344 cells..... 113

2.2.3 Co-culture of WB-F344 cells with hepatic stellate cells..... 120

2.2.4 Paracrine regulation of BMP4 and intracellular signaling pathways of BMP4 in WB-F344 cells..... 123

2.2.5 BMP4 regulation on C/EBP transcription factors expression in WB F344 cells..... 127

2.2.6 Effect of BMP4 on DNA binding activity of C/EBPα in WB-F344 Cells..... 131

2.2.7 Effect of BMP4 on WB-F344 cell proliferation..... 134

2.3 Discussion..... 137

3. Role of Extracellular Signal-regulated Kinase (ERK) and Protein Kinase C in Heterogeneous Population of Hepatic Stellate Cells

3.1 Introduction..... 142

3.2 Results

3.2.1 Morphology of CFSC-8B, 2G, 3H and 5H cells and expression of smooth muscle alpha actin in these cells..... 145

3.2.2 Effect of staurosporine on heterogeneous population of hepatic stellate cells apoptosis..... 146

3.2.3 Effect of staurosporine and U0126 on expression and phosphorylation of ERK in CFSC-8B and 5H cells..... 152

3.2.4 Effect of co-treatment of staurosporine and U0126 on hepatic stellate cells apoptosis.....156

3.3 Discussion..... 160

IV.SUMMARY.....162

V.CONCLUSION..... 163

VI. REFERENCES..... 168

LIST OF TABLES

Table 1 Human BMP antagonists based on the size of the cystine-knot.....10

Table 2 The pleiotropic biological functions of BMPs.....14

Table 3 The pleiotropic biological functions of BMP4.....19

Table 4 Factors involved in the initiation and perpetuation of hepatic stellate cells activation.....33

Table 5 Markers used in the identification of oval cells in liver.....47

Table 6 Markers used to identify the differentiation lineage of oval cells.....47

Table 7 Materials.....50

Table 8 Components for one PCR reaction.....60

Table 9 Primers, condition of polymerase chain reaction and siRNA sequence.....61

Table 10 The choice of the percent gel based on the molecular weight of proteins.....64

Table 11 Antibody and condition of western blot analysis.....65

Table 12 Oligodeoxynucleotide probes for C/EBP.....67

Table 13 Components for one labeling reaction.....67

Table 14 Components for EMSA reactions.....68

Table 15 Oligonucleotides encoding shRNA against rat BMP4.....74

Table 16 Components for annealing reaction.....75

Table 17 Components for ligation reaction.....76

LIST OF FIGURES

Figure 1 Molecular composition of the BMPs signaling pathway.....13

Figure 2 Rat BMP4 transcript and transcript neighborhood structure.....16

Figure.3 The structure model of BMP4.....17

Figure 4 Architecture of hepatic tissue.....22

Figure 5 The hepatic vascular system.....23

Figure 6 The composition in normal liver and blood flows through the sinusoids.....24

Figure 7 Signaling pathways involved in HSCs apoptosis.....41

Figure 8 Niche structure.....45

Figure 9 pENTR™/U6 vector.....78

Figure 10 pAd/BLOCK-iT™-DEST vector.....82

Figure 11 RT-PCR analysis of BMP4 and α-SMA expressions in the liver.....89

Figure 12 Western blot analysis of BMP4 and α-SMA expression in the liver.....92

Figure 13 Western blot analysis of BMP4 downstream signaling molecules expression in the liver after BDL.....95

Figure 14 mRNA expression of bone morphogenetic protein 4(BMP4) and its receptors.....99

Figure 15 Effect of BMP4 on T6 cell proliferation.....101

Figure 16 BMP4 Regulation of T6 cell trans-differentiation.....103

Figure 17 Western blot analysis of phospho-Smad1 in T6 cells stimulated with or without BMP4.....104

Figure 18 Western blot analysis of MAP kinases in T6 cells activated by BMP4.....106

Figure 19 The mRNA abundance of bone morphogenetic protein 4 (BMP4) and its receptors in CFSC-8B and WB-F344 cells.....112

Figure 20 Effect of BMP4 on the differentiation of WB-F344 cells.....116

Figure 21A Western blot analysis of BMP4 expression in WB-F344 cells after infection of adenovirus containing BMP4 cDNA.....118

Figure 21B RT-PCR analysis of the expression of hepatocyte and cholangiocyte markers in WB-F344 cells after infection of adenovirus containing either BMP4 cDNA or oligonucleotide encoding shRNA against BMP4.....118

Figure 22 Western blot analysis of albumin expression in WB-F344 cells after infection with adenovirus containing BMP4 cDNA.....119

Figure 23 RT-PCR analysis of the expression of hepatocyte and cholangiocyte markers in WB-F344 cells, CFSC-8B cells and the co-cultured cells.....122

Figure 24A Effects of BMP4 and Dexamethasone on BMP4 and its receptors mRNA abundance in WB-F344 cells.....125

Figure 24B Western blot analysis of intracellular signaling molecules in WB-F344 cells activated by BMP4.....126

Figure 25A RT-PCR analysis of mRNA levels of hepatic transcription factors, C/EBPα, C/EBPβ, C/EBPγ and C/EBPδ, in WB-F344 cells stimulated with or without BMP4.....129

Figure 25B Western blot analysis of expression of C/EBPα protein level in WB-F344 cells stimulated with or without BMP4.....130

Figure 26 Effect of BMP4 treatment on DNA binding activity of C/EBPα in WB-F344 cells as measured by electrophoretic mobility shift assay (EMSA).....133

Figure 27 Effect of BMP4 on the proliferation of WB-F344 cells.....136

Figure 28 Morphology of CFSC-8B, 2G, 3H and 5H cells and expression of smooth muscle alpha actin in four HSC clones.....145

Figure 29 Flow cytometric analysis of CFSC-8B, 2G, 3H and 5H cells after treatment with staurosporine.....148

Figure 30 Western blot analysis of ERK1 and phospho-ERK1/2 expression in CFSC-8B, 2G, 3H and 5H cells stimulated with or without staurosporine and U0126.....154

Figure 31 Flow cytometric analysis of CFSC-5H cells apoptosis after treatment of staurosporine alone or co-treatment of staurosporine and U0126.....158

Figure 32 Interaction of BMP4 and liver cells.....167

LIST OF ABBREVIATIONS

°C	degrees Celsius
%	percent
µCi	microcurie
µl	microliter
µg	microgram
aa	amino acid
ALD	alcoholic liver disease
ATP	adenosine triphosphate
α-SMA	α-Smooth muscle actin
bp	basepair(s)
BSA	bovine serum albumin
cDNA	complementary DNA
CO_2	carbon dioxide
DNA	deoxyribonucleic acid
DNase	deoxyribonuclease
dNTP	deoxyribonucleotide triphosphate
EB	ethidium bromide
E.coli	*Escherichia coli*
EDTA	ethylene diaminetetracetic acid
EGF	epidermal growth factor
EMSA	electrophoresis mobility shift assay
FBS	fetal bovine serum
FDA	Food and Drug Administration
g	gram
G	deocyguanosine
GAPDH	glyceraldehyde 3-phosphate dehydrogenase
GDF	growth differentiation factor

HCl	hydrochloric acid
HEPES	hydroxyethylpiperazine ethanesulfonic acid
hr	hour(s)
H_2O	water
IgG	Immunoglobulin G
KCl	potasium chloride
kDa	kilo daltons
LB	luria-bertani
M	molar
MgCl2	magnesium chloride
mM	millimolar
min	minute(s)
ml	milliliter
mRNA	messenger RNA
NaCl	sodium chloride
NaOAC	sodium acetate
NaOH	sodium hydroxide
ng	nanogram
OD	optical density
O/N	overnight
PAGE	polyacrylamide gel electrophoresis
PBS	phosphate buffered saline
PCR	Polymerase Chain Reaction
rpm	rotations per minute
RNA	ribonucleic acid
RNase	ribonuclease
RT-PCR	Reverse transcription PCR
SDS	sodium dodecyl sulfate
T	deoxythymidine
TBS	Tris buffered saline

TBS-T	Tris buffered saline with 0.1% Tween20
TE	Tris-EDTA
TEMED	N,N,N',N-tetramethylethylenediamine
Tris	tris(hydroxymethyl)amino methane
Tween-20	polyxyethylene-sorbitan monolaurate
UV	ultraviolet
v	voltage
WHO	world health organization
v/v	volume per volume
w/v	weight per volume

I. INTRODUCTION

Background

The liver is the largest and most complex internal organ within the human body. It carries out a number of vital functions, including regulation, synthesis, and secretion of many substances important in maintaining the body's normal state, storage of important nutrients, such as glycogen, vitamins, and minerals, and purification, transformation, and clearance of waste products, drugs, and toxins. In addition, under long-term evolutionary pressure, the liver acquired the remarkable regenerative capacity to help maintain these important functions. However, as powerful as the liver is, it is more vulnerable to many kinds of injuries and, therefore, maybe subject to different types of liver diseases including acute hepatitis, acute hepatic failure, chronic hepatitis, cirrhosis steatosis, alcoholic liver disease, iron overload, amyloidosis, metabolic diseases, and drug-induced and chemical-induced liver injuries. According to a report from *Health, United States, 2006*, chronic liver disease and cirrhosis is now the seventh leading cause of death in adults between the ages of 25~64 in United States. Moreover, in high prevalence areas, chronic hepatitis caused by hepatitis B virus (HBV) has become one of the major three causes of death in Africa, Asia and the Pacific Rim (Lavanchy, 2005).

Currently, hepatologists worldwide are making their efforts to deal with different types of liver diseases. The implementation of mass immunization programs and safe injection techniques has dramatically decreased the incidence of liver disease caused by HBV infection in many countries (WHO, 2000) (Lavanchy, 2005). However, the continuing occurrence of new infections and the presence of a large reservoir of chronically infected people are still big challenges. Furthermore, alcoholic liver disease

(ALD) remains one of the most common liver diseases in the world. Individuals with heavy consumption of alcohol don't always realize the seriousness of their problem, since not all heavy drinkers develop alcohol-induced liver disease, and the risk factors for alcohol-induced liver disease have not been fully elucidated. Moreover, unhealthy eating habits and sedentary lifestyles lead to a significant increase in non-alcoholic fatty liver disease (NAFLD) during the past several decades.

Numerous hepatologists and researchers worldwide have been actively engaged in looking for effective therapeutic approaches to liver diseases. Based on the pathogenesis of liver diseases with different origins, various treatments have been proposed, such as *Pegylated Interferons*, *Ribavirin* for virus infection, *Corticosteroids, antioxidants and antagonists of tumor necrosis factor alpha (TNFα)* for ALD (Diehl, 2002) (Lake-Bakaar, 2003), Cytoprotective agents: *Ursodeoxycholic acid, Taurine*; Insulin-sensitizing agents: *Metformin, Thiazolidinediones*; Antioxidants: *Vitamin E, betaine*; Lipase inhibitor: *Phlebotomy for NAFLD* (Bugianesi, Marzocchi et al., 2004). Unfortunately, these treatments can only slow but not stop the progression of liver injury, and treatments for hepatitis virus infection are somewhat disappointing due to the low response rates.

Without pharmacological intervention, the sustained wound-healing process that occurs in the liver in response to different chronic injuries would finally lead to liver fibrosis and progress to cirrhosis and hepatocarcinoma. During the past 20 years, huge progress was made in understanding the cellular and molecular basis of hepatic fibrosis. Dr. Friedmen first discovered that activated hepatic stellate cells (HSCs) were the major cell type responsible for the development of liver fibrosis in 1985. Subsequently, a number of pharmacological agents have emerged by using HSC as therapeutic target: (*i*)

direct anti-fibrogenic activity by regulating gene expression of activated HSCs (*Smad7, bone morphogenetic protein 7 (BMP7) and peroxisome proliferator activated receptor gamma (PPARγ) agonist*); (*ii*) indirect anti-fibrogenic activity by inhibiting the activation and promoting the apoptosis of HSCs (transforming growth factor beta (*TGFβ) inhibitors, interleukin 10 (IL-10)*); (*iii*) anti-oxidants which reduce the profibrogenic effects of reactive oxygen species (ROS) and intermediates *(α-tocopherol, glutathinne*) (Gressner and Weiskirchen, 2006). However, to date, due to the severe adverse effects and lack of significant benefits, the effective therapeutic approaches to liver fibrosis have not been identified yet. In recent years, researchers have turned to explore the possibility utilizing stem cells and gene therapy approaches to address the fibrosis problems while continuing to investigate the molecular mechanisms underlying HSCs activation and apoptosis. In this study, we investigated the roles of bone morphogenetic proteins 4 (BMP4) during liver fibrogenesis and the capacity of BMP4 to induce the differentiation of hepatic stem cells toward hepatocytes.

Bone Morphogenetic Protein 4

1. General introduction to BMPs

1.1 History of bone morphogenetic proteins

Bone morphogenetic proteins (BMPs) were first identified by Dr. Marshall Urist in 1965 when he found that demineralized bone matrix implanted in ectopic sites in rodents and rabbits could induce new bone formation (Urist, 1965). He named the active component contained in the bone extract "bone morphogenetic protein". The proteins responsible for bone induction remained unknown until purification of human BMPs was

accomplished in the 1980s (Urist, 2002). Recombinant techniques were broadly applied for the production of BMPs after gene sequences for various BMPs were deduced by two groups, one at Creative BioMolecules and the other at Genetics Institute in the 1990s (Takahashi, 2000). Thereafter, many researchers devoted their studies to understand the functions and clinical applications of BMPs. The landmark was the FDA approval of BMP7 for long bone defects and BMP2 for anterior lumbar interbody fusions in 2002 (Urist, 2002).

1.2 Classification and molecular structure of BMPs

Based on the similarities in amino acid sequences of BMPs found in the extract of bone, they are classified into five subfamilies. i) BMP2/BMP4 have 80% amino acid sequence homology between these two proteins. ii) BMP5/BMP6/BMP7/BMP8, almost 78% amino acid sequence homology is conserved among these BMPs. iii) BMP3 is significantly different in amino acid sequence from the other members of BMP family. iv) BMP12/ BMP13/BMP14 are cartilage derived morphogenic proteins. v) GDF5/GDF6/GDF7 and BMP15/BMP16 are growth and differentiation factors (Matthews, 2005).

BMPs belong to the TGFβ superfamily which composes of many multifunctional cytokines including TGF-βs, activins, inhibins, anti-müllerian hormone (AMH), bone morphogenetic proteins (BMPs), myostatin, and others. In the carboxy terminal portions of BMPs, there have seven highly conserved cysteine amino acid residues, which are identical to those present in all members of the TGFβ superfamily. Moreover, BMPs have a primary structure 40~50% similar to that of TGFβ. Like all members in the TGFβ superfamily, BMPs are synthesized as precursor proteins, which consist of a hydrophobic

secretive signal peptide of 15~25 amino acids, a poorly conserved prodomain of 50~375 amino acids, and a carboxyl terminal region of 100~125 amino acids (Rengachary, 2002). Once the mature carboxy terminal region is cleaved by proteolytic processing, they form mature dimeric proteins and are secreted to the outside of cells. Among the conserved seven cysteine residues in mature proteins, six residues are involved in the formation of intrachain disulphide bonds that form a rigid "cysteine-knot" molecular structure. The seventh cysteine residue contributes to the formation of either homo- or heterodimeric mature protein *via* interchain disulphide bond (Wozney, 2002). Accumulating evidence suggests that some heterodimers, such as BMP-2/7 and BMP-4/7 have more potent biological activity than the corresponding homodimers (Lin, Lerch et al., 2006). All BMPs are glycoproteins and have low molecular weight ranging from 15 to 30 kDa.

1.3 BMPs signaling transduction pathways

1.3.1 Smad-dependent signaling pathway

BMPs exert their biological activity *via* interaction with specific BMP receptors, which are serine/threonine kinase transmembrane receptors on cell surface. There are three type II receptors-BMPR2, activin receptor type II (ActR-II), and ActR-IIB and four different type I receptors-BMPR-1A (or activin receptor-like kinase3-ALK3), BMPR-1B (or ALK6), ALK2, and ALK1 (Yamashita, Ten Dijke et al., 1996; Rengachary, 2002). The binding of BMPs to the type II receptor on the cell surface results in the recruitment of type I receptor, then the formation of heterotetramer receptors complex. Once type II receptor phosphorylates and activates type I receptor, type I receptor phosphorylates and activates the regulatory signaling molecules Smad1, 5 or 8 proteins (receptor-activated Smads, R-Smads) at their C-terminal domain. Following the phosphorylation, Smad1, 5,

or 8 bind to Smad4 (common-partner Smad, Co-Smad) and form heterotetramer complex. The complex, in turn, translocates into nucleus and regulates target gene expression by binding to target DNA, interacting with DNA binding transcription factors, or recruiting co-repressors or co-activators (Sykaras and Opperman, 2003). It has been shown that the type I receptors are critical in determining the specificity of downstream Smad signaling pathways (ten Dijke, Korchynskyi et al., 2003). ALK1, ALK3 and ALK6 can activate all three Smads, but ALK2 only phosphorylates Smad1 and Smad5 (Sakou, 1998; Massague, Seoane et al., 2005) (Figure.1).

1.3.2 Smad-independent signaling through MAPK pathway

Besides Smad-mediated signaling pathway, BMPs also initiate signaling through MAPK pathway. Generally, receptor tyrosine kinases, cytokine receptors and some G protein-coupled receptors activate intracellular protein serine/threonine kinases which are termed mitogen activated protein kinases (MAPKs). MAPK is phosphorylated by an upstream protein kinase, MAPK kinase (MAPKK), whereas MAPKK in turn is phosphorylated by a third protein kinase, MAPK kinase kinase (MAPKKK). There are at least three MAPK pathways in mammalian cells: extracellular signal-regulated kinase (ERK) pathway, c-Jun amino-terminal kinase (JNK) pathway and p38 MAPK pathway (Lewis, Shapiro et al., 1998; Pearson, Robinson et al., 2001).

BMPs bind to type I receptor and then recruit type II receptor to form a receptor complex. The BMPs receptor complex can interact with an intracellular adaptor protein XIAP (X-linked inhibitor of apoptosis) which links TAB1 (TAK1 binding protein). TAB1, in turn, activates TGFβ activated kinase 1 (TAK1) a member of MAPKKK family (Yamaguchi, Nagai et al., 1999; Botchkarev and Sharov, 2004). Then TAK1

phosphorylates and activates MAPKK. Thus, JNK is subsequently activated through MAPKK4. P38 is activated through MAPKK3 or MAPKK6 (Shibuya, Iwata et al., 1998). In addition, BMPs can directly activate Ras which inturn phosphoralytes and activates ERK (Xu, Dong et al., 1996) (Figure.1). It has been shown that there is crosstalk between the Smad-dependent and Smad-independent signaling pathways (Massague, 2003; Aubin, Davy et al., 2004). ERK can phosphorylate serine or threonine residues in the linker region of Smads (Kretzschmar, Doody et al., 1997; Kaivo-oja, Jeffery et al., 2006). Although the ERK-phosphorylated Smads protein can form heterotetramer with Smad4, this complex can not translocate into nucleus. Therefore, BMPs initiating signaling pathway is inhibited.

1.4 Negative regulation of BMPs signaling

The pleiotropic functions of BMPs need tight regulation of their activities. Many studies have demonstrated that activities of BMPs are controlled at different molecular levels. The regulation of BMPs target genes expression in a specific cell type is dependent on the concentration of BMPs ligands for BMPRs, the availability of intracellular Smads proteins or the components of MAPK pathway, and the presence of inhibitors and co-activators or co-repressors of BMPs dependent gene transcription in the nucleus.

1.4.1 BMPs antagonists

Soluble inhibitory proteins outside the cell can directly bind to BMPs and inhibit the binding of BMPs to their receptors. Interestingly, BMPs can upregulate the expression of some of these inhibitors, indicating that a negative feedback loop may exist. BMP

antagonists have a secretory signal peptide and a cystine-knot structure (Yanagita, 2005). Based on the size of the cystine-knot, BMP antagonists are classified into three subfamilies (Table 1): the DAN family (eight-membered ring); twisted gastrulation (nine-membered ring); and chordin and noggin (ten-membered ring) (Yanagita, 2005).

1.4.2 Inhibitory Smads proteins

In the cytoplasm, several negative regulation mechanisms exist. Smad6 and Smad7 have MH2 domains but lack the C-terminal SSXS motif which is a conserved motif present at R-Smads proteins (Massague, Seoane et al., 2005). R-Smads proteins can be phosphorylated at the SSXS motif and activated to form complex with Co-Smad. It has been shown that Smad6 and Smad7 proteins can bind to BMPR-IB and inhibit the phosphorylation of Smad1 by BMPR-IB (Botchkarev and Sharov, 2004). Smad6 can also interfere with BMP/Smad1 signaling. It can specifically inhibit the binding of receptor-activated Smad1 to Smad4 and form an inactive Smad1/Smad6 complex. Therefore, Smad6 selectively regulate BMPs initiated Smad1 signaling pathway (Murakami, Watabe et al., 2003; Kaivo-oja, Jeffery et al., 2006). Moreover, BMPs are capable of upregulating the expression of Smad6, which constitutes another negative feedback regulative loop for BMPs signaling pathway.

1.4.3 Tob

Tob is a member of antiproliferative protein family. It can negatively regulate osteoblast proliferation and differentiation by inhibiting BMPs activated Smad-dependent signaling transduction pathway. It has been shown that Tob is negatively involved in BMP2 signaling. It interacts with Smad proteins and inhibits Smad-dependent

transcription. Upon BMP2 stimulation, Tob is induced and accumulates in the nucleus and thereafter recruits R-Smads to nuclear bodies by binding to the MH2 domain of the phosphorylated R-Smads. This allows a precise and timely regulation of BMP2 signaling pathway in osteoblasts (Yoshida, Tanaka et al., 2000; Ebara and Nakayama, 2002).

1.4.4 Smurf1

Smad ubiquitin regulatory factor 1 (Smurf1), is a new member of the Hect family of E3 ubiquitin ligases. It can negatively regulate the BMPs signaling pathway at several levels. In the cytoplasm, Smurf1 not only directly interacts with Smad1/5, but also indirectly associates with Smad1/5 through inhibitory Smad proteins Smad6/7. Finally, Smurf1 mediates Smads proteins ubiquitination and degradation. Moreover, in the nucleus, Smurf1 recognizes bone-specific transcription factor Runx2 and mediates its degradation in a uiquitin-proteasome-dependent manner. Smurf1 also forms a complex with Smad6 in nucleus. This complex is, in turn, exported into cytoplasm and targets the type I BMP receptors on the membrane for their degradation (Ebara and Nakayama, 2002; Murakami, Watabe et al., 2003; Yanagita, 2005).

1.4.5 CRIM1

The *Crim1*gene encodes a transmembrane protein containing six cysteine-rich repeats (CRRs). CRIM1 can interact with both BMP4 and BMP7 and acts as an antagonist to BMPs. It modulates the activity of BMPs by affecting BMPs processing and secretion to the outside of cells. CRIM1 binds to BMPs preprotein and leads to a

Table 1. Human BMP antagonists based on the size of the cystine-knot.

	BMP Antagonists	High Affinity	Low Affinity
	DAN	BMP2 and BMP4	
	Cer1	BMP2, BMP4 and BMP7	
	Coco	BMP4	
DAN family	PRDC	BMP2,BMP4,BMP6 and BMP7	
(Eight-membered ring)	Gremlin	BMP2, BMP4 and BMP7	
	USAG-1	BMP2, BMP4, BMP6 and BMP7	
	Sclerostin	BMP5, BMP6 and BMP7	BMP2 and BMP4
Twisted gastrulation ***(Nine-membered ring)***	Tsg	BMP and BMP4	
	Chordin	BMP4, BMP2 and BMP7	
Ten-membered ring	Noggin	BMP2 and BMP4	BMP6 and BMP7
	Follistatin	BMP2, BMP4, BMP7and BMP15	BMP6

reduction in the production of mature BMPs (Wilkinson, Kolle et al., 2003; Yanagita, 2005). Moreover, it can tether the pre-BMPs to the cell surface *via* CRRs, and thereafter inhibit the secretion of mature BMPs to the outside of cells.

1.5 Biological functions of BMPs

BMPs have been shown a variety of functions besides the induction of cartilage and bone formation. They play very crucial roles in embryogenesis, organogenesis and homeostasis in adult body through induction of cell proliferation, differentiation or apoptosis. It has been demonstrated that BMPs play different roles in different cell types, even at different states of same cell type (Table 2).

Figure 1 *Molecular events of the BMPs signaling pathway.* BMP-Smad pathway includes recruitment and phosphorylation of R-Smads followed by the formation of their complexes with Co-Smad and translocation into the nucleus to regulate gene transcription. BMP-MAPK pathway links BMP receptors with TAK1 kinase, which in turn activate p38 and JNK pathways. In addition, Erk could be activated by BMPs in a Ras dependent mechanism in BMP-MAPK pathway.

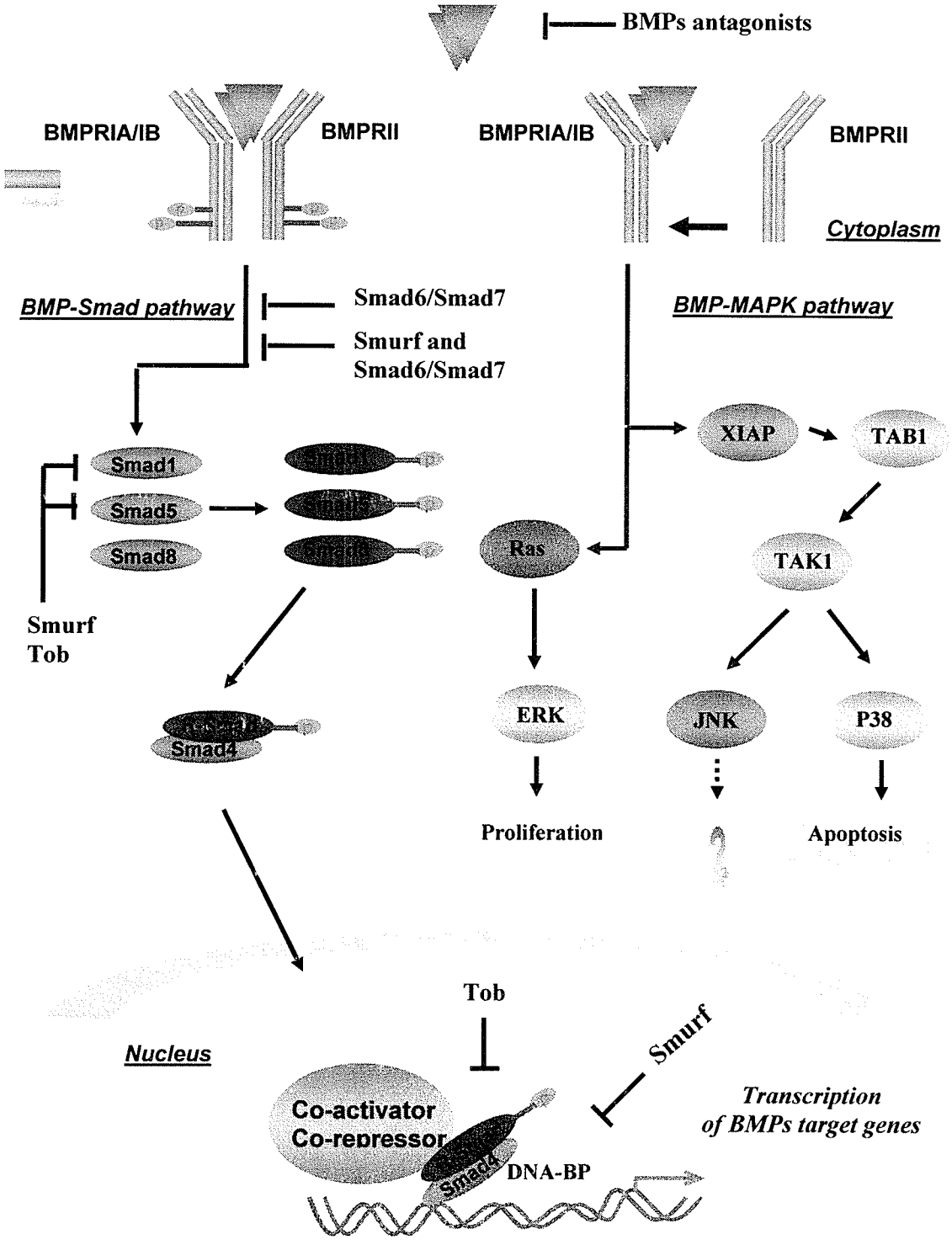
BMPs antagonists
BMPRIA/IB
BMPRII
BMPRIA/IB
BMPRII
Cytoplasm
BMP-Smad pathway
Smad6/Smad7
Smurf and
Smad6/Smad7
BMP-MAPK pathway
XIAP
TAB1
Smad1
Smad5
Smad8
Ras
TAK1
Smurf
Tob
ERK
JNK
P38
Smad4
Proliferation
Apoptosis
Tob
Nucleus
Smurf
Co-activator
Co-repressor
Smad4
DNA-BP
Transcription
of BMPs target genes

Table 2. The pleiotropic biological functions of BMPs

	Biological Activities	Ref.
BMP2	Induce cells differentiation	Itoh, 2006; Hsu, 2007
	Promote tumor angiogenesis	Raida, 2006
	Suppress tumorigenesis	Kumagai, 2006
	Promote cervical fusion	Shields, 2006
	Promote facial nerves regeneration	Wang, 2007
	Inhibit hepatocyte regeneration	Xu, 2006
	Induce bone formaiton	Kugimiya, 2005
	Induce endothelial activation	Csiszar, 2006
BMP4	Induce cells differentiation	Kim, 2002; Taha, 2006
	Inhibit cells differentiation	Faure,2007
	Promote cell proliferation	Paez-Pereda, 2003; Otani, 2007
	Antiproliferative effects	Giacomini, 2006; Hsieh, 2006
	Carcinogenesis	Deng, 2007; Montesano, 2007
	Suppress tumorigenesis	Nishanian, 2004
	Induce cells apoptosis	Israsena, 2002; Kiyono, 2003
	Tissue repair and remodeling	Jiang, 2006
	Promote development	Vogt, 2006; Yaar, 2006
BMP5	Promote ovarian folliculogenesis.	Pierre, 2005
	Inhibit growth and induce apoptosis	Ro, 2004
	Promote dendritic growth of neurons	Beck, 2001
BMP6	Induce bone formation	Simic, 2006
	Induce cells differentiation	Estes, 2006; Friedman, 2006
	Promote prostate cancer bone metastases	Dai, 2005
	Promote spinal fusion	Laurent, 2004
	Induce apoptosis in human myeloma cells	Ro, 2004
BMP7	Neurotrophic effects on striatum neurons	Gratacos, 2002
	Suppress corneal scarring	Fuchshofer, 2007
	Reverse chronic renal injury	Zeisberg, 2004

2. Bone morphogenetic protein 4

2.1 Gene and protein structure of BMP4

Rat BMP4 gene localizes at chromosome 15p14. The complete DNA sequence of a ~11kb region has been identified. The genomic region contains a transcription unit of 6.72kb, ~ 3kb of 5' flanking region and ~1kb of 3' flanking region (Feng, Chen et al., 1995; Shore, Xu et al., 1998). As shown in Figure 2, rat BMP4 mRNA are transcribed from four exons. 5' Rapid amplification of cDNA ends (RACE) analysis showed that there are two transcriptional start sites, located in different sites of exon1 (Shore, Xu et al., 1998). Two promoters have been identified to control the transcription of the BMP4 gene, one in upstream exon1, the other in exon1. 5'Flanking region of BMP4 exon1 contains both positive and negative transcriptional regulation elements, such as Esterase 1 (Ets-1),

Initiator (Inr), activated protein-1 (AP-1), AP-2, IFN stimulation response element (ISRE) and serum response element (SRE) (Shore, Xu et al., 1998). The promoter region is GC rich with no obvious TATA or CAAT consensus sequence. Interestingly, both exon1 and exon2 contain non-protein coding sequence. Having two promoters and noncoding exons may permit a more efficient translation of the BMP4 protein under certain specific conditions. They could control where the BMP4 mRNA is located in the cells and control the translation rate of mRNA in different cellular contexts.

After transcription, BMP4 is first synthesized as inactive preproteins, about 408 aa. The preprotein is subsequently cleaved by furin convertases within the Golgi apparatus at a conserved motif (Arg-XX-XX-Arg), and then forms an active dimeric protein

(Wilkinson, Kolle et al., 2003). Those preproteins remaining in uncleavage will be targeted for lysosomal degradation (Goldman, Hackenmiller et al., 2006). During development, BMP4 can specify cell types by forming precisely controlled concentration gradients through modulating protein processing.

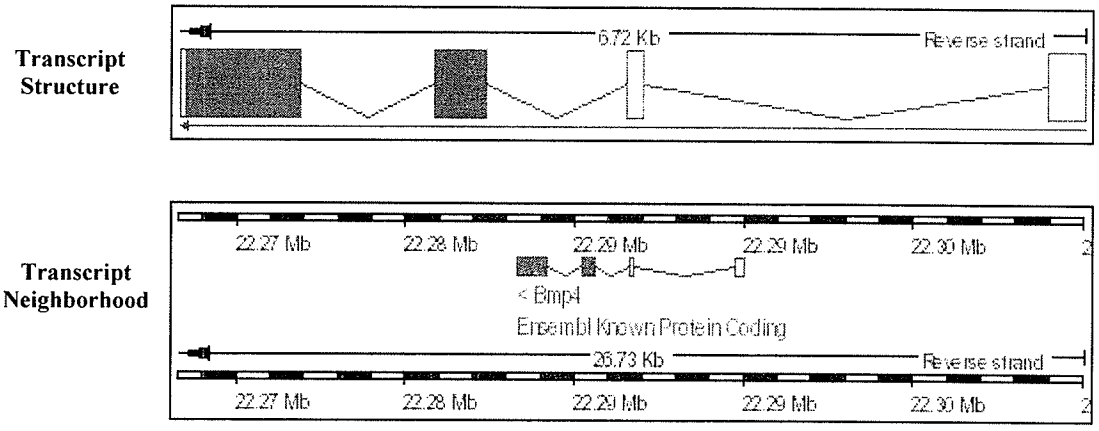

Figure 2 *Rat BMP4 transcript and transcript neighborhood structure from Ensembl website.*

Untranslated regions of the transcript

Translated regions of the transcript

http://www.ensembl.org/Rattus_norvegicus/transview?transcript=ENSRNOT00000012957;db=core

BMP4 is a member of TGFβ superfamily. It possesses the unique protein structure of these family members. It contains 408 amino acid residues. Figure 3 shows the structure model of BMP4, which comes from the *"Database of Comparative Protein Structure Model, University of California, San Francisco"*. The general structure of the monomeric BMP4 consists of two pairs of antiparallel β-strands forming a flattened surface and a long α-helix. The "cysteine-knot" formed from six cysteine residues is very important for BMP4 structural integrity. The homo- or heterodimer is formed through interchain disulphide bone which stabilizes the dimmer interface (Lin, Lerch et al., 2006).

Figure 3 The structure model of BMP4.

2.2 BMP4 signaling transduction pathways

Signaling transduction pathways initiated by BMP4 include Smad-dependent signaling pathway and Smad-independent signaling pathways (MAPK pathway). It exerts different physiological functions in different cell types through initiating different signaling pathways (Figure.1).

2.3 Biological functions of BMP4

BMP4 is a critical component in the formation of ventral mesoderm during embryo development. It can also initiate signals from mesoderm region to promote the specification of early hepatocytes in endoderm region. During the entire development process, BMP4 plays very important roles in tooth, eye, kidney, mandibular, hematopoietic system, and spinal cord oligodendrocyte development. In adults, the expression of BMP4 is still seen in some organs, such as heart, prostate, lung, kidney and eye. In some pathological conditions, the silent mechanisms are disrupted and the BMP4

gene is turned on again. Increased expression of BMP4 may indicate crucial roles in protection or injury of target cells. BMP4 functions identified from the studies during the past 10 years are summarized in Table 3.

3. BMPs and liver

BMPs, as members of the subclassification within the TGFβ superfamily, are very important in organ development and growth. BMPs knockout mice experiments have demonstrated that BMPs signaling is particularly involved in cell differentiation pathways. They direct the phenotypes when tissues are undergoing morphogenesis (Miller, Harvey et al., 2000). During embryo development, BMP4 secreted from septum transversum mesenchyme direct the endoderm hepatogenesis (Rossi, Dunn et al., 2001). In adult liver, mature hepatocytes show terminal cellularity differentiation and senescence features. However, the expression of BMPRs is still seen in some population of hepatic cell types, which may imply that hepatic cell types are capable of accepting the stimulation of BMPs in some specific physiologic or pathological situations when BMPs are available. TGFβ1, another member of the TGFβ superfamily, is considered to be a major factor in the progression of hepatic fibrotic and regenerative processes. Therefore, some studies have focused on the investigation of BMPs roles in liver, especially in pathological situations since liver fibrosis and carcinogenesis directly result from cell abnormal differentiation.

Recent investigations revealed that BMP6 and BMP9 transcripts were detectable in the liver in a cell type restricted expression pattern. BMP6 mRNA was observed in two nonparenchymal liver cells, Kupffer cells and hepatic stellate cells. (Knittel, Fellmer et al., 1997), whereas endothelial cells, Kupffer cells and hepatic stellate cells are the major

Table 3. The pleiotropic biological functions of BMP4

Differentiation	Cynomolgus monkey ES cells→ Cardiomyocyte	
	Embryonic stem cells → Lymphoid and myeloid hematopoietic cells	
	Mouse embryonic stem cells→Adipocyte	
	Mouse calvarial cells →Osteoblastic cells	
	Rhesus monkey embryonic stem cells→ Hematopoietic differentiation	
	Lung fibroblasts→Myocyte	
Apoptosis	Capillary endothelial cells	Smad1/5↑ , Bcl-XL ↑
	Ventricular zone progenitor cells	Msx2 and p21(CIP1/WAF1) ↑ , bax↑
	P19 Embryonal carcinoma cells	P21↑, Cdk4↓ p27↑
	Multiple myeloma cells	Induces cell cycle arrest / inhibits DNA synthesis
	Arterial endothelial cells	
	Human pulmonary artery smooth muscle cells	p38 and ERK1/2↑
	Pancreatic progenitor cell expansion	
Proliferation	Chondrocyte proliferation and hypertrophy	
	Myogenic progenitor proliferation	
	Adenocarcinomas / BMP4↑	Enhanced migration and invasion
	Corticotrophinomas / BMP4↓	Antiproliferative action, inhibits corticotroph tumor cells
Tumogenesis	Colon cancers / BMP4↑	Involved in epithelial cell differentiation,
	Breast cancer / BMP4↑	
	Malignant melanomas / BMP4↑	Angiogenesis
	Atherogenesis,elicit endothelial cells activation and dysfunction / BMP4↑	
Others	Regulation of ocular angiogenesis / VGEF↑	
	Tumor suppression / apoptosis↑, alterations in cell cycle profile	

cellular sources for BMP9 mRNA (Song, Celeste et al., 1995; Rossi, Dunn et al., 2001) There is high level expression of BMP2 around the central and portal veins in normal liver. The localization and timing of expression pattern of BMP2 in liver implied a negative regulation on hepatocyte proliferation (Xu, Ji et al., 2006). In addition, the introduction of BMP7 by adenoviral infection might suppress the profibrogenic response of the liver through triggering the expression of inhibitors of differentiation 2 (Id2) in HSCs, although the endogenous expression of BMP7 was hardly detectable in HSCs (Kinoshita, Iimuro et al., 2007). Further characterization of BMPs expression, signaling in HSCs will enable a more thorough understanding of the roles of these family members during liver fibrogenesis and carcinogenesis.

Liver Fibrosis and Hepatic Stellate Cells

1. Introduction to liver fibrosis

1.1 Liver structure

The human liver is a dark red-brown organ and located in the abdominal cavity in contact with diaphragm. It consists of four lobes: the right, left, quadrate and caudate lobes. Each lobe contains thousands of units called lobules that are the building blocks of the liver. The lobule is a roughly hexagonal arrangement of plates of hepatocytes radiating outward from a central vein in the center (Figure 4) (Hase and Brim, 1966). Liver has two blood supplies, from hepatic arteries (25%) and portal vein (75%) (carrying blood from the intestines, stomach, pancreas and spleen) (Takahashi, 1970; Urmanov, 1973). Terminal branches of hepatic portal vein and hepatic artery empty together and mix as they enter sinusoids in the liver (Figure 5). Sinusoids are distensible vascular channels lined with highly fenestrated endothelial cells and bounded circumferentially with hepatocytes (Revel, Yancey et al., 1981) (Figure 6). As blood flows through the sinusoids, a considerable amount of plasma is filtered into the space between endothelium and hepatocytes (the "space of Disse") (Urmanov, 1973). The sinusoid is a specific capillary network system where a variety of metabolic substances are exchanged between hepatic blood flow and hepatic parenchymal cells (Enomoto, Nishikawa et al., 2004).

1.2 Hepatic cell types and functions

The liver is composed of different cell populations with distinct functions. The parenchymal cells (hepatocytes) and cholangiocytes account for 60% of the total cell

population and 80% of the total volume of the organ. There are at least four major types of nonparenchymal cells in the liver. Almost half (40%) of the nonparenchymal cells are fenestrated endothelial cells. The remaining nonparenchymal cells consist of 33% of Kupffer cells, 22% of hepatic stellate cells (HSCs) and 1% of pit cells (or natural killer cells) (Williams and Iatropoulos, 2002).

Hepatocytes are the major functional cells in the liver and perform a variety of essential functions, including: (*i*) uptake, storage and controlled release of nutrients into the circulation; (*ii*) synthesis of proteins, glucose, fatty acids, cholesterol and phospholipids; (*iii*) digestion and absorption of dietary fats; (*iv*) degradation and detoxification of exogenous and endogenous compounds.

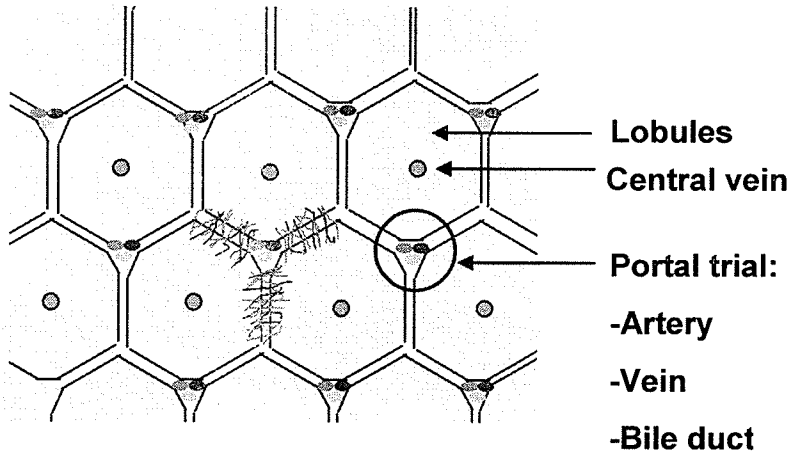

Figure 4 Architecture of hepatic tissue.

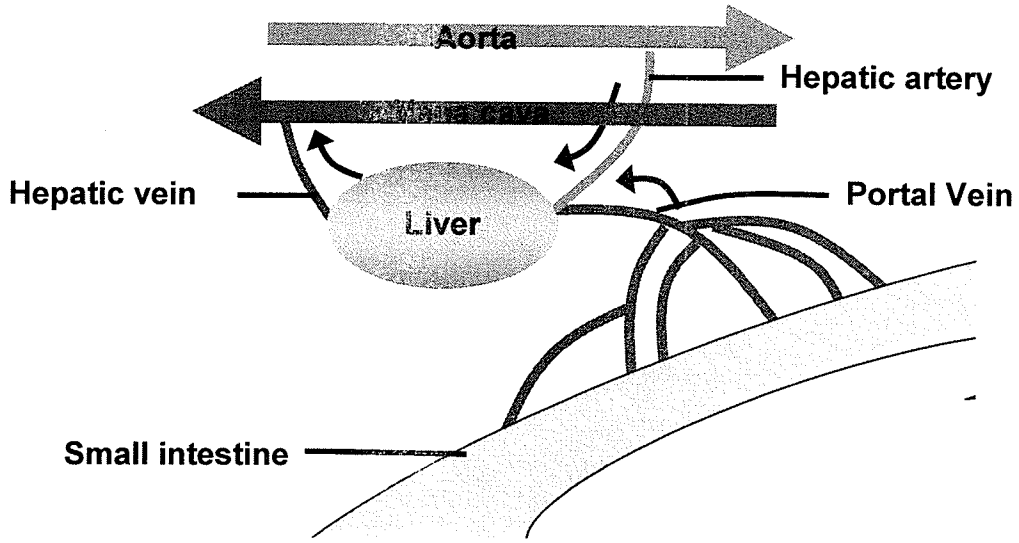

Figure 5 *The hepatic vascular system.* About 75% of the blood entering the liver is venous blood from the portal vein. The remaining 25% of the blood supply to the liver is arterial blood from the hepatic artery.

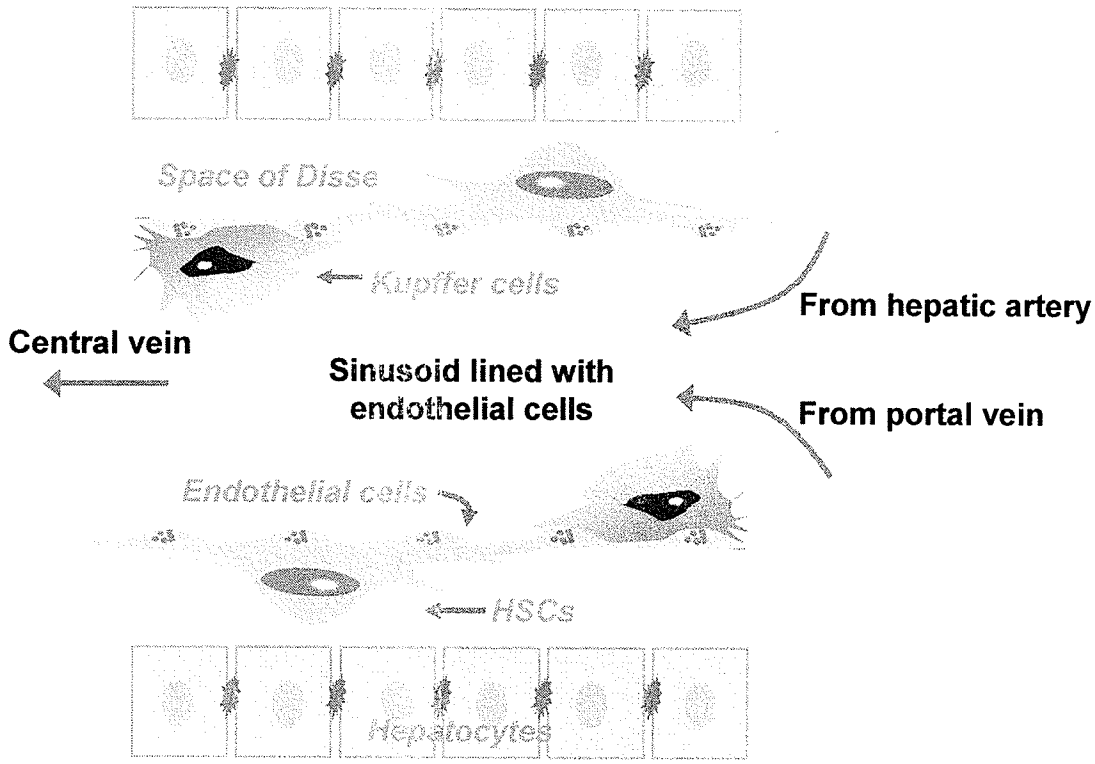

Figure 6 The composition in normal liver and blood flows through the sinusoids.

HSCs lie in the space between sinusoidal endothelial cells and hepatocytes. They have several important functions: (*i*) retinoid storage and homeostasis; (*ii*) remodeling of ECM by production of both ECM components and matrix metalloproteinases (MMPs); (*iii*) production of growth factors and cytokines; (*iv*) contraction and dilation of the sinusoidal lumen. HSCs mainly exhibit two phenotypes, quiescent phenotypes and myofibroblast-like phenotype. The activated process of HSCs is considered to be the key event during liver fibrogenesis (Sato, Suzuki et al., 2003; Gressner and Weiskirchen, 2006).

Endothelial cells express scavenger receptors on their surface and perform ***scavenger function*** for modified molecules, such as advanced glycation end products (AGE)-modified BSA, type I, III procollagen peptides and albumin. These cells can also exert ***antigen presentation function*** to present antigen to T lymphocytes. These antigens include bacterial components such as lipopolysaccarhides (LPS) and food antigens. Recently, it has been demonstrated that ECM components can be removed from the hepatic blood flow by endothelial cells (***Uptake function***) (Enomoto, Nishikawa et al., 2004).

Kupffer cells are predominantly located on the inside of the sinusoidal wall. They play an endocytic role to help blood-borne materials enter liver (***phagocytic capacity***). They are capable to clear pathogens, immune complexes, tumor cells, liposomes, lipid microspheres, iron and circulating endotoxin. Thus, Kupffer cells play a critical role in the host defense by acting as a biological filter (Arii and Imamura, 2000).

Pit cells are large granular cells that are anchored to the endothelial lining of the sinusoids in close apposition to endothelial and Kupffer cells. They are functionally

defined as liver-associated natural killer (NK) cells. Thus, pit cells are capable of preventing tumour cell metastasis to the liver by NK-mediated cytotoxicities (Nakatani, Kaneda et al., 2004).

1.3 Roles of different hepatic cell types in liver fibrosis

Hepatic cell types may have different fibrogenic potential.

Hepatocytes are ***initiators***. They are targets of most hepatotoxic agents. Damaged and apoptotic hepatocytes release ROS and fibrogenic mediators which act as the paracrine signaling molecules to induce the activation of HSCs.

Kupffer cells serve as the ***mediator***. They are involved in the pathogenesis of chemically mediated liver injury (carbon tetrachloride (CCl4), alcohol, and allyl alcohol) through release of biologically active mediators.

HSC acts as the ***effector***. It is the primary cell-type in the liver responsible for excess collagen synthesis during liver fibrogenesis. Following chronic injury, HSCs are activated or transdifferentiated into myofibroblast-like cells, acquiring contractile, proinflammatory, and fibrogenic properties (Luckey and Petersen, 2001).

In chronic cholestatic disorders (i.e., primary biliary cirrhosis), epithelial cells stimulate the accumulation of portal myofibroblasts, which initiate collagen deposition around damaged bile ducts (Luckey and Petersen, 2001).

1.4 Changes during fibrogenesis

In normal liver, the space of Disse contains low-density ECM. The defined lattice-like meshwork of ECM molecules provides cellular support and allows the transportation of cytokines and growth factors. Low-density ECM also provides signals that maintain

the differentiated function and morphology of resident liver cells (Friedman, 2003). During liver fibrosis, the activated HSCs produce a wide variety of collagenous and non-collagenous ECM proteins. The ECM composition is altered both quantitatively and qualitatively. Fibrotic liver contains approximately six times more ECM than normal liver. Although collagen types I, III, and IV are all increased, collagen type I increases much more significantly and therefore its ratio to collagen types III and IV increases (Eckes, Kessler et al., 1999; Sato, Suzuki et al., 2003; Gressner and Weiskirchen, 2006).

The deposition of ECM in the space of Disse leads to the capillarization of basement membranes. The incompleted basement membranes would hinder the bidirectional exchange processes between hepatocytes and sinusoidal blood stream and further impair the hepatocyte functions. Furthermore, an excessive amount of deposited ECM and contraction of myofibroblast-like HSCs narrow the sinusoidal lumen and lead to intraparenchymal hemodynamic resistance (portal hypertension) (Gressner and Weiskirchen, 2006).

1.5 Stimuli for liver fibrosis

1.5.1 Alcohol abuse

Alcohol is primarily metabolized in hepatocytes to acetaldehyde, a step that is catalyzed by alcohol dehydrogenase (ADH), or cytochrome P450 2E1 (CYP2E1). ROS and lipid peroxidation products are released during alcohol metabolism in hepatocytes. In addition, alcohol can lead to the increase in the concentration of LPS in portal blood. LPS further activates Kupffer cells to produce ROS. Finally, the released ROS and acetaldehyde can activate HSCs through paracrine mechanism. Lipid peroxidation

products, such as malondialdehyde (MDA) and 4-hydroxy-nonenal (4-HNE), could stimulate the collagen production in the liver (Bataller and Brenner, 2005).

1.5.2 NASH

Nonalcoholic steatohepatitis (NASH) is the most severe form of nonalcoholic fatty liver disease (NAFLD). NASH is a metabolic syndrome. It is characterized by obesity, type 2 diabetes mellitus, and dyslipidemia with insulin resistance as a common feature. The proposed mechanism of hepatic injury in NASH is associated with oxidative stress and lipid peroxidation. Hyperglycemia and insulin resistance lead to elevated serum levels of free fatty acids (FFA), which activate PPARα and result in FFA oxidation. The formation of ROS subsequently causes hepatocyte damage. Furthermore, FFA can induce the production of pro-inflammatory cytokines, such as TNFα and IL-6. ROS and inflammatory cytokines are considered as the contributor factors in NASH (Schuppan, Krebs et al., 2003; Bataller and Brenner, 2005; Farrell and Larter, 2006).

1.5.3 HCV

Hepatitis C virus (HCV) is known to induce liver fibrosis. However, the mechanism of this effect is poorly understood. It was known that HCV escapes surveillance of the HLA-II–directed immune response and then infects hepatocytes. Infected hepatocytes could cause oxidative stress and induce the recruitment of inflammatory cells into the liver, which subsequently lead to HSCs activation and collagen deposition. Moreover, activated HSCs express HCV receptors and thus, may be infected by HCV. It was shown that several HCV proteins (NS3, NS5) can induce fibrogenic effects in HSCs by increasing intracellular calcium concentration, ROS production and chemokine secretion

(Schuppan, Krebs et al., 2003; McCaughan and George, 2004; Purohit and Brenner, 2006).

2. Hepatic stellate cells

2.1 General introduction

Hepatic stellate cells (vitamin A-storing cells, lipocytes, fat-storing cells, Ito cells) were firstly identified by Boll and Von Kupffer in the 1870s. In 1968, Ito described their morphological features under light microscopy (Ito and Shibasaki, 1968). The function of HSCs in liver diseases was not thoroughly studied until the 1980s, during which HSCs were found to be the main producer of ECM in liver fibrogenesis. From that time, many studies have shown that HSCs are the important cell type associated with liver fibrosis (Senoo, 2004; Bataller and Brenner, 2005).

2.1.1 Basic cell biology

HSCs are localized in the perisinusoidal space of Disse. They have star-like dendritic cytoplasmic processes through which they are intimately contact with both hepatocytes and abluminal surface of sinusoidal endothelial cells. They are also in close proximity to hepatic nerves, which render HSCs responsive to neural stimulation of contractility. The intermediate filament proteins are the valuable markers for detecting HSCs by using immunohistochemistry technique. In normal liver, they are characterized by a low proliferative rate, very modest fibrogenic potential, little cytokine secretion, and lack of contractile properties (Senoo, 2004). As the major cell type to produce ECM, HSCs play very important roles in matrix homeostasis in the liver. Moreover, HSCs store almost 80% of retinoids in the whole body as retinyl palmitate in lipid droplets in

cytoplasm (Sato, Suzuki et al., 2003). In physiological conditions, HSCs play a pivotal role in the regulation of retinoid homeostasis. Another two possible functions of quiescent HSCs are to regulate the blood flow and control the sinusoidal tone to regulate the fluid exchange between the lumen of sinusoid and the Space of Disse through endothelial fenestrate (Wake, 2006).

2.1.2 Heterogeneous population of HSCs

It is known that fibrotic and cirrhotic liver constitute a heterogeneous population of HSCs that differ in their expression of cytoskeletal filaments, retinoid content and extracellular matrix components (Schaefer, Rivas-Estilla et al., 2003). Due to the different characteristics related to proliferative index, expression level of collagen, TIMP1 and MMPS, the heterogeneous population of HSCs exhibit different fates during resolution of hepatic fibrosis and cirrhosis. Currently, four different CCl_4-induced fibrotic stellate cell lines have been established. These HSC lines (CFSC-8B, CFSC-2G, CFSC-3H and CFSC-5H) represent different clones of HSCs, which were obtained from the liver of a CCl_4-induced-cirrhotic rat (Greenwel, Rubin et al., 1993). They provide convenient cell models to study the susceptibility of heterogeneous HSC population to apoptosis.

2.1.3 HSCs in pathological conditions

Following acute or chronic liver damage, HSCs undergo a process of activation. HSCs activation is considered as a two-stage process, initiation and perpetuation. Initiation process refers to early changes in gene expression and phenotype changes, including loss of vitamin A, increased proliferation and motility, enhanced cellular

contractility, and increased expression of cellular matrix metalloproteinase MMP2 and MMP9 (responsible for the degradation of collagen IV) and tissue inhibitor of metalloproteinase TIMP1 and TIMP2. The perpetuation process results from the persistent effects of stimuli on activated HSCs and finally leads to fibrosis. Initiation is largely due to paracrine stimulation, whereas perpetuation involves autocrine as well as paracrine loops.

Activated HSCs migrate and accumulate at the sites of tissue repair, where they secret large amounts of ECM, regulate ECM degradation and extend their long cytoplasmic processes along the sinusoidal wall (Kawai, Enzan et al., 2003). The morphology of these cells also changes from the star-shaped stellate cells to myofibroblasts. This process is termed transdifferentiation, which is considered to be the key event in the liver fibrogenesis. Moreover, the expression of a characteristic cytoskeletal protein, alpha-smooth-muscle actin (α-SMA), is significantly increased during this process.

2.2 Factors involved in the activation of HSCs

Factors involved in the activation of HSCs have been classified into two groups: one group of factors involved in the initiation of stellate cell activation and the other group factors involved in the perpetuation of stellate cell activation.

Factors in the initiation of stellate cell activation

The initiation of HSCs activation results from paracrine stimulation by all neighboring cell types, including sinusoidal endothelial cells, Kupffer cells, hepatocytes, and leukocytes. The factors secreted from these cells in response to most liver injuries

are responsible for HSCs early changes in gene expression and phenotype changes (Table 4).

Factors in the perpetuation of stellate cell activation

The perpetuation of HSCs activation is considered to be mediated by cytokines via autocrine and paracrine mechanisms. HSCs obtain a proliferative, fibrogenic and contractile phenotype during the transition process of activated HSCs to myofibroblast. It is also important to note that activated cells produce a number of chemokines such as monocyte chemotactic peptide (MCP-1) and promote further recruitment of inflammatory cells during the activation process (Table 4).

2.3 Intracellular events during hepatic stellate cells activation

Four principle intracellular signaling cascades in HSCs in response to liver injuries have been identified.

2.3.1 MAPK signaling pathway

Many studies have demonstrated that the MAPK signaling pathway may play an important role in the regulation of HSCs activation. MAPK signaling via ERK can promote HSCs mitogenesis and cell survival (Saxena, Titus et al., 2004). Both JNK and p38 MAPK signaling are required for α-SMA expression in early stage of HSCs activation. Activated p38 MAPK signaling can enhance the collagen α1(I) mRNA expression in HSCs, whereas JNK MAPK signaling inhibits its expression (Varela-Rey, Montiel-Duarte et al., 2002; Tsukada, Westwick et al., 2005). In addition, JNK signaling stimulates HSCs proliferation, whereas p38 signaling evokes a contrary effect on HSCs proliferation (Schnabl, Bradham et al., 2001).

Table.4 Factors involved in the initiation and perpetuation of hepatic stellate cells activation.

	Function	Factors (producer)
Initiation stage *(Paracrine mechanism)*	Proliferation	TGFα (*Kupffer cells*), Fibronectin (*Kupffer cells,Endothelial cells*) PDGF (*Platelets*), IGF-1 (*Hepatocytes*)
	Collagen degradation	IL-10 (*Kupffer cells*), INFγ (*Lymphocytes*)
	Collagen synthesis	MMP9 (*Kupffer cells*), ROS (*Kupfffer cells, Leukocytes*) TGFβ1(*Kupffer cells,Platelets,Hepatocytes*), ET-1 (*Endothelial cells*)
	Fibrogenesis	Lipid peroxides (H*epatocytes, Kupffer cells)*
	Inhibit proliferation and contractility	NO (*Kupffer cells, leukocytes*), IFNγ (*Lymphocytes*)
Perpetuation stage *(Autocrine mechanism)*	Proliferation	PDGF, EGF, TGFα, bFGF, IGF-1, CTGF
	Chemotaxis	PDGF, bFGF, IGF-1, M-CSF, MCP-1
	Fibrogenesis	TGFβ1, IL-1β, IL-6, TNFα, Lipid peroxidation products
	Contractility	ET-1, PAF, Thrombin
	Matrix degradation	MMP2, MMP9, TIMP1

Abbreviations: ET-1, endothelin 1; MCP-1, monocyte chemotactic protein 1; MMP 9, metalloproteinase 9; MMP 2, metalloproteinase 2; TIMP1, tissue inhibitor of metalloproteinase 1; PDGF, platelet-derived growth factor; TGF-β1, transforming growth (Abe, 2006)factor beta 1; TGFα, transforming growth factor alpha; IGF-1, insulin-like growth factor 1; INFγ, interferon gamma; NO, nitrogen monoxide; EGF, epidermal growth factor; bFGF, basic fibroblast growth factor; CTGF, connective tissue growth factor; M-CSF, macrophage colony-stimulating factor; TNFα, tumor necrosis factor alpha; PAF, platelet activating factor; IL-10, interleukin 10; IL-1β, interleukin 1beta; IL-6, interleukin6.

Reference: (Reeves and Friedman, 2002; Safadi and Friedman, 2002; Sokol, 2002; Friedman, 2003; Gabele, Brenner et al., 2003; Pinzani and Rombouts, 2004; Tsukada, Parsons et al., 2006)

2.3.2 Smad signaling pathway

Smad signaling pathway initiated by TGFβ plays a key role in the activation of HSCs. Active TGFβ binds to type II TGFβ receptor, which leads to the phosphorylation and activation of type I TGFβ receptor. The activated receptor phosphorylates Smad2 or Smad3 which subsequently forms a complex with Smad4 and translocates into nucleus to regulate target gene expression. TGFβ signaling via Smad3 plays an important role in the morphological and functional maturation of HSCs. However, the signaling via Smad2 seems to be a primarily antiproliferative role during HSCs activation (Uemura, Swenson et al., 2005).

2.3.3 Intracellular Ca^{2+} signaling pathway

Recently, it has been demonstrated that intracellular Ca^{2+} signaling pathway may play a particular important role in HSC biology (Kruglov, Correa et al., 2007). HSCs express G-protein-coupled metabotropic receptors (P2Y), which link extracellular ATP to downstream cytosolic Ca^{2+} signals. ATP binding to P2Y induces G protein oligomerization, activation of phospholipase C, and generation of inositol 1,4,5-trisphosphate (IP3). Binding of IP3 to the IP3R opens the IP3-gated Ca^{2+}-release channels, which allow localized increase in Ca^{2+} concentration. HSCs only express the type I IP3R, and the subcellular distribution of this receptor changes during HSCs activation. IP3 receptors locate in the endoplasmic reticulum (ER) in quiescent HSCs. However, they translocate into the nucleus and cell extensions upon activation with important functional consequences. In activated HSCs, the type I IP3R in nucleus may mediate proliferation and collagen gene transcription, whereas the receptor in cell

extensions may mediate HSCs contraction, gap junction signaling and exocytosis (Kruglov, Correa et al., 2007).

2.3.4 Wnt signaling pathway

Wnt signaling pathway has been recently identified in activated HSCs. Wnt5a, which expression is significantly enhanced in activated HSCs, activates a noncanonical Wnt signaling pathway through binding to cell surface receptor frizzled2. Activated frizzled 2 leads to the decrease in intracellular cyclic guanosine monophosphate (cGMP), attenuates the activity of protein kinase G (PKG), and thereafter enables a robust Ca^{2+} mobilization in activated HSCs. Finally, the transcription of nuclear factor of activated T cell (NF-AT) dependent target genes in response to Wnt stimulation are increased in HSCs. The NF-AT target genes play very important roles in HSCs differentiation into myofibroblasts. For example, WISPs promote the deposition of ECM. Follistatin is directly involved in TGFβ response during HSCs activation (Jiang, Parsons et al., 2006; Ma and Wang, 2006).

3. Signaling pathways contribute to the initiation of HSCs apoptosis

Many studies have demonstrated that activated HSCs have the capacity to undergo apoptosis both spontaneously (e.g., the resolution phase of HSC activation) and by specific targeting with apoptotic agents (McGee and Patrick, 1972; Friedman, 1993). The activated HSCs showed more susceptible to apoptotic stimulation than quiescent cells (Canbay, Friedman et al., 2004). Understanding of the control of HSCs apoptosis is very important since regulation of this process may provide a novel therapeutic approach

to the treatment of advanced hepatic fibrosis. Following are several signaling pathways that have been shown to contribute to the initiation of HSCs apoptosis (Figure7).

3.1 Fas/Fas-ligand

Fas ligand (FasL), a member of the tumor necrosis factor family, initiates apoptosis by binding to its surface receptor Fas. Binding of FasL to Fas triggers the formation of the death-inducing signaling complex (DISC) by recruiting intracellular adaptor proteins. These adaptor proteins subsequently bind and aggregate procaspase-8 molecules, which cleave and activate one another. The activated caspase-8 molecules then activate downstream procaspases to induce apoptosis (Kavurma and Khachigian, 2003). During *in vitro* culture, expression of both CD95 (Fas) and CD95L (Fas-ligand) are increased in activated HSCs. Moreover, myofibroblasts-like HSCs show higher sFasL-sensitivity than quiescent HSCs (Saile, Matthes et al., 2002). It was demonstrated that the physiological expression of CD95 and CD95/L during activation of HSCs could initiate HSCs apoptosis (Saile, Knittel et al., 1997). Some studies have shown that the Fas and FasL gene expression are regulated by stress and some cytokines. IL-10, a potent anti-inflammatory cytokine, can promote the apoptosis in HSCs by up-regulating the expressions of FasL and Bax, and down-regulating the expression of Bcl-2, which may contribute to the antifibrotic effect of IL-10. Moreover, stress-induced FasL transcription plays an important role in the regulation of FasL gene expression (Kavurma and Khachigian, 2003).

3.2 TRAIL Receptor2

Tumor necrosis factor-related apoptosis-inducing ligand (TRAIL) receptors (TRAIL-R) are another important family of death receptors (DRs). Four TRAIL-binding DRs have been identified: TRAIL-R1 and R2 (DR4/DR5) and TRAIL-R3 and R4 (decoy receptor). DR4/DR5 contains death domains, signals apoptosis by using the adapter protein FADD (Fas-associated death domain), and induces apoptosis via a caspase-dependent process (Degli-Esposti, 1999). Decoy receptor is associated with the NF-κB and c-Jun activation. These transcription factors exert an anti-apoptotic effect via the up-regulation of pro-survival genes. It has been shown that activated HSCs preferentially expressed TRAIL-R2 compared to less-activated cells, whereas the expression of the decoy receptors tended to decrease in HSCs during *in vitro* culture (Taimr, Higuchi et al., 2003). Therefore, activated HSCs were susceptible to TRAIL-mediated apoptosis.

3.3 Nerve Growth Factor Receptor p75

Nerve growth factor receptor (p75) is a death domain-containing member of the TNF receptor family. It is a receptor for the neurotrophin peptide family, of which nerve growth factor (NGF) is the paradigm member. There still exits another receptor that may mediate the action of NGF, the Trk family receptor tyrosine kinases (He and Garcia, 2004). The interaction of p75 with Trk receptor enhances the responsiveness of Trk receptor to never growth factor and promote cell growth (Kaplan and Miller, 2004). It is shown that NGF binding to p75 along can promote cell death, whereas binding to Trk receptor leads to a proliferative response (He and Garcia, 2004). Therefore, presence and localization of Trk receptors are pivotal to determine the potential role of NGF in HSCs.

It had been documented that the expression of p75 was not observed in quiescent HSCs but became detectable in activated HSCs. There was no expression of TrK receptor in normal or experimentally injured liver (Trim, Morgan et al., 2000). Moreover, the expression of NGF in hepatocytes paralleled the peak period of HSCs apoptosis during liver injury (Oakley, Trim et al., 2003). Therefore, the negative expression of TrK in liver suggested that the major response of HSCs to NGF was initiation of apoptosis.

3.4 Bcl-2 family proteins

The BCL-2 family proteins include pro- and anti-apoptotic molecules. The two subset members localize to separate subcellular compartments in the absence of a death signal. Anti-apoptotic members are localized in the mitochondria, endoplasmic reticulum (ER), or nuclear membrane and pro-apoptotic members are in cytosol or cytoskeleton (Hockenbery, Nunez et al., 1990; Krajewski, Tanaka et al., 1993). The pro-apoptotic BCL-2 members can be subdivided into two functional subcategories. One set of molecules, such as BCL-XS and BAD, would serve as upstream death ligands which function by binding to the BCL-2 or BCL-XL to inhibit their anti-apoptotic activity (Gross, McDonnell et al., 1999). The other set of molecules, such as BID, could integrate and become integral mitochondrial membrane proteins. Following a variety of death signals, pro-apoptotic molecules BAX, BAK, BCL-XS or BID translocate to the mitochondrial membrane and act independently or with BCL-2 or BCL-XL to alter mitochondrial membrane potential (MMP). This causes the release of cytochrome c, which activates downstream caspase cascade (Gross, McDonnell et al., 1999). Therefore, the ratio between pro and anti-apoptotic Bcl2 family member determines, in part, the susceptibility of cells to a death signal.

It has been demonstrated that freshly isolated HSCs showed prominent expression of BCL-2 and reduced expression of BCL-XL (Boise, Gonzalez-Garcia et al., 1993). Moreover, the expression of pro-apoptotic BAX and BCL-XS were increased dramatically in activated HSCs compared with quiescent HSCs (Gong, Pecci et al., 1998). Thus, the ratio of anti-apoptotic BCL-2 and BCL-XL to pro-apoptotic BAX, was shifted to the direction of pro-apoptosis in activated HSCs (Baliga and Kumar, 2002).

4. Animal models of cholestatic liver fibrosis

Bile duct ligation (BDL) can induce cholestatic hepatic fibrosis or cirrhosis in rat, rabbit, dog and monkey. In humans, several clinical conditions can lead to biliary fibrosis, such as primary sclerosing cholangitis and extrahepatic biliary atresia. This fibrosis model is characterized by primary pathological lesions occurred surrounding the bile duct epithelium. The operation of BDL introduces biomechanical stress to biliary epithelium and triggers the compensatory proliferation and expansion of biliary epithelial cells (BECs) (Rojkind and Greenwel, 1993; Wu and Norton, 1996). Following the proliferative response of BECs, chronic obstruction of bile duct causes massive activation of HSCs in the periductal region and ultimately results in liver fibrosis and cirrhosis (Wu and Norton, 1996). This model is often used to study differentiation and apoptosis of HSCs, expression and regulation of ECM, interaction of different hepatic cells, and proliferation of hepatocytes in fibrotic liver (Xia, Dai et al., 2006).

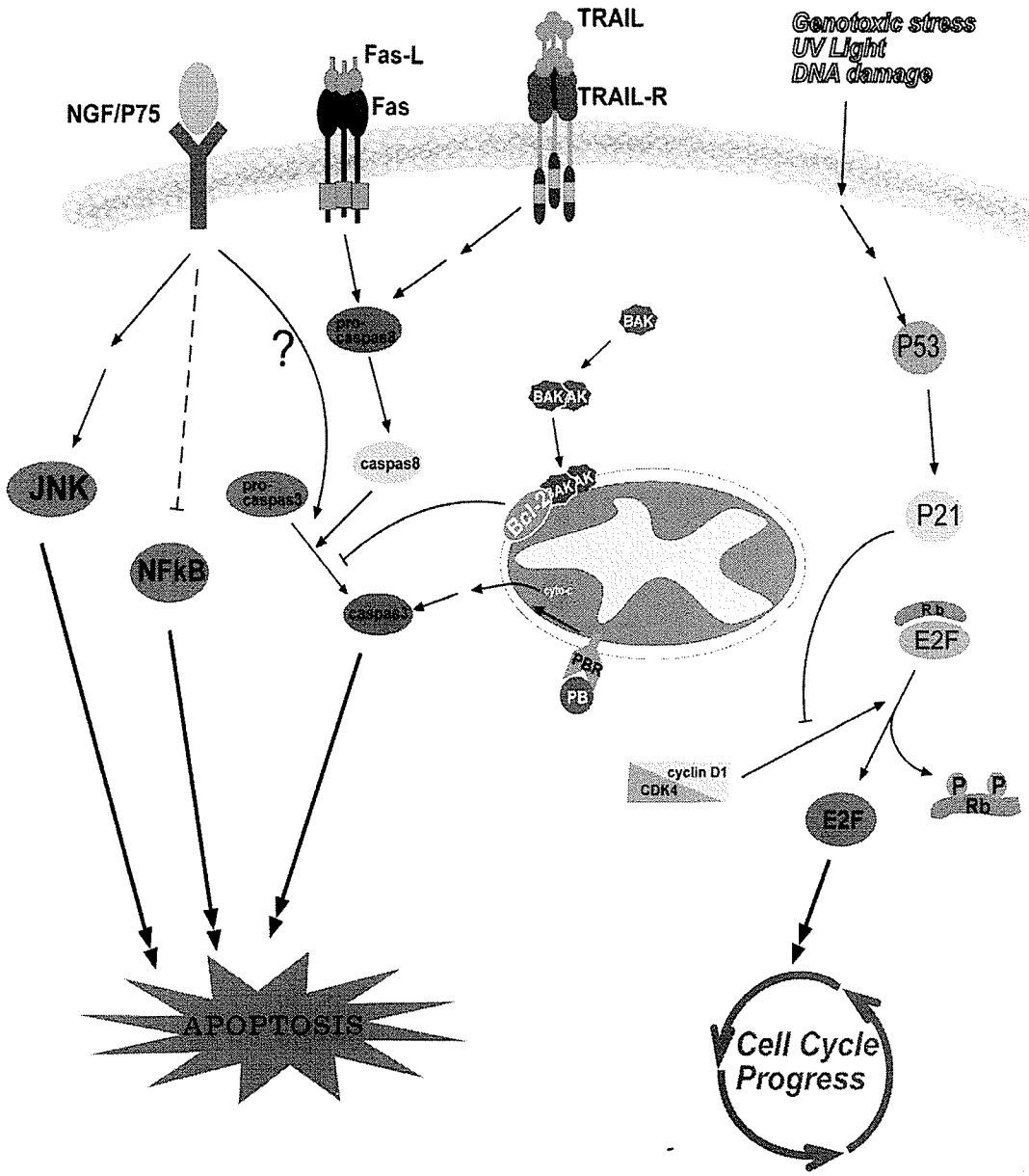

Figure 7 Signaling pathways involved in HSCs apoptosis

Oval Cells

1. General introduction

The "stem-like" cells in the liver were not identified until 1940s when Kinosita studied the capacity of liver regeneration using a hepatocarcinogenesis animal model (Vessey and de la Hall, 2001). Thereafter, many experiments provided evidence in support of the existence of a liver stem cell population (Solt, Medline et al., 1977; Dunsford, Maset et al., 1985; Alison, Poulsom et al., 1993). The concurrence of extensive hepatic injury and factors inhibitory to hepatocyte proliferation was the requirement for the rapid emergence of this cell population in the liver.

The stem-like cells are oval-shaped with scanty cytoplasm, termed "oval" cells in rodent and termed "progenitor" cells in human (Farber, 1956). They are 3~5 μm in diameter, smaller than the smallest cholangiocytes (6 μm) detected in rat liver and have a high nuclear to cytoplasmic ratio with a vesicular oval nucleus under conventional light microscopy. The oval cells can be detected by using immunohistochemistry with a mouse monoclonal antibody OV-6, which was raised against the hepatocytes isolated from liver nodules of 2-AAF treated rats (Dunsford and Sell, 1989; Crosby, Hubscher et al., 1998).

The oval cells are located at the smallest branches of the intrahepatic biliary tree, the canals of Hering. When severe damage occurs in the liver, proliferative oval cells are budding off portal bile ducts and forming tortuous ductular structures with the expression of alpha-fetoprotein (AFP), and then spreading out into the hepatic parenchyma (Alison, Poulsom et al., 1993).

2. Oval cells: stem cells

The classical definition for "stem cells" by Potten and Loeffler is "undifferentiated cells capable of proliferation, self maintenance, production of a large number of differentiated progeny, regeneration of tissue after injury and flexibility in the use of these options" (Potten and Loeffler, 1990). Essentially, there are two requirements for a cell to be "stem cell", self-renewing and pleuripotent.

The *in vivo* self-renewal capacity of oval cells has not been thoroughly documented since oval cells can not be easily detected in normal liver (Lowes, Brennan et al., 1999). Generally, the self renewal of quiescent stem cells is relatively slow, and differentiated daughter cells or intermediate cells can proliferate more rapidly. Increased oval cells can be easily detected in rat liver after induction with carcinogens by immunohistochemistry. The isolated oval cells from rat liver after treatment with 2-AAF can form colonies and maintain oval cell phenotype for at least 30 days in the absence of growth factors and ECM proteins (Leite, Correa-Giannella et al., 2007). As for the pleuripotency, it has been demonstrated that oval cells can give rise to either hepatocytes or cholangiocytes depending on the injury or the cell culture conditions. Oncostatin M, dexamethasone, bFGF and HGF all have the capacity to induce oval cell differentiation toward hepatocyte lineage (Germain, Noel et al., 1988; Dasgupta, Hughey et al., 2005; Okaya, Kitanaka et al., 2005). Moreover, several *in vivo* studies indicated that oval cells can differentiate into either hepatocellular or cholangiocyte lineage (Tee, Kirilak et al., 1994; Golding, Sarraf et al., 1995; Evarts, Hu et al., 1996).

3. Oval cells niche

The niche concept was first elucidated in the ovarian stem cell niche in Drosophila (Spradling, Drummond-Barbosa et al., 2001). Niche represents microenvironment around stem cells, which regulates stem cell activities, quiescence, proliferation or differentiation. Generally, niche includes stromal cells, base membrane and extracellular matrix (Figure 8).

Canals of Hering

Oval cells are located at the canal of Hering, which is the terminal branches of the intrahepatic biliary tree (Theise, 2006). It is partially lined by hepatocytes and cholangiocytes and forms the connecting channel between the bile ductules and bile canaliculi. The lined hepatocytes and cholangiocytes are morphologically and phenotypically intermediate cells, which are not found in normal tissue (Paku, Schnur et al., 2001). Confocal microscopy clearly showed that the oval cells form ductules surrounded by basement membrane, which derives from the canals of Hering and terminates on hepatocytes. The basement membrane and the contact between hepatocytes and oval cells may play an important role in regulating stem cell proliferation, differentiation and migration (Paku, Schnur et al., 2001).

Niche cells

In the liver, it has been suggested that one niche cell is HSCs. Ultrastructure of portal area of liver in 2-acetyl-aminofluren (AAF)-treated rat after partial hepatectomy clearly showed that HSCs moved across the basement membrane and formed direct cell-cell contact with oval cells (Paku, Schnur et al., 2001). However, the exact function of HSCs in regulating oval cells self-renewal and differentiation remains to be further

investigated. Moreover, the adhesive molecules that anchor stem cells to their niche play crucial roles not only in keeping stem cells within the niche but also in transducting the controlled signaling from niche to stem cells.

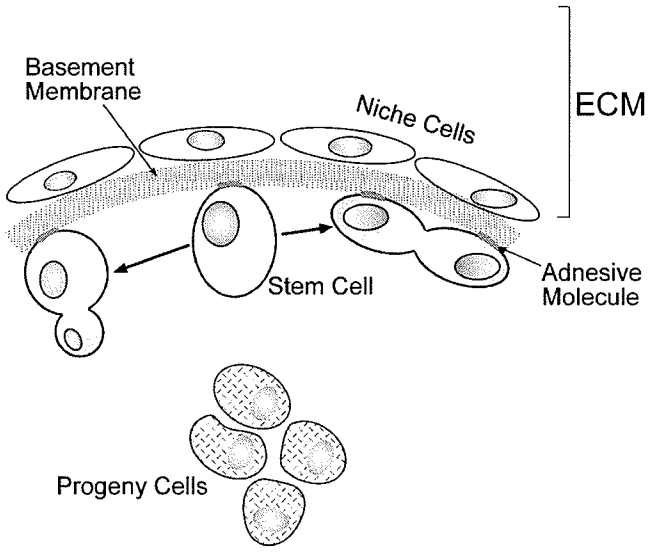

Figure 8 *Niche structure*. Niche cells underlying a basement membrane signal to stem cells to block differentiation and regulate division.

ECM

It has been demonstrated that ECM not only acts as scaffold physically connecting different cell types and maintaining the location but also recruits many kinds of cytokines, which regulate the activities of stem cells (Dasgupta, Hughey et al., 2005). In the liver, the basement membrane of bile ducts consists of laminin and type IV collagen, and the expression of integrin is also observed in biliary tree (Leite, Correa-Giannella et al., 2007). Since HSCs, the primary source of ECM in the liver, are structurally associated with oval cells, ECM may play an important role in regulation of the proliferation and differentiation of oval cells.

4. Hepatic and biliary markers for oval cells

A wide range of markers has been used to identify oval cells. OV-6 is mouse monoclonal antibody, raised against hepatocytes isolated from 2-AAF treated rat liver (Dunsford and Sell, 1989; Crosby, Hubscher et al., 1998). It recognizes a cytokeratin with epitopes shared on both CK 14 and CK 19 (Dunsford and Sell, 1989; Bisgaard, Parmelee et al., 1993). Oval cells can express hepatocellular markers and biliary differentiation markers. Moreover, some markers associated with haematopoietic cells can also be expressed by oval cells, which may imply the bone marrow origin of oval cells (Petersen, 2001). These markers can be used to immunochemically detect and sort oval cells (Table 5).

Differentiation of oval cells toward biliary or hepatocellular lineage is determined by using the expression pattern of hepatic and biliary markers, which are often used to elucidate the oval cells hepatic and biliary lineage mature (Table 6).

Table 5. Markers used in the identification of oval cells in liver.

Oval cells	**OV-6**
monoclonal antibodies	**OC.2, OC.3, OC.4, OC.5, OC.10**
Biliary epithelial phenotype	**BDS7**
	Gamma-glutamyltranspeptidase (GGT)
	Thy-1
Haematopoietic cells	**c-kit**
	CD34
	flt-3 ligand/flt-3
Haematopoietic stem cells marker	**ABCG2/BRCP1**
Biliary differentiation markers	**CK7, CK19, CK14**
Hepatic phenotype	**AFP**
Hepatocellular carcinoma marker	**Placental form of glutathione-S-transferase (GST-P)**
Deleted in malignant brain tumour 1	**DMBT1**
Gap junction protein	**Connexin 43**

Table 6. Markers used to identify the differentiation lineage of oval cells.

Hepatocytes	Biliary Cells
➢ **Early hepatic marker:**	**CK19, CK7**
Fetoprotein (AFP)	**β4 integrin**
➢ **Mid-hepatic marker:**	**Yp**
Albumin	**CX43**
➢ **Late hepatic marker:**	**GGTmRNA IV**
Glucose-6-phosphatase(G6Pase)	
Tyrosine-aminotransferase (TAT)	

HYPOTHESIS AND OBJECTIVES

Rationale

Many studies have proved that BMP4 signaling plays an important role during liver development. BMP4 expressed in mesoderm is required for the induction of liver-specific markers, such as albumin, and the exclusion of expression of a pancreas gene in endoderm. In adult liver, even though BMP4 expression appears undetectable in normal liver, stable expression of BMPRs in hepatocytes, hepatic stellae cells and hepatic stem cells obviously renders these cells responsive to BMP4. TGFβ, another member of TGFβ superfamily, is directly involved in liver fibrogenesis through initiating Smad and MAPK signaling pathways in HSCs. It has been shown that BMP4 can initiate a wide variety of biological activities in different cell types depending on the different spatial and temporal expression patterns of ligand and interaction of downstream signaling molecules with various partners. Some partners associated with BMP4 downstream signaling molecules have shown changes in activity and expression levels during liver fibrogenesis, such as RUNX (Miyazono, Kusanagi et al., 2001; Bertrand-Philippe, Ruddell et al., 2004), p300 and C/EBP (Yavrom, Chen et al., 2005). Therefore, it is reasonable to hypothesize that BMP4 is an important cytokine involved in liver fibrogenesis.

Hypothesis:

BMP4 and its induced signaling pathway play crucial roles in trans-differentiation and apoptosis of hepatic stellate cells as well as differentiation of hepatic stem cells.

Objectives:

- To investigate BMP4-induced differentiation of hepatic stellate cells.
- To investigate intracellular signaling pathway initiated by BMP4 during the differentiation of hepatic stellate cells.
- To investigate BMP4-induced differentiation of rat hepatic stem cells, WB-F344 cells, toward hepatocytes.
- To investigate intracellular signaling pathway initiated by BMP4 during the differentiation of WB-F344 cells.
- To investigate BMP4 signaling in determination of the susceptibility of hepatic stellate cells to apoptosis.

II. MATERIALS AND METHODS

1. Materials

Table 7 Materials

Product	**Company**
$25cm_2$ Cell Culture Flask	Fisher
15ml Centrifuge Tubes	Fisher
50ml Centrifuge Tubes	Fisher
100bp DNA Ladder (250ug)	Invitrogen
10ul Pipet Tips	VWR
200ul Pipet Tips	VWR
1000ulPipet Tips	VWR
100mM dNTP set, PCR Grade	Invitrogen
[γ-^{32}P]-ATP	Amersham
Adeno-X™ Expression Systems	Clontech
Adeno-X™ Rapid Titer Kit	Clontech
7-Aminoactinomycin D	Sigma
Annexin V-Cy3 Apoptosis Kit	CEDARLANE
Acrylamide	Sigma
Anti-mouse IgG (HRP linked)	Amersham
BCA Protein Assay Reagent	PIERCE
BLOCK-iT™ U6 RNAi Entry Vector kit	Invitrogen
Collagenase Type IV	Sigma
Costar 96-well Easy Wash ELISA Plate	Fisher
BD Adeno-X Rapid Titer Kit	BD Biosciences
Bis-acrylamide	Sigma
Charcoal stripped fetal bovine serum	Hyclone

Product	Company
Dexamethasone	Sigma
Dnase I	Roche
Dulbecco's Modified Eagle Medium	GIBCO/BRL
ECL Plus Reagents	Amersham
Essential amino acids	GIBCO/BRL
G-25 Sephadex Column	Roche
GFX PCR DNA and Gel Band Purification Kit	GE health care
Glycerol	Sigma-Aldrich
Kodak Biomax XAR film	GE health care
L-Glutamine	Fisher
LB Broth	Fisher
Lipofectamine2000	Invitrogen
MEM	Hyclone
Methanol	VWR
MicroSpin G25 column	GE health care
MLV-Reverse Transcriptase	Invitrogen
Noggin	R&D Systems
Non-essential amino acids	GIBCO/BRL
Nonidet P40 substitute	Sigma-Aldrich
Nuclei EZ prep kit	Sigma-Aldrich
Nycodenz AG	Invitrogen
One Shot® Top10 competent cells	Invitrogen
Oligo(dT) 12-18 Primer	Promega
PCR Thermowell Tubes	Fisher
Penicillin, Ampicillin	GIBCO/BRL
Pac I	New England

Product	Company
Phenol/Chloramform/Isomyl Alcohol(25:24:1)	Sigma-Aldrich
Plasmid DNA Spin Miniprep Kit	Qiagen
Polyd(I-C)	GE health care
Polaroid Film Type 667	Fisher
Ponceau S solution	Sigma-Aldrich
Pronase	Roche
Protein assay kit	Bio-Rad
Proteinase inhibitor	Invitrogen
Proteinase K	Invitrogen
QIAGEN Plasmid Mini Kit	Qiagen
QIAquick PCR Purification	Qiagen
Rainbow protein marker	Amersham
RNaseOut Rnase Inhibitor	Invitrogen
RNase, DNase-free	Roche
RNeasy Plus Mini Kit	Qiagen
Staurosporine	Sigma
Sodium pyruvate	Sigma
T4 DNA ligase	Promega
T4 polynucleotide kinase	Invitrogen
Taq DNA Polymerase	Qiagen
The BLOCK-iT™ Adenoviral RNAi Expression System	Invitrogen
Trichloroacetic Acid	VWR
Tris Base	Sigma-Aldrich
Tween-20	Sigma
U0126	Promega
Western Blot Membrane	Fisher

2. Methods

2.1 Animal model of liver fibrosis

Male Sprague–Dawley rats (450-550gram body weight) were purchased from Central Animal Breeding Facility of the University of Manitoba and maintained under temperature controlled conditions (22-28°C) and an artificial 12 hrs light/dark cycles with food and water ad libitum. In conducting the research described in this thesis, all animals received humane care in compliance with the Institution's guidelines (animal protocol no.98–053), which is in accordance with the Canadian Council on Animal Care's criteria.

Rats were randomly divided into bile duct ligation (BDL) and sham surgery groups. After being anesthetized with pentobarbital, the common bile duct of rats was exposed by median laparotomy and occluded by double ligature with a non-resorbable suture (7-0 silk). The first tie was made below the junction of the hepatic ducts and the second was made above the entrance of the pancreatic ducts (Ackerman, Karmeli et al., 1996). The common bile duct was cut completely between these two ties. For sham-operated rats, laparotomy was performed but the common bile duct was neither ligated nor cut.

Following surgery, rats were kept in individual cages until being sacrificed at 1, 2, 3, 4, 5, and 6 weeks, respectively. At the end of the experiment, the common BDL was confirmed to be intact with proximal dilatation of the common bile duct. Liver tissue was collected. Sectors of the liver were immediately frozen in liquid nitrogen and stored at -70°C for subsequent determination.

2.2 Isolation of rat hepatic stellate cells

Hepatic stellate cells were isolated from rat liver by two steps of collagenase and pronase methods (Shen, Zhang et al., 2002). The liver was perfused via the portal vein first with Ca^{2+} free Hanks' balanced salt solution (HBSS), pH7.4, for 10 minutes at 37°C and then with Ca^{2+} HBSS containing 0.125 mg/ml collagenase D, 0.5 mg/ml pronase and 15 μg/ml DNase 1 for 20 minutes. After being dispersed gently, cells were incubated with 0.025mg/ml collagenase D, 1 mg/ml pronase, 15 μg/ml DNase 1 and 1 mg/ml BSA for another 12 minutes with constant low speed stirring at 37°C.

The cell suspension was filtered through a 100μm mesh. After removing hepatocytes by centrifugation at 480*g* using a bench-top centrifuge, Hepatic stellate cells were separated from other non-parenchymal cells by density gradient centrifugation on 11.3 % Nycodenz with sodium chloride at 1500g for 17 minutes at 4°C. Hepatic stellate cells were harvested from the interface between suspension buffer on the top and 11.3% Nycodenz solution, and then cultured on uncoated plastic tissue culture dishes (Costar) at a density of 25,000 cells/cm^2. Hepatic stellate cells were identified by the typical star-like configuration under light microscopic appearance. Purity was always greater than 95%.

Hepatic stellate cells were incubated in DMEM supplemented with 10% FBS, antibiotics (100 IU/ml penicillin and 100 mg/ml streptomycin) and 2mM L-glutamine at 37°C in a humidified atmosphere of 5% CO_2. The first change of culture medium was made 24 hrs after seeding and then changes were made every 48 hrs.

2.3 Cell line and culture conditions

2.3.1 Rat hepatic stellate cell line-T6 cells

Rat HSC line-T6 cells was the generous gift of Dr. Scot Friedman (Mount Sinai School of Medicine, NY, USA). T6 cells were maintained in DMEM supplemented with 10% fetal bovine serum, 4.5g/l glutamine, 100 IU/ ml penicillin, 100mg/ml streptomycin, and 2mmol/l L-glutamine at 37°C in a humidified atmosphere of 5% CO_2 and 95% air. Cells were sub-cultured in 10cm culture dishes for experiments. One day before addition of BMP4, culture medium was removed and cells were incubated with DMEM with 0.01% FBS for the rest of experiments.

T6 cells were derived from healthy male Sprague-Dawley rat hepatic stellate cells and immortalized through infecting a temperature-sensitive mutant SV40. With regard to the expression of retinoid-related proteins, T6 cells resemble more quiescent hepatic stellate cells as found *in vivo* or in primary culture rather than an activated stellate cell.

2 3.2 Rat hepatic stellate cell lines-CFSC-8B, CFSC-2G, CFSC-3H, and CFSC-5H

CFSC-8B, 2G 3H, and 5H (cirrhotic fat-storing cell-8B, 2G, 3H and 5H) were kindly provided by Dr. Marcos Rojkind (The George Washington University, DC). Cells were cultured in MEM supplemented with 1% non-essential amino acids, 10% FBS, 100U/ml penicillin and 100μg/ml streptomycin at 37°C in a humidified atmosphere of 5% CO_2 and 95% air. Cells were sub-cultured in 10 cm culture dishes for experiments. One day before treatment, culture medium was removed and cells were incubated with serum-free MEM. CFSC cell lines were originally isolated from cirrhotic rat liver and used as

an *in vitro* model for activated HSCs based on their expression levels of collagen I and TIMP1. (Schaefer, Rivas-Estilla et al., 2003).

2.3.3 Rat hepatic stem cells-WB-F344 cells

WB-F344 cells were kindly provided by Dr. William B. Coleman (The University of North Carolina at Chapel Hill, Chapel Hill, NC). Cells were cultured in MEM with 50% increased concentrations of essential and non-essential amino acids, and supplemented with 110 mg/l sodium pyruvate, 10 mM HEPES, 10% FBS, 100U/ml penicillin and100μg/ml streptomycin at 37°C in a humidified atmosphere of 5% CO_2 and 95% air. Only the cells at passages 11~22 were used throughout the study. Cells were sub-cultured in 10cm culture dishes for experiments. One day before treatment, culture medium was removed and cells were incubated with medium described above supplemented with 5% charcoal stripped FBS.

WB-F344 cell line was isolated and cloned from the liver of a young adult male Fischer 344 rat and established as an immortalized cell line under conditions that excluded differentiated hepatocytes or biliary epithelial cells. They were genetically tagged with the *E. coli* lac Z gene (β-galactosidase) by infection with the CRE BAG2 retrovirus. WB-F344 cells are diploid, anchorage-dependent, express contact inhibition *in vitro*, and are not tumorigenic.

2.3.4 Human kidney cells-293A cells

Human kidney cell line - 293A cells was purchased from Invitrogen (Carlsbad, CA) and maintained in DMEM supplemented with 10% FBS, 100 IU/ml penicillin, 100 mg/ml

streptomycin, and 2mmol/l L-glutamine at 37°C in a humidified atmosphere of 5% CO_2 and 95% air.

The 293 cell line is a permanent cell line established from primary embryonic human kidney transformed with sheared human adenovirus type 5 DNA (Graham, Smiley et al., 1977; Harrison, Graham et al., 1977). The 293A cell line is a subclone of the 293 cell line. It can supply the E1 proteins as trans factors that are required for the expression of adenoviral late genes, with which adenovirus can replicate. The cells exhibit a fatted morphology, enabling easier visualization of viral plaques.

2.4 Cell co-culture

The co-culture of hepatic stem cells with hepatic stellate cells was employed to investigate the effect of hepatic stellate cells on hepatic stem cell differentiation. A mixture of hepatic stem cells ($1X10^4$ cells) and hepatic stellate cells ($1X10^3$ cells) was seeded in a 35mm well and cultured in the serum free standard hepatic stem cell culture medium with medium changes every 2~3 days. The mixture of cells was cultured for 1 week.

2.5 Microphotography

Cells were imaged and photographed on an Olympus inverted-phase microscope (CK-40) using a mounted Olympus 35-mm camera (Carsen Group, Markham, ON, Canada) and TMAX400 Kodak black-and-white film (Eastman Kodak, Rochester, NY).

2.6 RNA isolation

Total RNA was extracted from liver tissues and cells using TRIzol® Reagent according to the manufacturer's instructions (Invitrogen, Carlsbad, CA, USA). RNA was eluted in RNase-free water and the concentration was determined by using a spectrophotometer (Bio-Rad SmartSpec 3000 Spectrophotometer, Life Science Research Division, Mississauga, ON). Good quality RNA had an $A_{260/280}$ ratio of 1.8 to 2. Working stocks of 1μg/μl RNA in RNase-free water were prepared and used for all RT-PCR reaction. RNA was stored at -70°C.

2.7 Reverse transcription polymerase chain reaction (RT-PCR)

The first-strand cDNA was synthesized by an Advantage RT-for-PCR kit (CLONTECH, Palo Alto, CA). Briefly, 1μg of total RNA was dissolved in diethylpyrocarbonate (DEPC)-treated doubled-distilled water (ddH_2O) to achieve a final volume of 12.5μl. Subsequently, 1μl oligo(dT) primer, 4μl 5X reaction buffer, 1μl 10mmol/l dNTP mix, 0.5μl recombinant RNase inhibitor, and 1μl Moloney murine leukemia virus reverse transcriptase were added and incubated for 1 hr at 42°C. At the end of reverse transcription, the reaction mixture was heated to 94°C for 5 minutes to denature reverse transcriptase and brought up to a final volume of 100μl with DEPC-H_2O.

PCR reactions were performed using Taq DNA Polymerase kit (Qiagen, Mississauga, ON). Taq DNA Polymerase is a high quality recombinant polymerase originally isolated from *Thermus aquaticus*, and expressed in *E. coli*. This kit includes two unique PCR buffers. QIAGEN PCR Buffer contains both KCl and $(NH_4)_2SO_4$ providing a wide

annealing temperature window and tolerance to variable Mg^{2+} concentration. Q-Solution facilitates amplification of difficult templates by modifying the melting behavior of DNA.

A typical 50µl PCR reaction was setup as seen in Table 8. Primers were designed using Oligo5 program according to the DNA sequence and synthesized by Invitrogen (Invitrogen, Burlington, ON). PCR reactions were performed in an Eppendoff MasterCycler (Eppendoff, Westbury, NY). The cycling conditions were as follows: initial denaturation at 95°C for 5 minutes, followed by 25 to 38 cycles of denaturation at 95°C for 1 minute, annealing for 45 seconds at different annealing temperatures listed in Table 9, extension at 72°C for 90 seconds, and then followed by 10 minutes of final extension at 72°C. PCR products were analyzed by electrophoresis in a 1.2% agarose gel. Identity of PCR products was confirmed by sequencing at DNA sequencing facility of Manitoba Institute of Cell Biology.

Table 8 Components for one PCR reaction

Component	Volume (µl)
cDNA template	5
10X PCR Buffer	5
5X Q Buffer	10
25mM $MgCl_2$	4
dNTP mix (10 mM each)	1
Forward Primer	1
Reverse Primer	1
Taq DNA Polymerase	0.4
RNase-free Water	22.6

2.8 Protein isolation

2.8.1 Nuclear protein

Cell nuclear protein was isolated by Nuclei EZ prep kit (Sigma-Aldrich, Okaville ON). Cells were washed with ice-cold PBS two times. After aspirating the PBS, 800µl of ice cold Nuclei EZ lysis buffers was added to lyse cells. Cells were then harvested by thoroughly scraping the dish with a small bladed cell scraper. Cell lysates were set on ice for 5 minutes and then centrifuged at 500Xg for five minutes at 4°C. The supernatant was carefully aspirated and the nuclei pellet was set on ice. The nuclei pellet was then washed with 400µl of ice-cold Nuclei EZ lysis buffers as described above. Finally, the nuclei pellet was resuspended in 200µl of ice-cold Nuclei EZ storage buffer supplemented with 2µl protease inhibitor cocktail (Sigma-Aldrich, Oakville ON). The nuclei fraction was stored at -70°C. The nuclear protein concentration was determined by the BCA (PIERCE, Rockford, IL) assay. Appropriate amount of nuclear proteins was subjected to western blot analysis and DNA and protein binding reaction experiments.

2.8.2 Whole cellular protein

For isolation of whole cellular protein from liver tissues, 100mg liver tissue was homogenized in 2ml ice-cold lysis buffer (50 mM Tris pH8.0, 0.5mM EDTA, 150mM NaCl, 0.5% NP-40 and 20µl protease inhibitor cocktail) by a power Brinkman homogenizer (Brinkman Instrument, Westbury, NY). Following homogenization, the insoluble material in the homogenate was removed by centrifugation at 12,000X *g* for 10 minutes.

Table 9 Primers, condition of polymerase chain reaction and siRNA sequence.

Gene		Primers	Temperature (℃)	Size (bp)
Albumin	sense	5'-ACCAGGCCACTATCTCCAGCA-3'	60	1040
	anti-sense	5'-CGCCTTCAGCACAGCACTTCTC-3'		
G6Pase	sense	5'-ATCGGGAGGAGGGGGAGTGTTTGG-3'	60	332
	anti-sense	5'-CAGCAGCGTGGTCAGGGAAGCAGT-3'		
Tyrosine Aminotransferase	sense	5'-GAGAAGCAGAAGACGGAGGAT-3'	54	431
	anti-sense	5'-CTACGAGAAGACAAGGAGGAAGAT-3'		
Cytokeratin 19	sense	5'-CGCTTTGGGTCAGGGGGTGTTTTC-3'	63	168
	anti-sense	5'-CAGCAGCCCATCGGTCACAGTCA-3'		
Integrin β4	sense	5'-GGAAATACTGTGCCTGCTGC-3'	60	749
	anti-sense	5'-GTGATGTTTACCAGGCGTCG-3'		
BMPRII	sense	5'-GCTAACTGGAAATCGGCTGGTG-3'	59	506
	anti-sense	5'-GCATAGCAGTTGACATTGGGTTGA-3'		
BMPR1A	sense	5'- TGAAGAAAGCAGCAGGTGAAAG-3'	56	190
	anti-sense	5'-GAA CAGACAGGCTCCCAGTAATCT-3'		
BMP4	sense	5'-CCTTTCCAGCAAGTTTGTTCAA-3'	60	1368
	anti-sense	5'-GTGGTCGGATGGGCTTTGT-3'		
BMP4	sense	5'-CCCTGGCTCTGCTCTTCT TC-3'	59	587
	anti-sense	5'-CCCTGGCT CTGCTCTTCTTC-3'		
GAPDH	sense	5'-GGGATGGAATTGTGAGGGAGATG-3'	64	981
	anti-sense	5'-TGATGCTGGTGCTGAGTATGTCGT-3'		
BMP4 si RNA	sense	5'-CACCGGATTACATGAGGGATCTTTACGAATAAAGATCCCTCATGTAATCC-3'		
	anti-sense	5'-AAAAGGATTACATGAGGGATCTTTATTCGTAAAGATCCCTCATGTAATCC-3'		
Non-silencing siRNA	sense	5'-CACCGTTCTCCGAACGTGTCACGTCGAAACGTGACACGTTCGGAGAA-3'		
	anti-sense	5'-AAAATTCTCCGAACGTGTCACGTTTCGACGTGACACGTTCGGAGAAC-3'		

For isolation of whole cellular protein from cells, after washing with ice-cold PBS two times, 600μl cold lysis buffer was added directly in the culture dish. Cells were harvested by thoroughly scraping the dish with a small bladed cell scraper. The insoluble material from the lysate was removed by centrifugation at 12,000X *g* for 10 minutes.

Protein concentration was determined by the BCA (PIERCE, Rockford, IL) assay. For liver tissues, working stocks of 5μg/μl protein in lysis buffer were prepared. Reconstituted protein samples were aliquoted into 500μl fractions. Protein samples were stored at -70°C. Appropriate amount of proteins was subjected to western blot analysis.

2.9 Western blot analysis

Different amount of total protein was employed to detect different target proteins in western blot analysis (Table 11). Proteins of samples were boiled for five minutes in 4X gel loading buffer (250mmol/l Tris-HCl, pH=6.8,0.8% sodium dodecyl sulfate (SDS), 20% glycerol, 0.2% bromophenol blue and 5% β-mercaptoehanol). The purpose of this step was to denature and unfold the proteins. The SDS surrounded the protein with a negative charge and the β-mercaptoethanol prevented the reformation of disulfide bonds. Then the proteins were separated completely according to the molecular weight using sodium dodecyl sulfate-polyacrylamide gel electrophoresis (SDS-PAGE). The choice of the percent gel was based on the molecular weight of proteins (Table 10). Once separated, proteins were electrophoretically transferred to a Nitroplus-2000 membrane (Micron Separations Inc., Westborough, MA). Nonspecific antibody binding was blocked by pre-incubation of the membranes in TBS-T solution (Tris-buffered-saline-Tween, 2.42g Tris base, 29.25g NaCl, and 1ml Tween 20 per liter) containing 5% skim milk for 1 hr at room temperature. This blocking step can eliminate false positives and

lead to clearer results. After blocking, membranes were then incubated overnight at 4°C with appropriated primary antibodies at different dilutions in TBS-T solution containing 2% skim milk (Table 11). After washing the membranes with TBS-T to remove unbound primary antibody, the membranes were subsequently incubated with donkey anti-rabbit IgG or sheep anti-mouse IgG at 1:1,000 dilutions for 1 hr at room temperature. The second antibody is linked to a reporter enzyme, horseradish peroxidase, which converts a luminol substrate to a light releasing substance in proportion to the amount of protein. The protein-antibody complexes were detected by enhanced chemiluminescence kit (ECL system, GE health care) according to the manufacturer's instruction and the densitometry of the bands was determined by using ImageJ program.

Table 10 The choice of the percent gel based on the molecular weight of proteins

Gel percentage (%)	Protein size (kDa)
20	4~40
15	12~45
12.5	10~70
10	15~100
8	25~200

2.10 Electrophoretic Mobility Shift Assay (EMSA)

The EMSA is a common technique to study protein-DNA interaction *in vitro*. The interaction of proteins with DNA regulates DNA replication, DNA recombination, and DNA repair. In addition, it also regulates transcription of gene expression. The technique is based on the fact that protein: DNA complexes migrate more slowly than free DNA molecules when they are electrophoresized on non-denaturing polyacrylamide gel.

The consensus double-strand oligodeoxynucleotide probes for C/EBP (Table12) (Santa Cruz Biotechnology, Santa Cruz, CA) were radiolabeled using [γ-^{32}P]-ATP (GE Healthcare, Pittsburgh, PA) and T4 polynucleotide kinase (Invitrogen, Burlington, ON). T4 polynucleotide kinase possesses a 5' polynucleotide kinase and a 3' phosphatase activity. The enzyme converts transfer of a phosphate of ATP at γ-position to the 5' hydroxyl group of DNA. A typical labeling reaction was set up as seen in Table13.

Table 11 Antibody and condition of western blot analysis

Primary antibody	Type	Host	Total proteins used (μg)	Working dilution	Source
β-actin	Monoclonal	Mouse	10	1:2000	Sigma-Aldrich (Okaville, ON)
GAPDH	Monoclonal	Mouse	20	1:2000	IMGENEX (San Diego, CA)
Histon H1	Monoclonal	Mouse	50	1:2000	Santa Cruz (California, CA)
α-SMA	Monoclonal	Mouse	10	1:2000	Sigma-Aldrich (Okaville, ON)
BMP4	Monoclonal	Mouse	40	1:1000	Santa Cruz (Santa Cruz, CA)
ERK1	Polyclonal	Rabbit	10	1:2000	Santa Cruz (Santa Cruz, CA)
p-ERK1/2	Polyclonal	Rabbit	40	1:500	Santa Cruz (Santa Cruz, CA)
p38	Monoclonal	Mouse	60	1:500	Santa Cruz (Santa Cruz, CA)
p-p38	Monoclonal	Mouse	60	1:500	Santa Cruz (Santa Cruz, CA)
JNK1	Monoclonal	Mouse	60	1:500	Santa Cruz (Santa Cruz, CA)
p-JNK1/2	Polyclonal	Rabbit	40	1:1000	R&D System (Minneapolis, MN)
Smad1	Polyclonal	Rabbit	60	1:1000	Upstate (Hornby, ON)
p-Smad1	Polyclonal	Rabbit	60	1:1000	Upstate (Hornby, ON)
C/EBPα	Polyclonal	Rabbit	40	1:500	Santa Cruz (Santa Cruz, CA)
Albumin	Polyclonal	Rabbit	60	1:500	Immunology Consultants Lab (Newberg,OR)

After centrifugation, reaction mixture was incubated at 37°C for 10 minutes and then was stopped by adding EDTA to a final concentration of 5mM. Radiolabeled probes were purified by passing reaction mixture through a G-25 Sephadex Column (Roche Laval, QC) to remove free [γ-^{32}P]-ATP. TE buffer (90µl) was added to reaction mixture. The final concentration of radiolabeled probes is 0.05pmol/µl.

For EMSA, 6µg of nuclear protein was preincubated in a reaction mixture consisting of 1µg of poly (dI-dC) (GE health care), and appropriate amount of 5X binding buffer (20% glycerol, 5mM $MgCl_2$, 2.5mM EDTA, 2.5mM DTT, 250mM NaCl, and 50mM Tris-HCl pH7.5) for 15 minutes on ice to block nonspecific binding. Radiolabeled probes (0.2 pmol) were than added and incubated for 20 minutes at room temperature (Table 14).

Specificity of the EMSA was tested by competition experiment in which a 100 mol excess of unlabeled wild-type or mutated oligonucleotide was added to the reaction mixture and preincubated for 20 minutes at room temperature before the addition of oligonucleotides. Supershift analysis was performed by adding 2mg antibody against C/EBPα and incubated for 20 minutes at room temperature before the addition of oligonucleotides (Table 14).

Resulting protein/DNA complexes were separated on a 4% polyacrylamide gel (6.7ml of 30% polyacrylamide, 1.25ml of 2% bi-acrylamide, 2ml of 10XTBE, 150ul of 20% APS, 30ml of water, and 34ul of TEMED) in 0.5XTBE buffer. Gel was pre-run at 100v for 30 minutes and then samples were mixed with 10Xgel loading buffer (250mM Tris-HCl (pH 7.5), 0.2% bromophenol blue, 40% glycerol) and run on a gel for 3 hrs at 200V at 4°C. The gel was dried under vacuum for 2 hrs at 50°C using Slab Gel Dryer-

2000 (Fisher Scientific Limited) and exposed to X-ray film (Kodak Biomax XAR film) for 3~6 days.

Table 12 Oligodeoxynucleotide probes for C/EBP

C/EBP Consensus Oligonucleotide
(binding site for CCAAT enhancer binding proteins)
5' – TGC AGA TTG CGC AAT CTG CA – 3'
3' – ACG TCT AAC GCG TTA GAC GT – 5'
C/EBP Mutant Oligonucleotide
(an eight base pair substitution in the binding motif)
5' – TGC AGA **GAC TAG TC** T CTG CA – 3'
3' – ACG TCT **CTG ATC AG** A GAC GT – 5'

Table 13 Components for one labeling reaction

Component	**Volume (µl)**
Dephosphorylated DNA fragments	5pmol
5X Forward Reaction Buffer	5µl
T4 Polynucleotide Kinase	10units
[γ-^{32}P]ATP (10 µCi/ µl)	2.5µl
Rnase-free water	to 25µl

Table 14 Components for EMSA reactions

Reaction 1: Negative control group

Component	Volume (µl)
Gel Shift 5X Binding Buffer	4µl
Nuclear Protein	0µg
Radiolabeled probe	1µl
Poly (dI-dC)	1µg
Nuclease-free Water	to 20µl

Reaction 2: Experiment group

Component	Volume (µl)
Gel Shift 5X Binding Buffer	4µl
Nuclear Protein	6µg
Radiolabeled probe	1µl
Poly (dI-dC)	1µg
Nuclease-free Water	to 20µl

Reaction 3: Competition or supershift group

Component	Volume (µl)
Gel Shift 5X Binding Buffer	4µl
Nuclear Protein	6µg
cold or mutant oligo or antibody	20pmol/2mg
Poly (dI-dC)	1µg
Radiolabeled probe	1µl
Nuclease-free Water	to 20µl

2.11 Cell proliferation

Cell proliferation is the measurement of number of cells that are dividing in culture. Since DNA synthesis is closed related to cell division, measurement of DNA synthesis can be used to assess cell proliferation. The labeled DNA precursors (^{3}H-thymidine) can incorporate into DNA during DNA replication. The incorporation is directly proportional to amount of cell division in the culture. However, the incorporation might also represent DNA repair and possibly RNA synthesis. Therefore, another indicator such as metabolic activity of viable cells can also be used to determine cell proliferation. Increase in number of viable cells results in an increase in overall activity of mitochondrial dehydrogenases, which can cleave WST-1 (a proliferating reagent from Roche) to form a formazan dye. The amount of formazan dye is directly correlated to number of metabolically active cells in the culture. The disadvantage of this method is sometimes increase in the enzyme activity is a result of gene expression. Direct cell counting offers the most direct method to determine cell proliferation and it can also provide direct cell doubling time, which is calculated according to the following formula (Gong, Deng et al., 2002).

Doubling time= t x log 2/ logNt/Ni

t= time between the count

Nt= cell number at day 6

Ni= cell number at day 2

2.11.1 ^{3}H Thymidine incorporation assay

Cells ($5X10^{4}$) were seeded onto 6-well plates. After 24 hrs of quiescence in serum free medium, cells were treated with BMP4 (R&D System, Minneapolis MN) at the indicated concentrations and time points, and cultured in culture medium supplemented with 2% FBS. Culture medium was changed every other day. At the end of experiment, cells were incubated with 1μCi [^{3}H] thymidine (GE health care) for 4 hrs at 37C°. Then the medium was aspirated and cells were washed with PBS two times. Cells were subsequently fixed with 10% trichloroacetic acid (Sigma-Aldrich, Okaville ON) for 10 minutes at room temperature. After washing the cells with PBS, the lysis solution (0.3 M NaOH and 1%SDS) was added into the culture dishes to lyse cells with gently shaking for 2 hrs. Finally, 50μl of cell lysate was added into liquid scintillation solution (Ultima Gold; Packard Bioscience), and activity of ^{3}H in each sample was measured by use of a liquid scintillation detector (1217 Rackbeta; Wallac Oy) equipped with Utmac 1.1 (Wallac Oy) software.

2.11.2 WST-1

Cells ($4X10^{3}$) were seeded into 96-well plates. After 24 hrs of quiescence in serum free medium, cells were treated with BMP4 (R&D System, Minneapolis MN) at the indicated concentrations and time points, and cultured in 100μl culture medium supplemented with 2% FBS. Culture medium was changed every other day. At the end of experiment, 10μl of cell proliferation reagent WST-1 was added into each well and incubated the cells for 3 hrs at 37C°. Then the plate was placed on a shaker to thoroughly

shake for 1 minute. Absorbance was measured using ELx 808 microplate (ELISA) reader (Bio-TEK Instruments, Winooski, VT). Wavelength for measuring the absorbance of the formazan product is 490nm and the reference wavelength is 600nm.

2.11.3 Cell counting

Cells ($5X10^4$) were seeded into 6-well plates. After 24 hrs of quiescence in serum free medium, cells were treated with BMP4 (R&D System, Minneapolis MN) at the indicated concentrations and time points, and cultured in culture medium supplemented with 2% FBS. Culture medium was changed every other day. At the end of experiment, cells were trypsinized with 1ml 0.25% trypsin at 37°C for 2~3 minutes until cells detached completely from the plate. Cell numbers were counted in triplicate using an electronic Couler Cell Counter (model ZM, Coulter Electronics Ltd).

2.12 Cell apoptosis detection

Cell apoptosis was detected using a Annexin V Apoptosis Detection Kit (BioVision, Mountain View, CA). This method is based on the observation that after initiating apoptosis, cells translocate the membrane phosphatidylserine (PS) from the inner face of the plasma membrane to the cell surface. Once on the cell surface, PS can be easily detected by staining with a fluorescent conjugate of Annexin V, a protein that has a high affinity for PS. 7-Amino-actinomycin D (7-AAD) (Sigma-Aldrich, Okaville ON) can only incorporated into late apoptotic or necrotic cells which have lost membrane integrity.

Therefore, Annexin V-PE staining identifies apoptosis at an earlier stage (Annexin V-PE positive, 7-AAD negative), whereas cells at late stage of apoptosis or necrosis show both Annexin V-PE and 7-AAD positive.

Cells ($2X10^5$) were seeded onto 6-well plates. After treatment with the apoptosis inducer staurosporine at the indicated concentrations and time points, the medium was collected and attached cells were trypsinized with 0.5ml 0.25% trypsin at 37°C for 2~3 minutes until cells detach completely from the bottom. The trypsinized cells were combined with medium and subjected to centrifugation at 480*g* for 5 minutes. After discarding the supernatant, the cell pellet was resuspended in 500µl binding buffer (10 mM Hepes /Na OH (pH 7.4), 140mM NaCl, and 2.5mM $CaCl_2$). Five microlitres of Annexin V-Cy3 and 1µl 7-AAD (1mg/ml) were added to the resuspended cells. The cells were incubated at room temperature for 15 minutes in the dark. Cell apoptosis was detected by analyzing the Annexin V-Cys binding and the 7-AAD incorporating using a Beckman Coulter EPICS ALTRA Flow Cytometer (Beckman Coulter Canada Inc., Mississauga).

2.13 Construction of recombinant adenovirus (short hairpin RNA (shRNA))

Recombinant adenovirus containing oligonucleotide encoding shRNA to rat BMP4 was constructed using BLOCK-iT™ Adenoviral RNAi Expression System kit (Invitrogen, Carlsbad, CA).

2.13.1 Structural features of shRNA and oligonucleotide encoding shRNA

Oligonucleotide encoding shRNA can be cloned into expression vectors to express siRNA (19-21nt RNA duplex) for RNA interference studies. shRNA has the following structural features: A short nucleotide sequence ranging from 19-29 nucleotides derived from the target gene, followed by a short spacer of 4-15 nucleotides (i.e. loop) and a 19-29 nucleotide sequence that is the reverse complementary to the initial target sequence. Oligonucleotide encoding shRNA against rat BMP4 was designed using the software - BLOCK-iT™ RNAi Designer (Invitrogen, Carlsbad, CA). Three oligonucleotide sequences were selected to examine their effects on knocking down BMP4 gene expression (Table 15). CACC was added to the 5' end of the top strand oligonucleotide and AAAA was added to the 5' end of the bottom strand oligonucleotide. The purpose of adding these two 4 nucleotides is to enable directional cloning of the double-stranded oligonucleotide into vector.

Table 15 Oligonucleotides encoding shRNA against rat BMP4

Select	No.	Start	Oligo Type	Oligo Sequence
☑	1	640	Top Strand	5'- CACCGGATTACATGAGGGATCTTTACGAATAAAGATCCCTCATGTAATCC -3'
			Bottom Strand	5'- AAAAGGATTACATGAGGGATCTTTATTCGTAAAGATCCCTCATGTAATCC -3'
			ds Oligo	5'- CACCGGATTACATGAGGGATCTTTACGAATAAAGATCCCTCATGTAATCC -3' 3'- CCTAATGTACTCCCTAGAAATGCTTATTTCTAGGGAGTACATTAGGAAAA -5'
☑	2	924	Top Strand	5'- CACCGCTTCCACCGTATAAACATTTCGAAAAATGTTTATACGGTGGAAGC -3'
			Bottom Strand	5'- AAAAGCTTCCACCGTATAAACATTTTTCGAAATGTTTATACGGTGGAAGC -3'
			ds Oligo	5'- CACCGCTTCCACCGTATAAACATTTCGAAAAATGTTTATACGGTGGAAGC -3' 3'- CGAAGGTGGCATATTTGTAAAGCTTTTTACAAATATGCCACCTTCGAAAA -5'
☑	3	1297	Top Strand	5'- CACCGCGCTCCAGGAAGAAGAATAACGAATTATTCTTCTTCCTGGAGCGC -3'
			Bottom Strand	5'- AAAAGCGCTCCAGGAAGAAGAATAATTCGTTATTCTTCTTCCTGGAGCGC -3'
			ds Oligo	5'- CACCGCGCTCCAGGAAGAAGAATAACGAATTATTCTTCTTCCTGGAGCGC -3' 3'- CGCGAGGTCCTTCTTCTTATTGCTTAATAAGAAGAAGGACCTCGCGAAAA -5'

https://rnaidesigner.invitrogen.com/rnaiexpress/

2.13.2 Generation of double-stranded oligonucleotides

The complementary single-stranded DNA oligonucleotides were synthesized by Invitrogen (Invitrogen, Burlington, ON) and double-stranded oligonucleotides were generated in the laboratory. Annealing reaction was set up as seen in Table 16. Equal amounts of single-stranded complementary oligonucleotides were mixed with 10X oligo annealing buffer (100mM Tris-HCl pH 8.0, 10mM EDTA pH8.0 and 1M NaCl).and incubated at 95°C for 4 minutes in a heating block (Isotemp*125D heating block, Fisher Scientific Limited, Nepean, ON). The heating block was then turned off allowing the temperature cool down slowly to room temperature for 1 hr. The single-stranded oligonucleotides were annealed to form double-stranded oligonucleotides during this time. Final concentration of the oligonucleotide mixture is 50µM. Integrity of the annealed double-stranded oligonucleotides was verified by electrophoresing on 4% agarose gel. Appropriate concentration of oligo (5nM) was made in 1X oligo annealing buffer for further ligation reaction and stored at -20°C.

Table 16 Components for annealing reaction

Component	Volume (µl)
Top strand DNA oligo (200µM)	5µl
Bottom strand DNA oligo (200µM)	5µl
10X Oligo Annealing Buffer	2µl
DNAase/Rnase Free Water	8µl
Total volume	20µl

2.13.3 Ligation reaction

Double-stranded oligonucleotides were cloned into the linearized pENTR™/U6 vector (Figure 9). Ligation reaction was set up at room temperature according to the Table 17. Reaction solution was mixed by pipetting up and down and incubated for 2 hrs at room temperature, where T4 DNA ligase forms a phosphodiester bond between juxtaposed 5'-phosphate and 3'-hydroxyl termini in duplex DNA or RNA with blunt or cohesive-end termini. Reaction solution was then used to transform One Shot® Top10 competent cells.

Table 17 Components for ligation reaction

Component	Volume (µl)
5X Ligation Buffer	4µl
pENTR™/U6 (0.5ng/µl)	2µl
ds Oligo (5nM)	1µl
Dnase/Rnase-Free Water	12µl
T4 DNA Ligase (1U/µl)	1µl
Total volume	20µl

2.13.4 Bacterial transformation

Ligation reaction (10µl) was mixed gently with 50µl One Shot® Top10 competent cells, incubated on ice for 30 minutes and then subjected to heat shock for 30 seconds at 42°C. After heat shocking, reaction mixture was immediately put on ice and then the reaction mixture was incubated in a shaking incubator (C_{24} incubator shaker, New Brunswick Scientific, NJ) at 37°C for 30 minutes (200rpm) after addition of 250µl room

temperature SOS medium (Invitrogen, Burlington, ON). After shaking incubation, the solution (100µl) was spread on a pre-warmed LB agar plate containing 50µg/ml kanamycin and the plate was incubated overnight in a 37°C incubator (Precision incubator, Precision Scientific Inc., Chicago, IL).

2.13.5 Plasmid DNA isolation

Plasmids are non-obligate, circular, extrachromosomal bacterial replicons. Plasmid DNA isolation requires separation of this DNA from the chromosomal DNA in the bacterial cell as well as from the polysaccharides, lipids and proteins. In the experiment, an alkaline lysis method was used to isolate plasmid DNA. Bacteria were lysed by strong alkali (NaOH). After lysis of bacteria, proteins and chromosome DNA were precipitated by high salt solution (NH_4OAC) and detergent (SDS). Since plasmid was relatively small and stable in alkali solution, it remained in the solution and was separated from proteins and chromosome DNA after centrifugation. A single kanamycin-resistant colony was picked up and cultured in 2ml LB containing 50µg/ml of kanamycin at 37°C with vigorous shaking (300rpm) overnight. Bacteria were centrifuged at 1350g for 15 minutes. Bacteria pellet was resuspended in 100µl of ice-cold suspension solution (50mM glucose, 25mM Tris-Cl, pH 8.0, and 10mM EDTA pH 8.0) by pipetting up and down. Alkaline solution (200µl) (0.2N NaOH and 1% SDS) was freshly prepared and added into bacterial suspension. The solution was mixed by inverting the tube gently 5 times and incubated on ice for 5 minutes. High salt solution (150ul) (3.0 M NaOAc, pH 5.0) was added into the tube and was mixed thoroughly by inverting the tubes 4–6 times to ensure complete precipitation. (Be careful, the pAd/BLOCK-^{iT}TM-DEST plasmid is large and excessive manipulations can shear the DNA.) Proteins and chromosome DNA were precipitated by

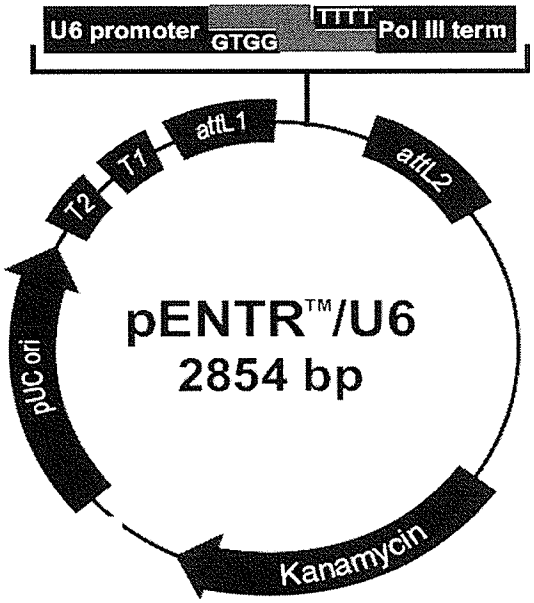

Figure 9 *pENTR™/U6 vector cited from Invitrogen web page.* Expression of the oligonucleotide is driven by human U6 promoter, which can transcribe small RNAs by RNA polymerase III and this transcription is terminated when polymerase meets Pol III terminator. The pENTR™/U6 vector contains attL1 and attL2 sites, which are bacteriophage λ-derived recombination sequences and allow recombinational cloning of oligonucleotides in the pENTR™/U6 vector to recombinant expression acceptor vector. The pENTR™/U6 vector also possesses a kanamycin resistance gene, which allows selection of the recombinant vector in *E. coli*. In addition, there are three sequencing primer sites for convenient sequencing purpose - U6 forward priming site, M13 forward primer site and M13 reverse primer site.

incubation of the tube on ice for 5 minutes. Plasmid DNA was separated by centrifugation at 10,000g for 15 minutes. The supernatant containing plasmid was transferred to a new eppendorf tube. Phenol: chloroform: isoamylalcohol (25:24:1) (400µl) was added into the supernatant to extract DNA. The solution was mixed by inverting the tubes for 2 minutes and centrifuged at 10,000g for 5 minutes. Aqueous layer was transferred to a new eppendorf tube and plasmid DNA was precipitated with addition of two volumes of 100% ethanol and incubated at -70°C for 2 hrs. After centrifugation of plasmid DNA at 10,000g for 8 minutes at 4°C, DNA pellet was washed with 70% ethanol twice, air dried for 15 minutes and redissolved in 20µl of TE buffer containing 0.2µl of 100µg/ml DNase-free RNase (Roche Mississauga, ON). The concentration of plasmid DNA was determined using a spectrophotometer (Bio-Rad SmartSpec 3000 Spectrophotometer, Life Science Research Division, Mississauga, ON). Good quality DNA had an $A_{260/280}$ ratio of 1.65 to 1.85. Recombinant plasmids were confirmed by DNA sequencing (University Core DNA & Protein Services, University of Calgary, Canada).

2.13.6 Recombination of pAd/BLOCK-iT™-DEST and pENTR™/U6 vector

Gateway is one of the most popular recombination cloning technologies. It includes two sets of reactions: LR and BP recombinations. The BP reaction is catalyzed by the BP Clonase which recombines *att*B sites with *att*P sites. The LR Clonase is responsible for recombination of *att*L sites with *att*R sites. The recombination reactions are based on the *Escherichia coli* bacteriophage lambda integrase/*att* system.

LR recombination reaction was performed between the pAd/BLOCK-iT™-DEST vector (Figure 10) and pENTR™/U6 entry clone. The pENTR™/U6 vector (300ng) was mixed with about 300ng of pAd/BLOCK-iT™-DEST vector in a 16µl reaction that contained 4µl LR Clonase in 5X reaction buffer. After 1 hr incubation at room temperature, proteinase K (2µl at 2mg/ml) was added and the reaction mixture was incubated at 37°C for 10 minutes. The reaction was transformed into 50µl of One Shot® Top10 competent E. coli as described above. The LB plates contained 100mg/ml ampicillin. The putative expression clone was tested for growth on LB plate containing 30µg/ml chloramphenicol. The true expression clones were ampicillin-resistant and chloramphenicol-sensitive. The *ccdB* gene encodes CcdB protein, which is a natural analogue of the quinolone antibiotics. Vector carrying the *ccdB* gene cannot grow in medium, as well as the medium containing ampicillin or chloramphenicol. Therefore, only true expression clone can grow in medium containing ampicillin.

2.13.7 Preparation of the expression clone

The pAd/BLOCK-iT™-DEST vector contains *Pac I* restriction sites. Digestion of the vector with *Pac I* allows exposure of the left and right viral ITRs and removal of the bacterial sequences (i.e. pUC origin and ampicillin resistance gene).

The purified plasmid DNA of pAd/BLOCK-iT™-DEST pENTR™/U6 (5µg) was mixed with 10U *Pac I* (New England Biolabs, Ipswich, MA) in 1XNEBuffer (total volume up to 20µl) (10 mM Bis-Tris-Propane-HCl,10 mM MgCl2 and 1 mM Dithiothreitol), supplemented with 100µg/ml BSA. After 2 hrs incubation at 37°C, the digested plasmid DNA was purified using phenol/chloroform and ethanol

precipitation method. The purified plasmid DNA was resuspended in sterile water to a final concentration of 1μg/μl.

2.13.8 Package of adenovirus in 293A cells

The 293A cells can provide E1 protein of adenovirus that is required for package of adenovirus. In this experiment, Lipofectamine™ 2000 (Invitrogen, Carlsbad, CA), a cationic lipid transfection reagent, was used to transfect the pAd/BLOCK-iT™- DEST expression construct into 293A cells. The positively-charged components of Lipofectamine™ 2000 form a complex with the negatively-charged plasmid DNA, and then "escort" it through the membranes into cells.

293A cells were plated at $5X10^5$ cells per well in a 6-well plate in 2ml DMEM with 10% FBS. One day after plating, the medium was replaced with 1.5 ml DMEM without antibiotics. Plasmid DNA (4μg) and Lipofectamine™ 2000 (10μl) was diluted in 250μl DMEM without FBS and antibiotics, respectively. After incubation for 5 minutes at room temperature, the diluted plasmid DNA and Lipofectamine™ 2000 were mixed gently, and incubated for 20 minutes at room temperature to allow the formation of DNA/lipofectamine complexes. The 293 cells were transfected by adding the complexes dropwise into each well and incubated overnight at 37°C in an incubator. On the next day, medium was changed to DMEM with 10% FBS and antibiotics, and cells were cultured for another 48 hrs. After 48 hrs, cells were trypsinized and transferred to a 10cm culture dish. Then the 293A cells were cultured in DMEM with 10% FBS and antibiotics, and medium was changed every 3 days until approximately 80% cytopathic effect (CPE) was observed (about 10 days post-tranfection). The adenovirus-containing cells and media

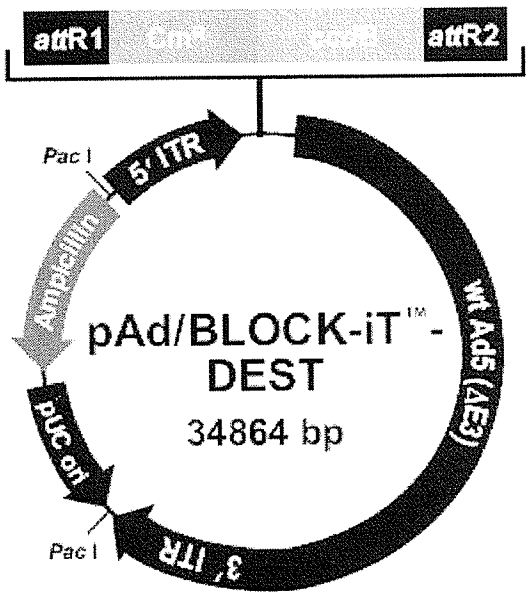

Figure 10 *pAd/BLOCK-iT™-DEST vector cited from Invitrogen web page.* This vector includes all elements (except E1 and E3 proteins) required to produce replication-incompetent adenovirus including left and right inverted terminal repeats (ITRs), encapsidation signal for packaging, E2 and E4 regions and late genes. Expression of the oligonucleotide encoding shRNA is driven by *bla* promoter. The pAd/BLOCK-iT™-DEST vector also contains attR1 and attR2 sites, which are bacteriophage λ-derived DNA recombination sequences that permit recombination of oligonucleotide encoding shRNA in pENTR™/U6 vector with a pAd/BLOCK-iT™-DEST vector. Two antibiotic resistance genes were included in this expression vector. One is chloramphenicol resistance gene (CmR), which will be lost in recombined vector. Another is ampicillin resistance gene (β-lactamase), which allows selection of the plasmid in E. coli. This vector possesses two *Pac I* restriction sites. After digestion, left and right ITRs, required for viral replication and packaging, were exposed. There are two sequencing primer sites, pAd forward priming site and pAd reverse priming site.

were harvested by pipetting cells off the dish and transferred to 15ml capped tubes. The intracellular viral particles were released by three cycles of freeze/thaw at -70°C and 37°C (15 minutes at each temperature). After centrifugation at 1500g for 15 minutes, the supernatant containing viral particles was transferred to cryovials in 1 ml aliquots and was stored at -70°C.

2.13.9 Amplification of adenoviral stock

293A cells were plated at $3X10^6$ cells per 10cm dish in 10ml DMEM with 10% FBS. One day after plating, the cells were at 90% confluence, and the crude adenovirus stock (200µl) was then added into the dish. After cells were infected with recombinant adenovirus for 3 days, approximately 80% of the cells were rounded up and floated in the medium. Cells were collected and viral particles were prepared by freeze/thaw method as described above.

2.13.10 Titration of adenoviral stock

293A cells were plated at $2.2X10^5$ cells per well in a 24-well plate in 0.5ml DMEM with 10% FBS and antibiotics. Three 10-fold dilution series of viral stock from 10^{-3}-10^{-5} were prepared. Each viral dilution (100µl) was added to cell culture wells. Assays were performed in triplicate. Cells were then incubated at in a 37°C incubator for 48 hrs. After aspirating off the medium, the cell culture dishes were dried in a hood for 10 minutes, and then ice cold 100% methanol (0.5ml) was added into each well to fix cells at -20°C for 10 minutes. After washing the cells with 0.5ml PBS containing 1% BSA twice, 0.25ml of the mouse anti-hexon antibody (1:500) was added into each well and incubated

at 37°C for 1 hr. After washing the cells with PBS as described above, 0.25ml of the HRP-conjugated goat anti-mouse antibody (1:1000) was added into each well and incubated at 37°C for 1 hr. After washing the cells with PBS as described above, 0.25 ml of diaminobenzidine (DAB) substrate (prewarmed to room temperature) in 1Xworking solution (0.015% H_2O_2 in PBS, pH 7.2) was added into each well and incubated at room temperature until the desired staining color was developed. Under inverted microscope (Olympus inverted-phase microscope) with 20X objective, 10 fields were randomly selected and hexon positive cells were counted. The titer of virus stock was calculated using the following formula and expressed as IFU (infectious unit per ml).

$$\text{IFU} = \frac{\text{Average number of positive cells/field} \times \text{fields/well}}{\text{Volume of diluted virus used in each well (ml)} \times \text{dilution factor}}$$

2.14 Construction of recombinant adenovirus containing BMP4 cDNA

Recombinant adenovirus containing BMP4 cDNA was constructed using Adeno-X™ Expression Systems (Clontech, Mountain View, CA)

The methods used in the construction of recombinant adenovirus containing BMP4 cDNA are the same as used in the construction of recombinant adenovirus containing oligonucleotide encoding shRNA. PCR method was used to generate a full length of BMP4 cDNA with restriction enzyme sites at two ends by using appropriate primers containing the restriction enzyme sites. After purification, the full length of BMP4 cDNA was ligated into the adaptor vector, which was linearized by digestion with restriction enzyme. Then the ligation reaction was transformed into DH5α cells. After the correct entry clone was identified, the recombination reaction was performed to

generate an expression clone. Finally, the expression clone was transfect into HEK 293 cells to produce an adenoviral stock. After amplification and titration, the adenovirus containing BMP4 cDNA was used in my studies.

2.15 Statistical analysis

To analyze differences between different groups, ANOVA and Fisher's PLSD post hoc test were perfomed via a computer software StatView (version 5.0) (SAS Institute, Inc., Cary,NC). Differences with P-values less than 0.05 were judged as significant.

III. RESULTS AND DISCUSSION

1. The Effect of Bone Morphogenetic Protein 4 on Rat Hepatic Stellate Cells Proliferation and Differentiation

1.1 Introduction

BMP4 plays pleiotropic roles in different cell types by initiating different signaling pathways. For example, it has been demonstrated that activation of BMP4 downstream Smad1 signaling induced cell death in human lung cancer cell line A549 cells (Buckley, Shi et al., 2004). Moreover, Smad1 and JNK pathways played an important role in BMP4-induced anti-proliferation and differentiation of lung fibroblasts (Jeffery, Upton et al., 2005). Furthermore, BMP4 could utilize p38 and ERK1/2 signaling pathways to stimulate proliferation of human pulmonary artery smooth muscle cells (Frank, Abtahi et al., 2005).

In the past 40 years, research in the field of liver fibrosis and cirrhosis has undergone a rapid development and a lot of knowledge has been gained, such as the roles of HSCs in hepatic fibrogenesis. It is known that TGFβ, a member of TGFβ superfamily, is the most important cytokine during hepatic fibrogenesis and HSC trans-differentiation (Bedossa and Paradis, 1995). However, expression of TGFβ in activated HSCs only showed a temporary increased expression pattern. Therefore, other cytokines could play an important role in HSCs activation during liver fibrogenesis. These factors could belong to the same family with TGFβ or other growth factor families. BMP4 is a member of TGFβ superfamily. It has been shown that BMP4 could induce α-SMA expression in

lung fibroblasts (Jeffery, Upton et al., 2005), which is also the marker for activated HSCs. Moreover, in previous work, we observed that BMP2 and BMP4 could increase the expression of α-SMA in primary cultured HSCs (Shen, Huang et al., 2003). However, the exact role of BMP4 in HSC activation and trans-differentiation and hepatic fibrogenesis remains to be determined. In order to further understand the role of BMP4 in hepatic fibrogenesis, we conducted an experiment to examine the expression of BMP4 and BMP receptors in primary cultured HSCs and in bile duct ligation (BDL)-induced liver fibrosis model. We also investigated the effect of BMP4 on transformed HSC proliferation and differentiation, and examined BMP4 down-stream signal transduction pathways in these cells.

1.2 Results

1.2.1 BMP4 expression in the liver of BDL rats

To investigate the role of BMP4 in hepatic fibrogenesis, we first examined the expressions of BMP4 and α-SMA in the liver of BDL rats. As shown in Figure 11, abundance of BMP4 mRNA was significantly elevated after 1 week of BDL while abundance of α-SMA mRNA was significantly increased after 4 weeks of BDL. With increase in BMP4 mRNA after BDL, there was an increase in BMP4 protein after 2 weeks of BDL (Figure 12). The abundance of BMP4 protein after BDL showed two peaks with the first peak at 3 weeks after BDL and the second peak at 6 weeks after BDL (Figure 12). The α-SMA protein level was gradually elevated from 3 weeks after BDL and peaked at 4 weeks and gradually decreased but still remained higher level than that in sham rats (Figure 12).

Figure 11 *RT-PCR analysis of BMP4 and α-SMA expressions in the liver*. A represents typical agarose gel pictures of BMP4 and α-SMA expressions after BDL. B and C display density histogram of BMP4 and α-SMA band densities, respectively. Data represent mean±SE from four rats. Abundance of BMP4 mRNA was significantly increased after 1 week of BDL and abundance of α-SMA mRNA was significantly increased after 4 weeks of BDL. N represents negative control without reverse transcription. P represents positive control with Marathon-ready Liver cDNA. (+) and (−) indicate the presence and absence of BDL, respectively. Glyceraldehyde 3-phosphate dehydrogenate (GAPDH) was used for loading control. *indicates $P<0.05$ between sham and BDL groups at the same week.

A

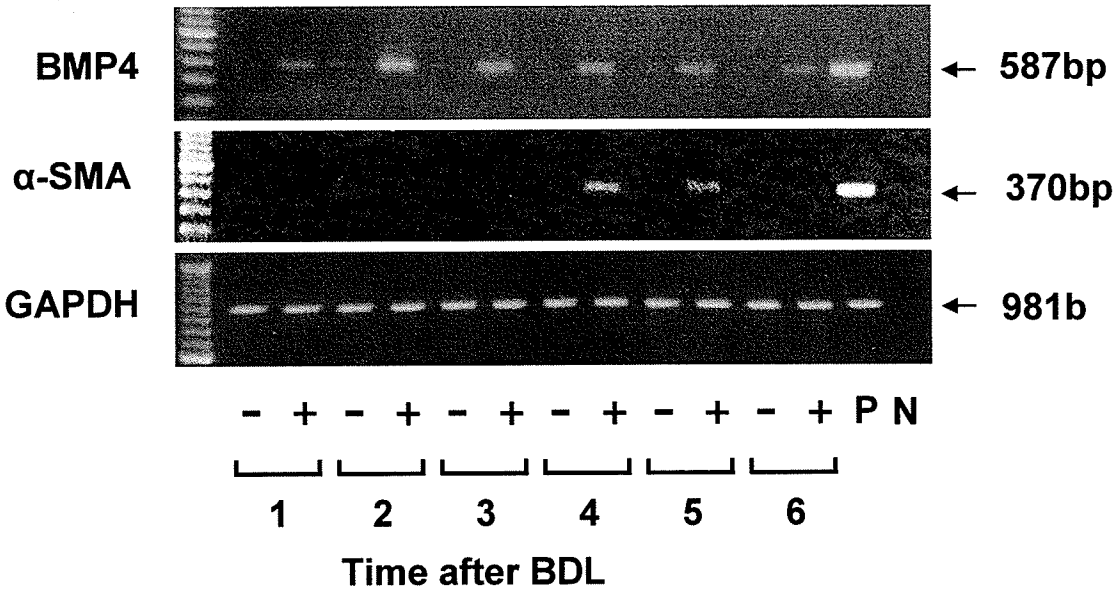
BMP4
α-SMA
GAPDH
587bp
370bp
981b
- + - + - + - + - + - + P N
1 2 3 4 5 6
Time after BDL

B

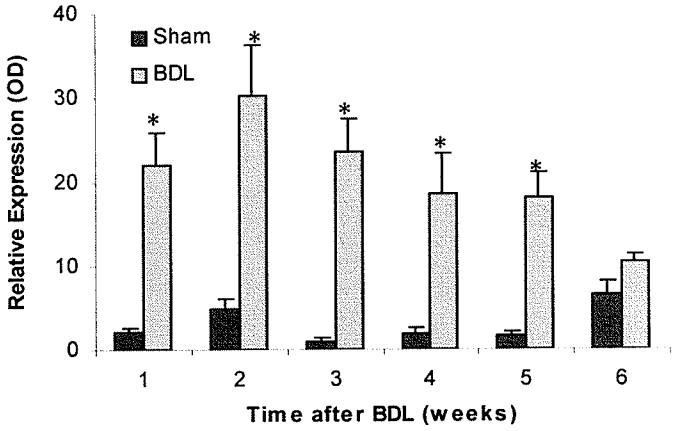
Sham
BDL
Relative Expression (OD)
40
30
20
10
0
1 2 3 4 5 6
Time after BDL (weeks)

C

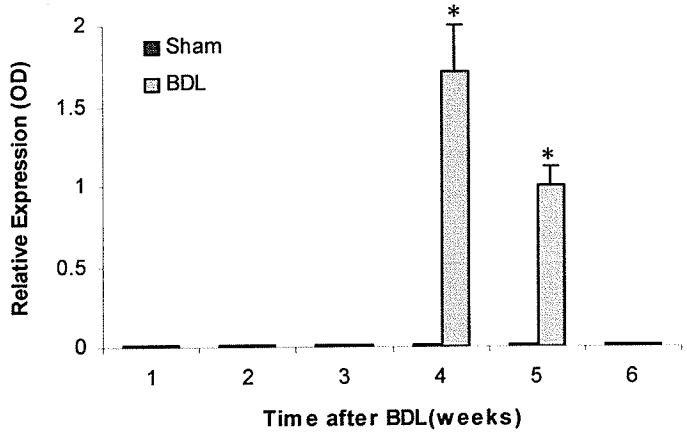
Sham
BDL
Relative Expression (OD)
2
1.5
1
0.5
0
1 2 3 4 5 6
Time after BDL(weeks)

Figure 12 *Western blot analysis of BMP4 and α-SMA expression in the liver.* The figure shows the expression of BMP4 and α-SMA protein levels in the liver after BDL. The abundance of BMP4 protein was increased after two weeks of BDL. The expression of BMP4 showed two peaks with the first peak at the third week after BDL and the second peak at the sixth week after BDL. The α-SMA protein level was gradually increased from the third week after BDL and peaked at the fourth week. GAPDH was used for loading control. (+) and (-) indicate the presence and absence of BDL, respectively. A represents typical SDS-PAGE gel pictures of BMP4 and α-SMA expressions after BDL. B and C display the density histogram of BMP4 and a-SMA, respectively. Data are from four rats and represent mean±SE. *indicates $P<0.05$ between sham and BDL groups at the same week.

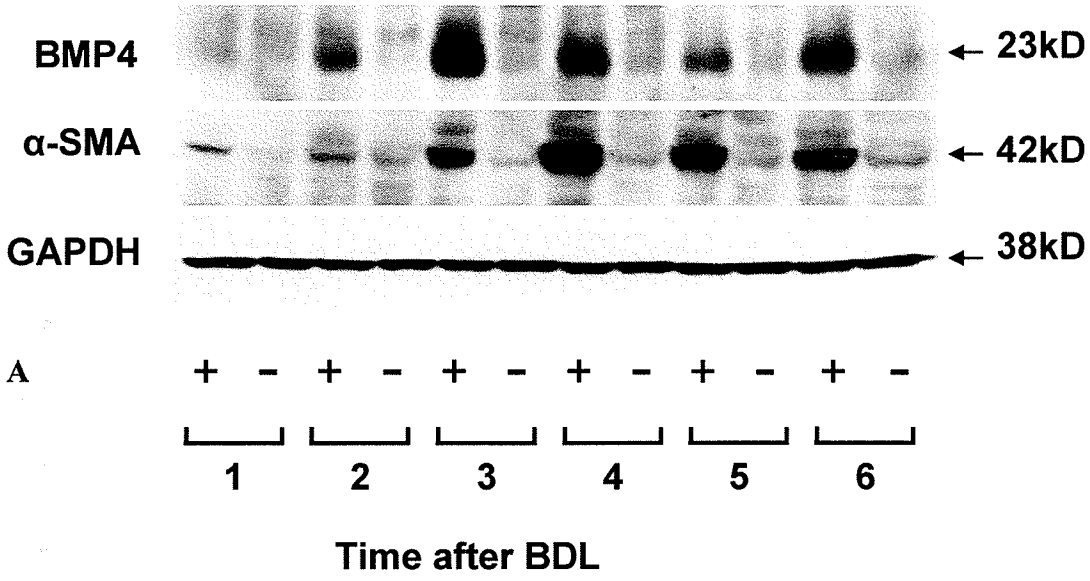
BMP4
α-SMA
GAPDH
23kD
42kD
38kD
A
+ - + - + - + - + - + -
1 2 3 4 5 6
Time after BDL

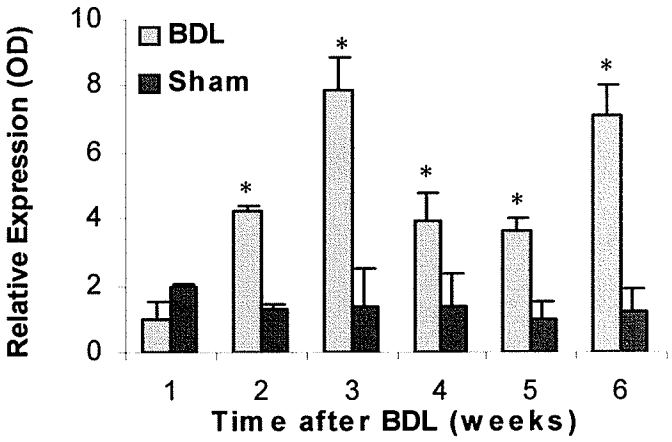
B
BDL
Sham
Relative Expression (OD)
Time after BDL (weeks)

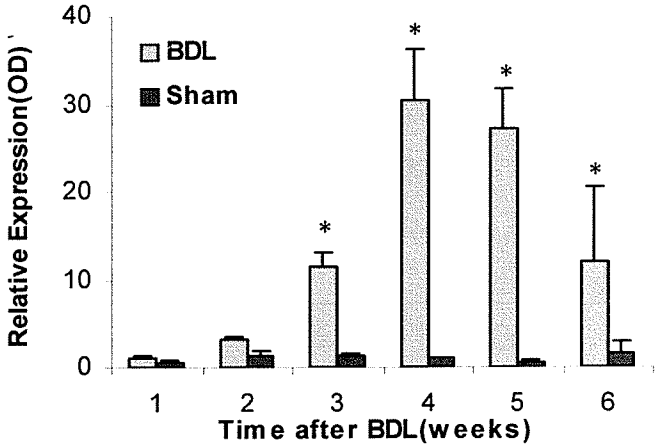
C
BDL
Sham
Relative Expression(OD)
Time after BDL(weeks)

1.2.2 Expression of BMP4 downstream signaling molecules after BDL

To understand BMP4 involvement in BDL-induced hepatic fibrosis, we examined downstream signaling molecules of BMP4 in the liver of BDL and sham rats. As shown in Figure 13, there were increase in phospho-Smad1, Smad1, phospho-ERK1/2, ERK1, phospho-p38 and p38 in the liver after BDL, indicating that Smad1, ERK1, and p38 signal transduction pathways might mediate BMP4 activity during liver fibrogenesis.

Figure 13 *Western blot analysis of BMP4 downstream signaling molecules expression in the liver after BDL.* The top part shows the expression of phospho-Smad1, Smad1, phospho-ERK1/2, ERK1, phospho-p38 and p38 in the liver after BDL. The abundance of these protein levels were all increased in the liver after BDL. GAPDH was used for loading control. (+) and (-) indicate the presence and absence of BDL. The lower part displays the density histogram data from four rat samples (mean±SE), which represent the relative expression of phospho-Smad1 (A), Smad1 (B), phospho-ERK1/2 (C), ERK1 (D), phospho-p38 (E) and p38 (F) protein, respectively. *indicates $P<0.05$ between sham and BDL groups at the same week. **indicates $P<0.001$ between sham and BDL groups at the same week.

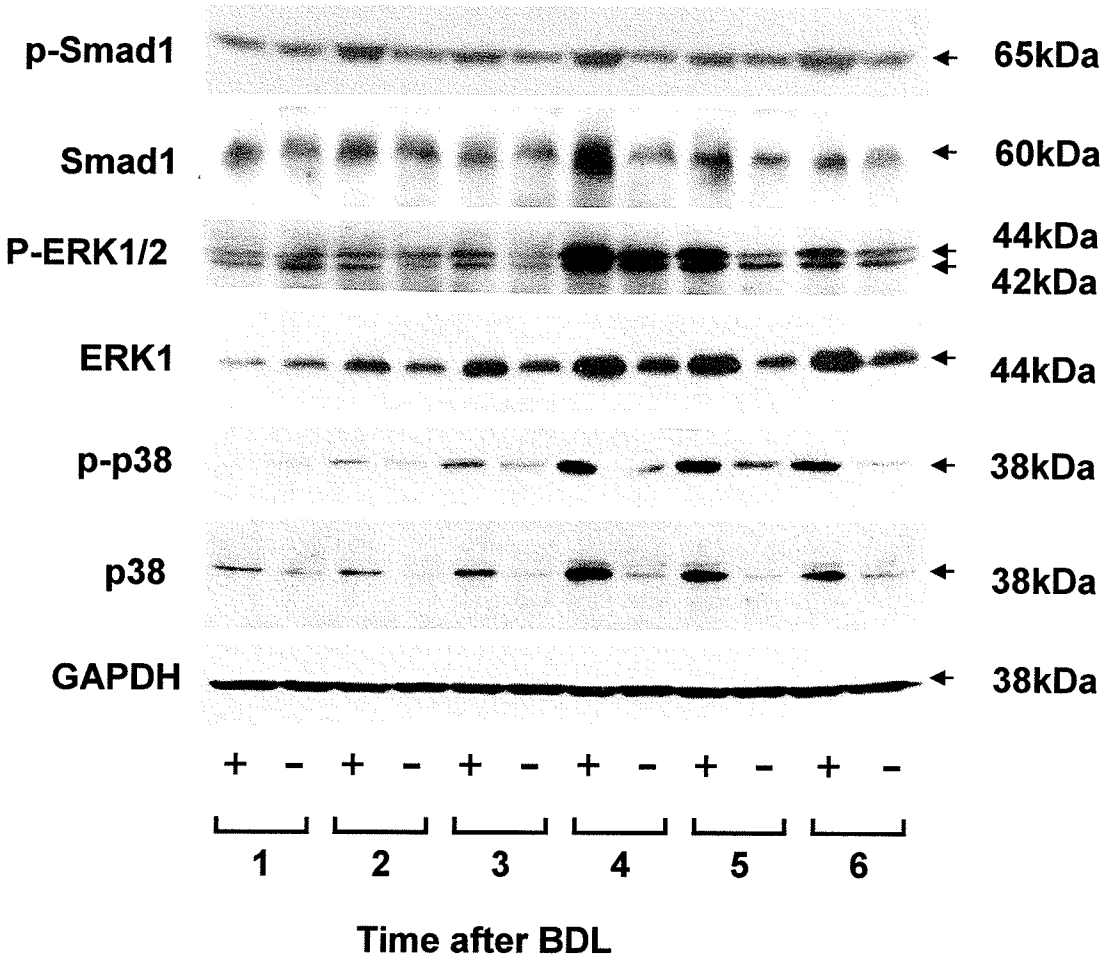
p-Smad1
65kDa
Smad1
60kDa
P-ERK1/2
44kDa
42kDa
ERK1
44kDa
p-p38
38kDa
p38
38kDa
GAPDH
38kDa
+ - + - + - + - + - + -
1 2 3 4 5 6
Time after BDL

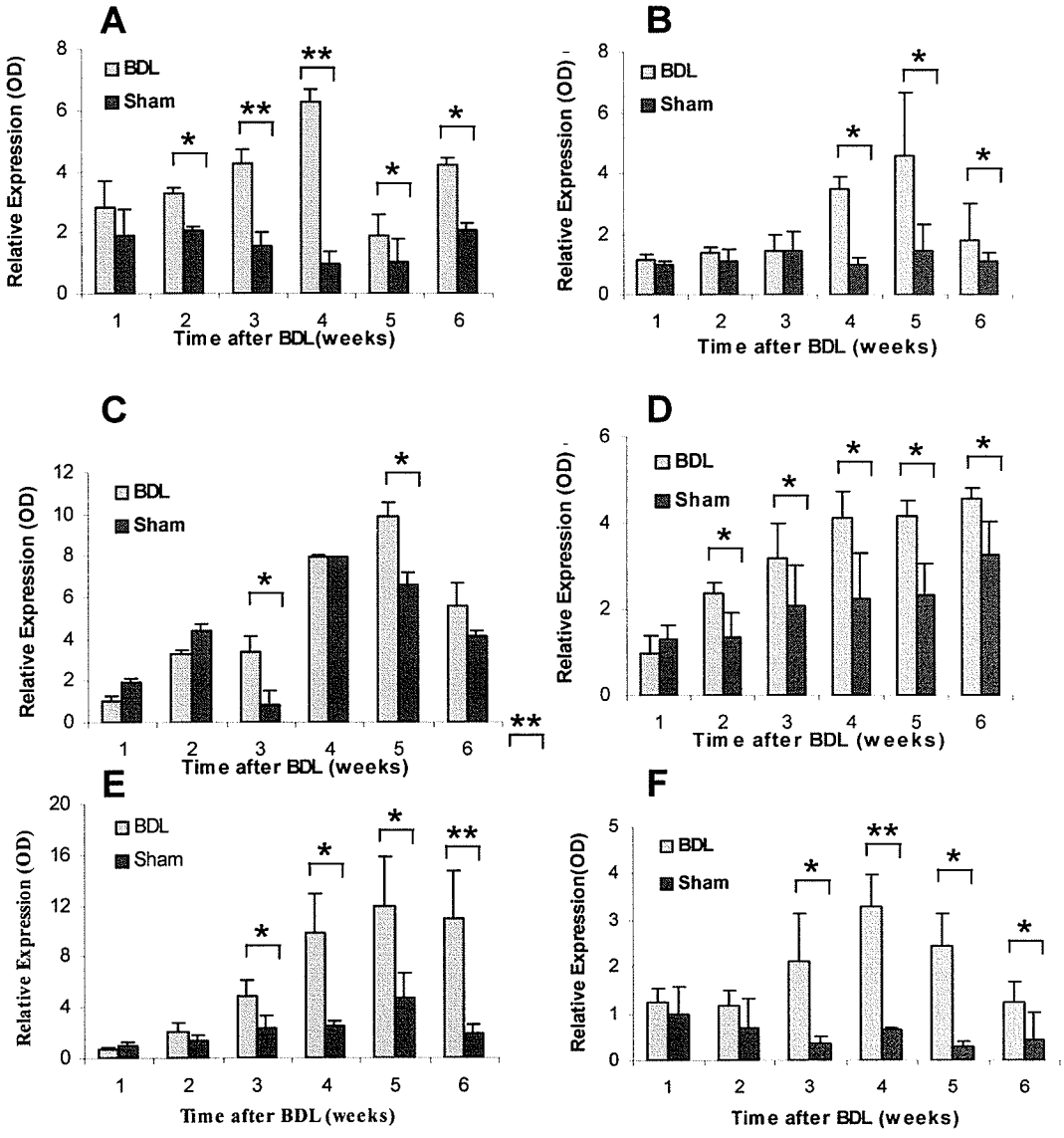
A
BDL
Sham
Relative Expression (OD)
Time after BDL(weeks)
B
BDL
Sham
Relative Expression (OD)
Time after BDL (weeks)
C
BDL
Sham
Relative Expression (OD)
Time after BDL (weeks)
D
BDL
Sham
Relative Expression (OD)
Time after BDL (weeks)
E
BDL
Sham
Relative Expression (OD)
Time after BDL (weeks)
F
BDL
Sham
Relative Expression(OD)
Time after BDL (weeks)

1.2.3 BMP4 expression in rat hepatic stellate cells

To investigate the role of BMP4 in hepatic fibrogenesis, we also employed primary cultured HSCs and a rat HSC line - T6 cells. Expressions of BMP4 and its membrane receptors were examined in these cells. As shown in Figure 14A, there were strong expressions of BMP4 and BMPRII in T6 cells and primary cultured HSCs. A moderate expression of BMPR1A was observed in both T6 cells and primary cultured HSCs. Expression of BMPR1B was lowest among these genes in both T6 cells and primary cultured HSCs. Moreover, expression pattern of BMP4 during *in vitro* activation of HSCs was documented in Figure 14B. Increased expression of BMP4 was observed at day 9 of *in vitro* culture and a significant increase in BMP4 mRNA level was documented at day 24.

Figure 14 *A: mRNA expression of bone morphogenetic protein 4 (BMP4) and its receptors.* Representative ethidium bromide-stained gels demonstrated the abundance of mRNAs for BMP4, BMPR1A, BMPR1B and BMPRII in primary culture HSCs and T6 cells. Total RNA from rat bone marrow stromal cells was used as a positive control. *B: Expression of BMP4 mRNA level during primary culture of HSCs from day 1 to 24.* The abundance of BMP4 mRNA was increased at day 9 and significantly increased at day 24 during *in vitro* cultures. N represents negative control without reverse transcriptase. P represents positive control with rat bone marrow stromal cells. GAPDH was used as the loading control.

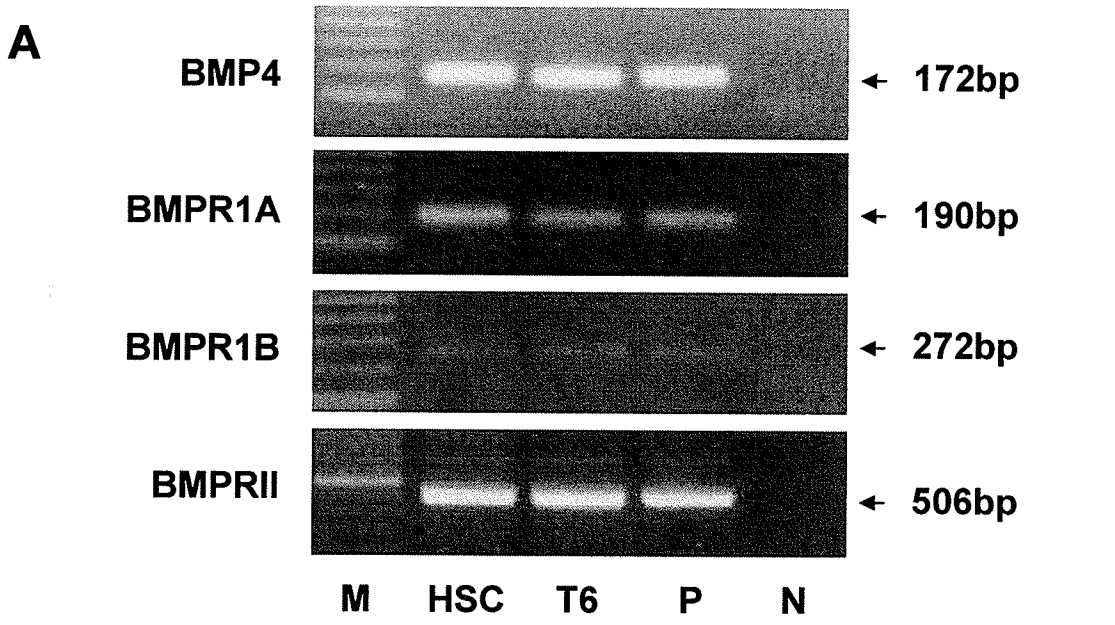
A
BMP4
172bp
BMPR1A
190bp
BMPR1B
272bp
BMPRII
506bp
M
HSC
T6
P
N

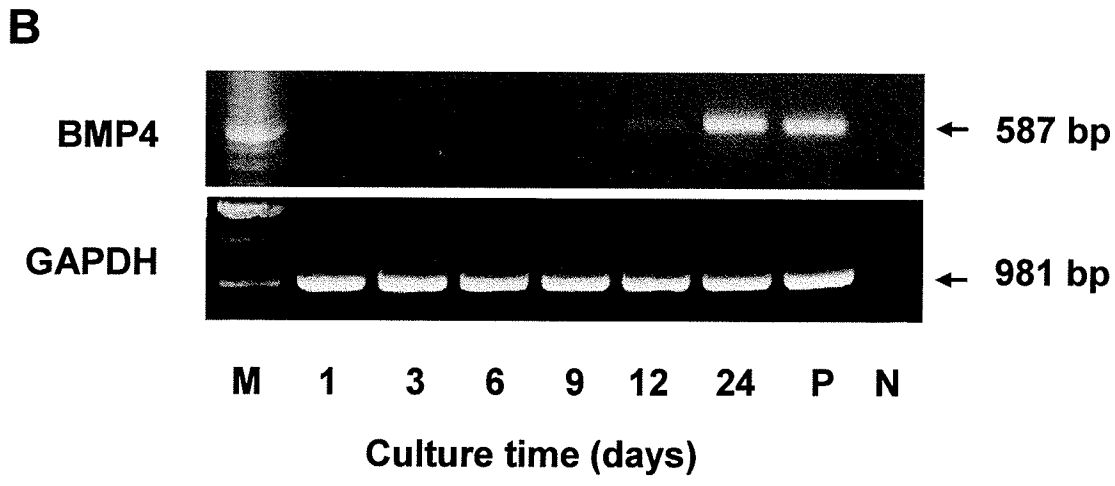
B
BMP4
587 bp
GAPDH
981 bp
M
1
3
6
9
12
24
P
N
Culture time (days)

1.2.4 Effects of BMP4 on T6 cells

The biological effect of BMP4 on T6 cells was next examined. The effect of BMP4 on T6 cell proliferation was determined by WST-1 reagent, ^{3}H-thymidine incorporation assay and cell counting. As shown in Figure 15, BMP4 had no effect on T6 cell proliferation. In culture, T6 cells expressed low but detectable levels of α-SMA as seen by Western blot analysis. However, when T6 cells were incubated with BMP4, there was a significant increase in α-SMA protein level (Figure 16). The increase in α-SMA abundance occurred in a time-dependent manner with the peak at 48 hrs after BMP4 stimulation (Figure 16A). In addition, the increased α-SMA expression in response to BMP4 stimulation was dose-dependent as shown in Figure 16B. To determine the intracellular signaling pathways initiated by BMP4 in T6 cells, we first examined Smad pathway, which is classic BMP4 signaling pathway. After incubation of T6 cells with BMP4, there was an increase in Smad1 phosphorylation at 5 minutes, reaching maximum at 15 minutes and then back to normal at 60 minutes (Figure 17). We also examined the MAPK pathway, which is shown to be involve in BMP4 signaling recently. In this study, ERK1/2, p38, and JNK were investigated and results showed that BMP4 induced phosphorylation of ERK1/2 and p38 in T6 cells. BMP4, however, did not induce phosphorylation of JNK (data not shown) (Figure 18). The phosphorylation of ERK1/ 2 and p38 appeared to occur at 5 minutes and then back to normal at 30 minutes after BMP4 stimulation.

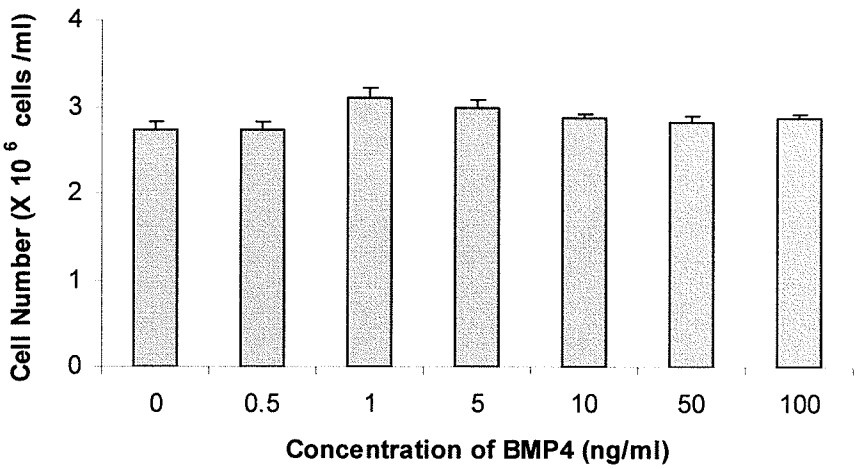

Figure 15 *Effect of BMP4 on T6 cell proliferation.* T6 cells were incubated with different concentrations of BMP4 (0-100ng/ml) as described in Materials and methods. Cell numbers were counted 48 hrs later. The data represent mean±SE from 6 wells. No significant differences were found between treated and control groups.

Figure 16 *BMP4 Regulation of T6 cell trans-differentiation.* A: T6 cells were incubated with BMP4 (50ng/ml) for different time periods as indicated. Western blot was performed as described in Materials and methods. The top part represents typical Western blot of α-SMA. The lower part represents the density diagram data from three-separated Western blot analysis (mean±SE). B: T6 cells were incubated with different concentrations of BMP4 (0-100ng/ml) for two days. Western blot was performed as described in Materials and methods. The top part represents typical Western blot of α-SMA. The lower part represents the density histogram data from three-separated Western blot analysis (mean±SE). *indicates $P<0.05$ between treated and control groups. **indicates $P<0.001$ between treated and control groups.

A

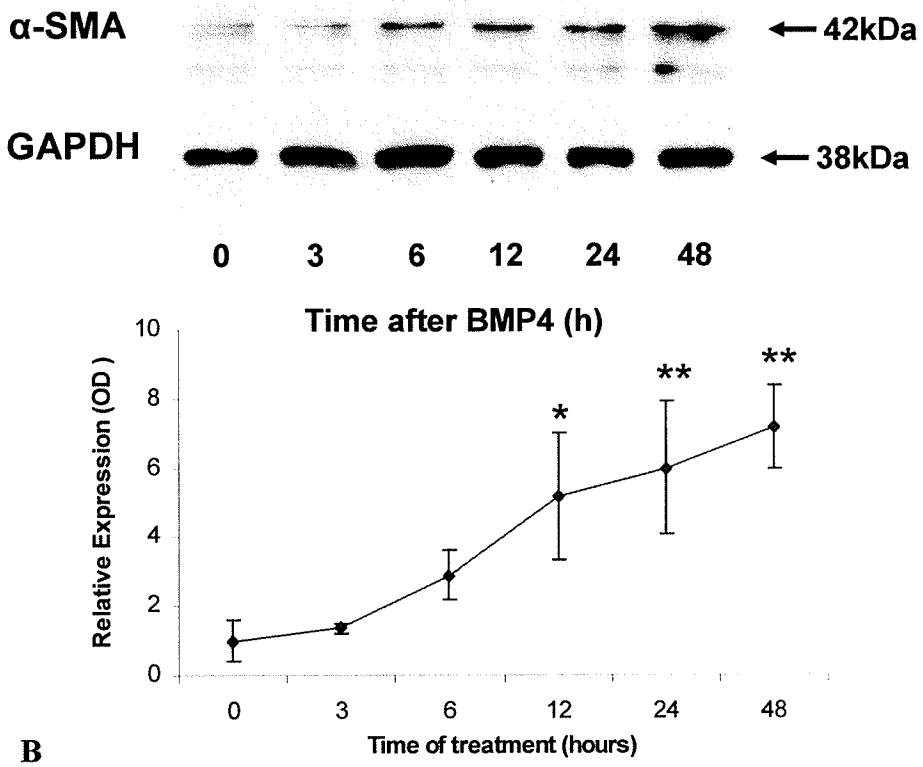
α-SMA
42kDa
GAPDH
38kDa
0 3 6 12 24 48
Time after BMP4 (h)
Relative Expression (OD)
10
8
6
4
2
0
*
**
**
0 3 6 12 24 48
Time of treatment (hours)

B

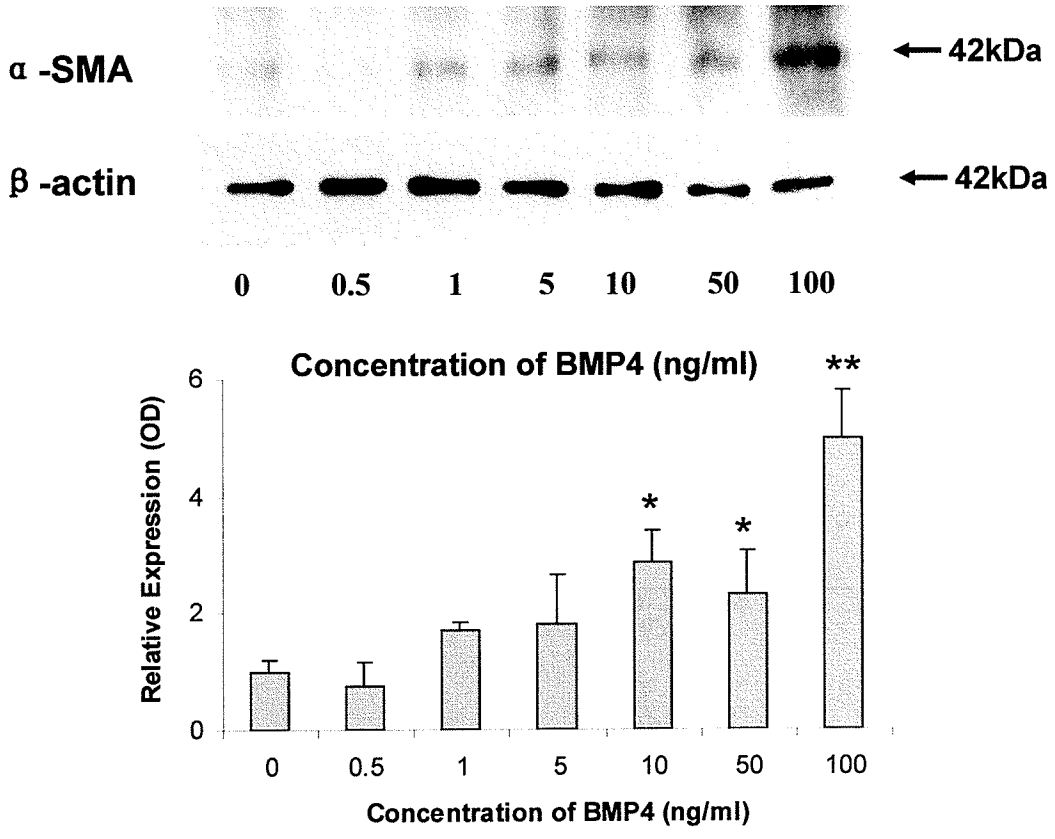
α -SMA
42kDa
β -actin
42kDa
0 0.5 1 5 10 50 100
Concentration of BMP4 (ng/ml)
Relative Expression (OD)
6
4
2
0
*
*
**
0 0.5 1 5 10 50 100
Concentration of BMP4 (ng/ml)

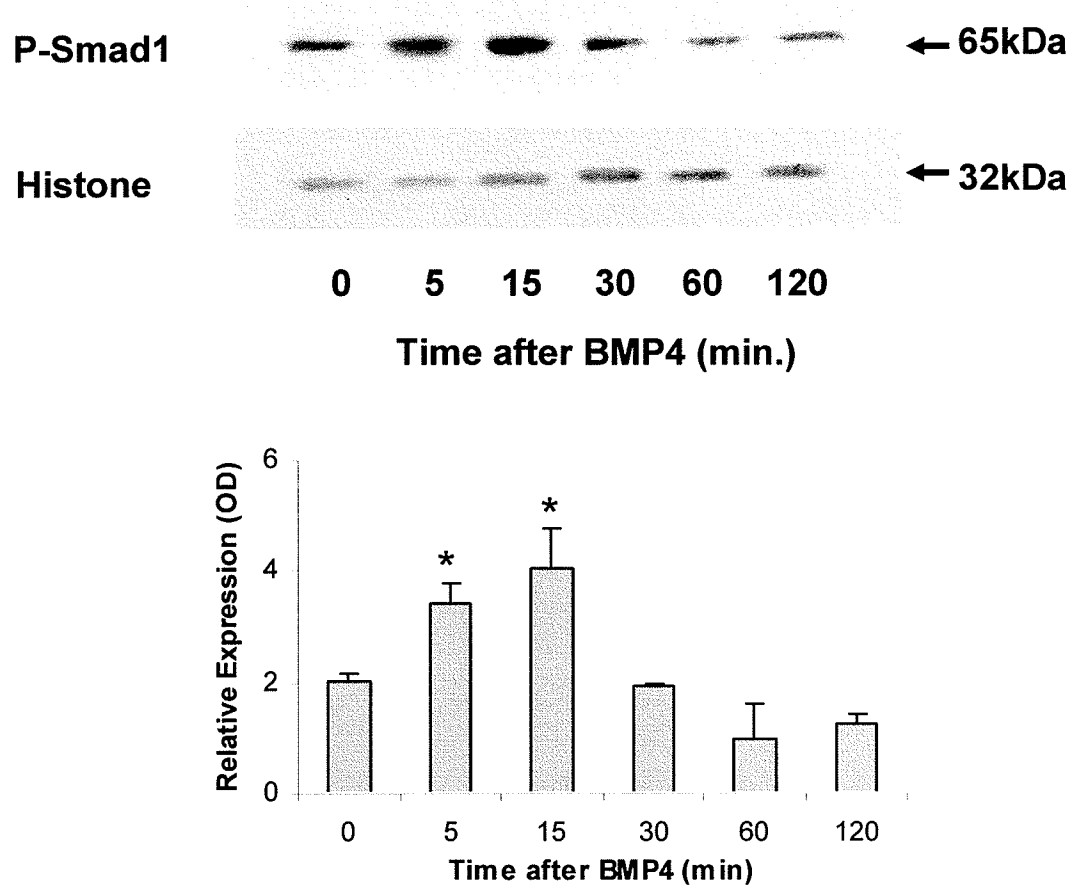

Figure 17 *Western blot analysis of phospho-Smad1 in T6 cells stimulated with or without BMP4 (50 ng/ml).* Nuclear proteins were isolated from T6 cells at different time points as indicated. Abundance of phospho-Smad1 was analyzed by Western blot analysis as described in Materials and methods. Histone was used as the loading control of nuclear protein. The top part represents typical Western blot of phospho-Smad1. The lower part represents the density histogram data from three-separated Western blot analysis (mean±SE). *indicates $P<0.05$ between treated and control groups.

Figure 18 *Western blot analysis of MAP kinases in T6 cells activated by BMP4.* The figure shows the expression of phospho-ERK1/2, ERK1, phospho-p38 and p38 in T6 cells stimulated with or without BMP4 (50ng/ml) at different time points as indicated. GAPDH was used for loading control. The lower part displays the density histogram data from three-separated Western blot analysis (mean±SE), which represents the relative expression of phospho-ERK1/2 (A), ERK1 (B), phospho-p38 (C) and p38 (D) protein, respectively. *indicates $P<0.05$ between treated and control groups.

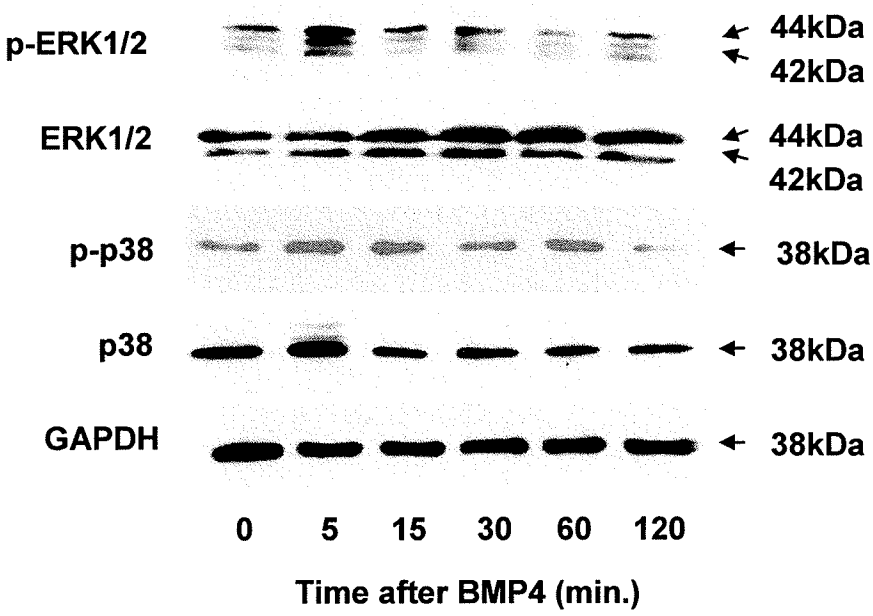
p-ERK1/2
44kDa
42kDa
ERK1/2
44kDa
42kDa
p-p38
38kDa
p38
38kDa
GAPDH
38kDa
0 5 15 30 60 120
Time after BMP4 (min.)

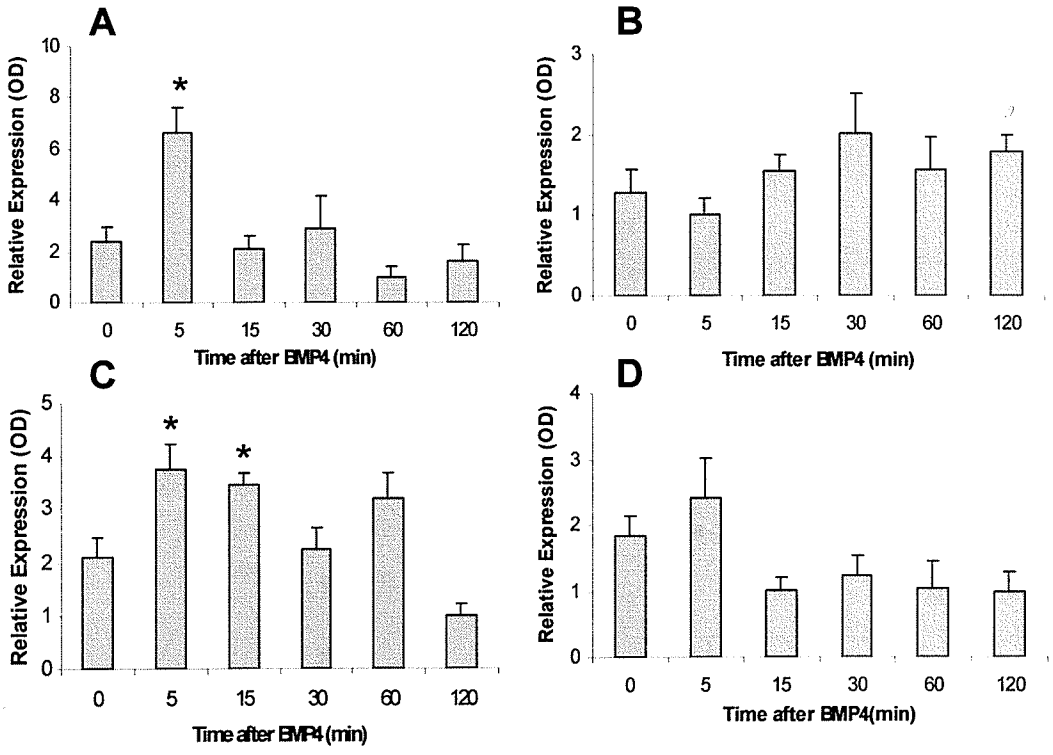
A
Relative Expression (OD)
Time after BMP4 (min)
B
Relative Expression (OD)
Time after BMP4 (min)
C
Relative Expression (OD)
Time after BMP4 (min)
D
Relative Expression (OD)
Time after BMP4(min)

1.3 Discussion

Liver fibrosis and cirrhosis is common sequel of different liver diseases. It has been widely investigated during last four decades. Different models of liver fibrosis and cirrhosis have been established and one of them is the BDL model (Tsukamoto, Matsuoka et al., 1990). BDL model of fibrosis in rats shows similar changes in morphology of the liver and the activation of HSCs as observed in human liver diseases (Ohata, Lin et al., 1997; Tieche, De Gottardi et al., 2001), especially liver fibrosis and cirrhosis caused by cholestatic liver diseases. HSCs have been recognized as a major cell type in the liver mediating the development of liver fibrosis and cirrhosis (Gressner, 1996). During liver injury, there are proliferation and trans-differentiation of HSCs in the liver, which are regulated by different cytokines such as transforming growth factor beta1 (TGF-β1) (Gressner, Weiskirchen et al., 2002), platelet-derived growth factor (Pinzani, Gentilini et al., 1995; Kinnman, Goria et al., 2001), and endothelin 1(Rockey and Chung, 1996). Among these cytokines, it is considered that TGFβ1 is the most important cytokine during hepatic fibrogenesis and the activation of HSCs (Bedossa and Paradis, 1995).

BMPs belong to TGF-β superfamily but TGF-β and BMPs have different functions in different tissues (Heckman, Ehler et al., 1999). The expression and biological activities of TGF-β in HSCs have been extensively investigated while the role of BMPs in HSC activation is still unclear. We have observed that BMP2 and BMP4 stimulated the expression of α-SMA in HSCs, indicating a role of BMPs in HSC trans-differentiation (Shen, Huang et al., 2003). This is in consistent with the general consideration of BMPs in other tissues. However, recently numerous studies have

demonstrated that multiple TGF-β superfamily members and their receptors are dynamically co-expressed during cell proliferation, differentiation, and apoptosis, and can reciprocally regulate related gene expression. During vascular smooth muscle cell (VSMC) differentiation and phenotypic modulation, TGF-β1 upregulated the expression of α-SMA while BMP4 downregulated the expression of α-SMA (Nakajima, Yamagishi et al., 2002). BMP2 can enhance TGF-β induced initial phenotypic changes associated with endothelial-mesenchymal transformation during generation of the endocardial cushion (Nakajima, Yamagishi et al., 2000). Therefore, the distinct spatio-temporal expression profiles of each subfamily members may determine the development of organs and the fate of cells.

During HSC activation, TGF-β1 mRNA transcripts increased significantly at the second day of HSCs primary culture and the first day after trypsinization and reseeding. After this short-term elevation, there was a decrease in TGF-β1 mRNA abundance during *in vitro* activation of HSCs (Gong, Roth et al., 1998). The temporal expression pattern of TGF-β1 mRNA in HSCs is different from those of BMP4 and BMP2 mRNA in HSCs described in our study. The expression of BMP4 mRNA was significantly increased during HSCs activation. The initial expression was observed at day 9 of HSCs primary culture and a dramatic increase was observed at day 24 of HSCs primary culture. The expression of BMP2 remained unchanged during this course (data not shown). The different expression patterns of TGF-β1, BMP4, and BMP2 mRNAs during HSCs activation suggest that these three growth factors may play different roles in the regulation of HSCs. Previous studies have demonstrated that TGF-β1 significantly inhibited HSCs proliferation, whereas BMP2 and BMP4 did not affect the proliferation of

HSCs. Although both TGF-β1 and BMPs were important in the transdifferentiation of HSCs, BMP2 and BMP4 were more potent in the trans-differentiation of HSCs than TGF-β1 (Shen, Huang et al., 2003). The difference can be due to the different signaling proteins involved in TGF-β1 and BMPs signal transduction. Indeed the expression of signaling protein involved in BMPs signal transduction - Smad1 was significantly increased during HSC activation (Shen, Huang et al., 2003) while the expression of Smad2 and Smad3 remained unchanged (Dooley, Delvoux et al., 2001). Moreover, study with TGF-β1 gene knockout mouse indicated that HSCs could still be activated when cultured in *vitro* (Hellerbrand, Stefanovic et al., 1999). Therefore, it is reasonable to believe that dominant BMP signal transduction pathway in HSCs is more important on cell trans-differentiation and keeps myofibroblast-like phenotype.

Previous studies have shown that blocking p38 MAPK pathway in HSCs with the specific inhibitor SB203580 has no effect on the up-regulation of α-SMA in HSCs during *in vitro* culture. However, collagen I and MMP-13 mRNA expression was strongly reduced (Lechuga, Hernandez-Nazara et al., 2004; Lindert, Wickert et al., 2005). Our results showed that BMP4 can induce the activation of p38 MAPK in HSCs. This may imply that BMP4-mediated p38MAPK signaling pathway contributed to the ECM gene expression during trans-differentiation of HSC, but not the phenotypic changes of HSC trans-differentiation.

The present study is the first to report that Smad1 dependent signaling pathway is involved in the activation of HSCs. In addition, it is also documented that BMP4-initiated Smad1 signaling was capable to promote cell differentiation in fibroblast.

2. The effect of Bone Morphogenetic Protein 4 on Rat Hepatic Stem Cells Proliferation and Differentiation

2.1 Introduction

It has been debated by researchers in the field of hepatic fibrogenesis and hepatocarcinogenesis why hepatocellular carcinoma developes from the cirrhotic liver. It was demonstrated that during early hepatic fibrosis there is a so-called ductual response or oval cell response which occurs at the terminal of bile duct at the portal triad (Clouston, Powell et al., 2005). Our previous studies indicated that there was a significant increase in BMP4 expression in both the fibrotic liver and activated HSCs *in vitro* (Fan, Shen et al., 2006). Moreover, it is known that in the early fibrosis, HSCs migrate toward the portal triad (Craig, Quaglia et al., 2004). Therefore, during hepatic fibrogenesis, direct interaction between HSCs and hepatic progenitor cells (HPCs) is possible and there could be some paracrine interaction between HSCs and HPCs (Clouston, Powell et al., 2005). The patterns of spatial and temporal expression of BMP4 in HSCs indicate that they may exert an important effect on HPCs differentiation toward hepatocytes.

Several soluble factors such as hepatocyte growth factor, fibroblast growth factors, oncostatin M, extracellular matrix (ECM), and cell surface associated molecules can regulate the differentiation of HPCs toward hepatocytes (Heng, Yu et al., 2005). Differentiation of HPCs toward hepatocytes are indicated by several hepatic markers such as alpha fetoprotein (AFP), albumin, glucose-6-phosphatase (G6Pase) and tyrosine-aminotransferase (TAT). Expression of these markers are regulated by several hepatic nuclear transcription factors such as hepatocyte nuclear factors (HNFs),

CCAAT/enhancer-binding proteins, and GATA-binding proteins (Suzuki, Iwama et al., 2003; Heng, Yu et al., 2005). Moreover, several *in vitro* studies demonstrated that dexamethasone has the potential to induce multiple end-phenotypes (Grigoriadis, Heersche et al., 1990; Shalhoub, Conlon et al., 1992) by binding to its cognate nuclear receptor and thus modulating the transcriptional activity of target genes (Tanaka, Murphy et al., 2004). Dexamethasone is known to suppress DNA synthesis and upregulate albumin and G6Pase production during specific hepatic maturation in embryonic stem cells (Dasgupta, Hughey et al., 2005). Furthermore, in a recent investigation of mouse embryonic stem cells, it was found that BMP4 was required for hepatic specification of mouse embryonic stem cell-derived definitive endoderm (Gouon-Evans, Boussemart et al., 2006). However, there is a little information regarding the role of BMP4 in HPC differentiation. The current study is the first to examine the role of BMP4 in HPC differentiation and connect the link between HPCs and HSCs to investigate the role of BMP4 in hepatic fibrogenesis and hepatocarcinogenesis.

2.2 Results

2.2.1 BMP4 and its receptors expression in WB-F344 cells and CFSC-8B cells

To investigate the autocrine and paracrine stimulation of BMP4 on HPCs, the expression of BMP4 and its receptors in one rat HPC cell line (WB-F344 cells) and one transformed rat HSC cell line (CFSC-8B) were examined. As shown in Figure 19, there was expression of BMP4 and its receptors BMPRII and BMPR1A in both WB-F344 and CFSC-8B cells. Presence of BMP4 receptors on the cellular membrane of WB-F344 cells indicates a functional activity of BMP4 on WB-F344 cells.

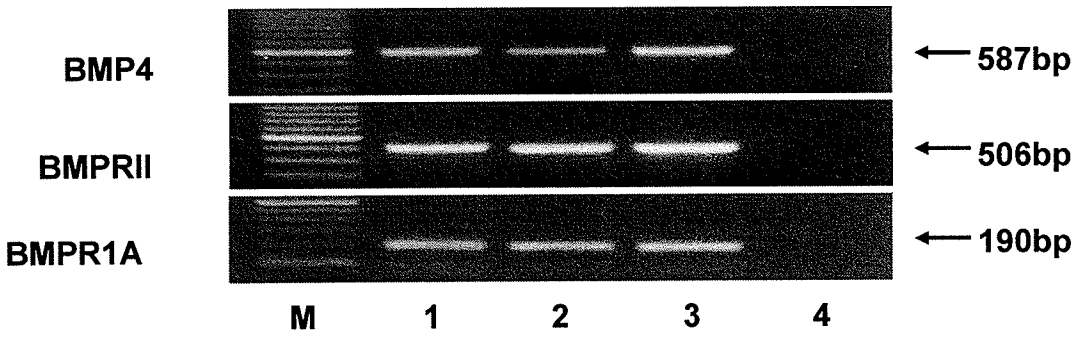

Figure 19 *The mRNA abundance of bone morphogenetic protein 4 (BMP4) and its receptors in CFSC-8B and WB-F344 cells.* RT-PCR analysis demonstrated the presence of mRNAs for BMP4, BMPR1A and BMPRII in both WB-F344 and CFSC-8B cells. Bone marrow stromal cells were used as a positive control and negative control is the reaction without reverse transcriptase. M: Marker, 1: CFSC-8B, 2: WB-F344 3: Positive control, 4: Negative Control.

2.2.2 Effect of BMP4 on differentiation of WB-F344 cells

The differentiation of WB-F344 cells was assessed by examination of several hepatocyte and cholangiocyte marker genes. As shown in Figure 20, after treatment with BMP4 (50ng/ml) for 8 days, albumin (mid-hepatic marker), G6Pase and TAT (late hepatic markers) were all expressed in WB-F344 cells, whereas fetoprotein (early hepatic marker) could not be detected (data not shown). In terms of cholangiocyte markers, CK-19 and β4-integrin were not detectable. The pattern of marker genes expression indicated that BMP4 could promote the differentiation of WB-F344 cells toward hepatic lineage. As a positive control, dexamethasone also induced hepatic marker genes expression. Moreover, there was a synergetic action between BMP4 and dexamethasone in the induction of WB-F344 cells differentiation toward hepatocytes. Furthermore, specificity of BMP4 activity on WB-F344 cells differentiation was evaluated by employing a specific inhibitor of BMP4 - Noggin, which was able to block the effect of BMP4 on hepatic marker genes expression in WB-F344 cells.

The effect of BMP4 on WB-F344 cells was also examined by employing recombinant adenovirus vectors carrying BMP4 cDNA or oligonucleotide encoding shRNA against BMP4, which were constructed in our laboratory. After infection of WB-F344 cells with adenovirus containing BMP4, BMP4 protein level was significantly increased in the cytoplasmic compartment (Figure 21A). Expression of hepatocyte and cholangiocyte markers were examined after infection of WB-F344 cells with recombinant adenoviruses as shown in Figure 21B. There were significant increases in mRNA abundance of hepatocyte markers while no cholangiocyte markers were detected. After infection of cells with adenovirus containing oligonucleotide encoding shRNA against BMP4, the

differentiation of WB-F344 cells was blocked. The protein level of albumin was also examined as shown in Figure 23. A dose dependent increase in albumin protein levels was observed after infection of WB-F344 cells with adenovirus carrying BMP4 cDNA.

Figure 20 *Effect of BMP4 on the differentiation of WB-F344 cells.* WB-F344 cells were treated with BMP4 (50ng/ml), dexamethasone (10^{-7}M), Noggin (200ng/ml) or cotreated with BMP4 and dexamethasone or BMP4 and Noggin for 8 days. Total RNA was extracted as described in Materials and methods. The expression of hepatocyte markers (Albumin, TAT-1, and G6Pase) and cholangiocyte markers (CK-19 and β4-integrin) were determined by using RT-PCR analysis. GAPDH was used for loading control and liver cells were used as positive control. The lower part displays the density histogram data from three-separated RT-PCR analysis (mean±SE), which represents the relative expression of albumin, G6Pase and TAT-1, respectively. *indicates $P<0.05$ between treated and control groups. **indicates $P<0.001$ between treated and control groups. M: Marker, 1: Control, 2: BMP4 (50ng/ml), 3: Dexamethasone (10^{-7}M), 4: BMP4+Dexamethasone, 5: Noggin (200ng/ml), 6: Noggin+ BMP4, 7: Positive control, 8: Negative Control.

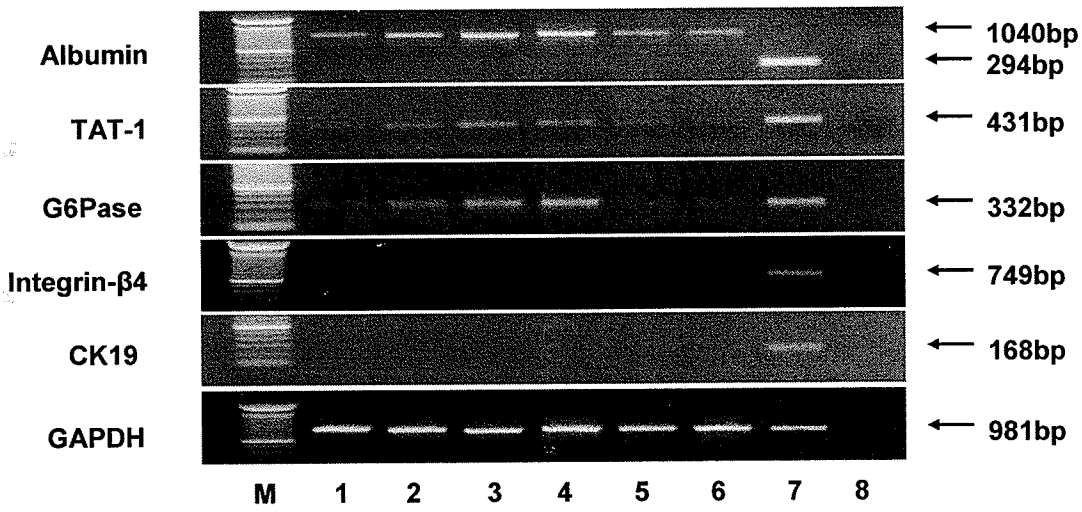
Albumin
TAT-1
G6Pase
Integrin-β4
CK19
GAPDH
1040bp
294bp
431bp
332bp
749bp
168bp
981bp
M 1 2 3 4 5 6 7 8

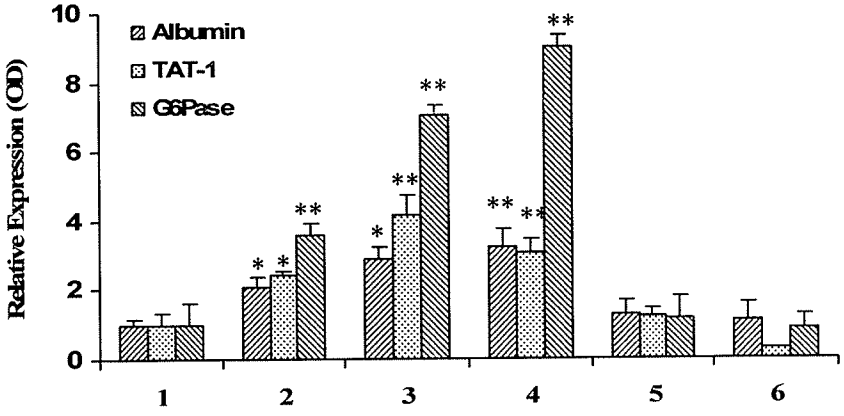
Albumin
TAT-1
G6Pase
Relative Expression (OD)
10
8
6
4
2
0
1 2 3 4 5 6

Figure 21 ***A:*** *Western blot analysis of BMP4 expression in WB-F344 cells after infection of adenovirus containing BMP4 cDNA.* WB-F344 cells were infected with adenovirus containing BMP4 cDNA for 72hr. Western blot was performed as described in Materials and methods. Ad-GFP was used as vector control. C: control; GFP: green fluorescent protein; CFU: colony forming unit. ***B:*** *RT-PCR analysis of the expression of hepatocyte and cholangiocyte markers in WB-F344 cells after infection of adenovirus containing either BMP4 cDNA or oligonucleotide encoding shRNA against BMP4.* WB-F344 cells were infected with adenovirus with 5cfu/cell for 72hrs. Total RNA was extracted for RT-PCR as described in Materials and methods. GAPDH was used for loading control and liver cells were used as positive control. Ad-GFP and Ad-non-silencing shRNA were used as vector control. The lower part displays the density histogram data from three-separated RT-PCR analysis (mean±SE), which represents the relative expression of albumin, G6Pase and TAT-1, respectively. **indicates $P<0.001$ between Ad-BMP4 and Ad-GFP treated groups or Ad-shRNA and Ad-non-silencing shRNA treated groups. M: Marker; 1: Control, 2: Ad-GFP; 3: Ad-BMP4; 4: Ad- shRNA; 5: Ad- non-silencing shRNA; 6: Positive control; 7: Negative control.

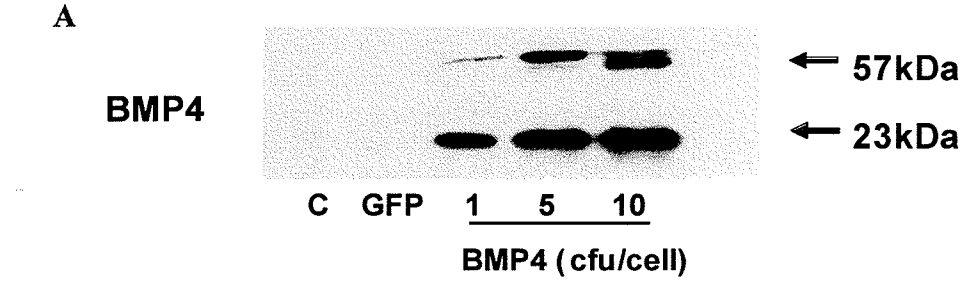
A
BMP4
57kDa
23kDa
C GFP 1 5 10
BMP4 (cfu/cell)

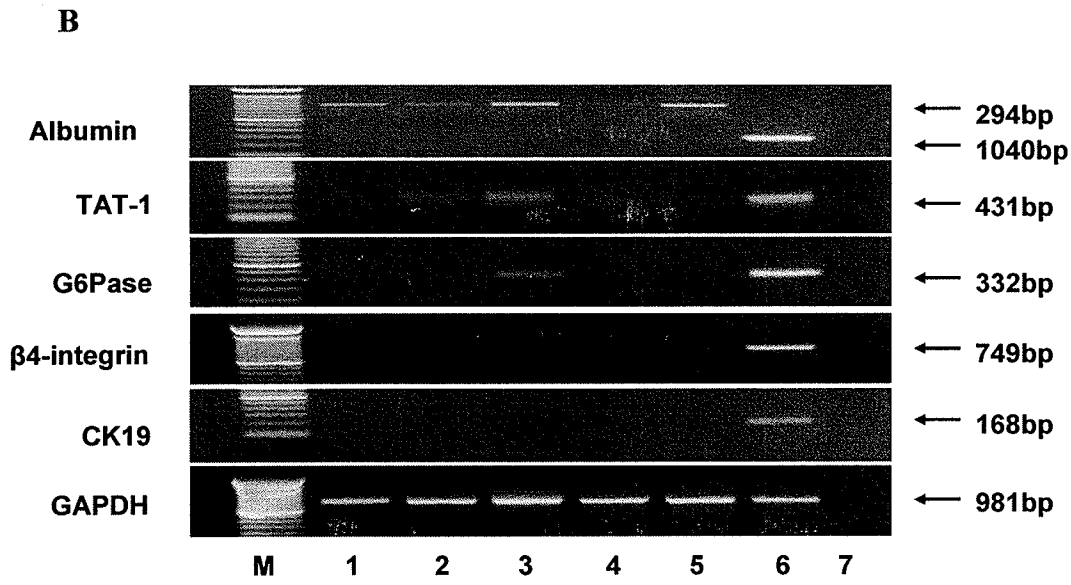
B
Albumin
TAT-1
G6Pase
β4-integrin
CK19
GAPDH
294bp
1040bp
431bp
332bp
749bp
168bp
981bp
M 1 2 3 4 5 6 7

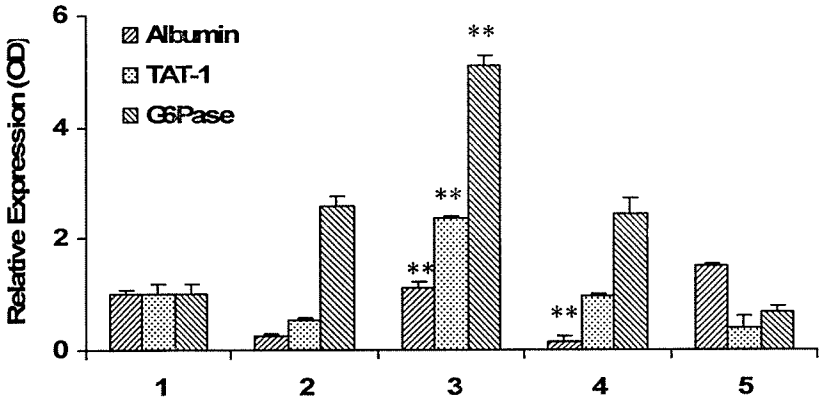
Albumin
TAT-1
G6Pase
Relative Expression (OD)
0
2
4
6
1 2 3 4 5
**

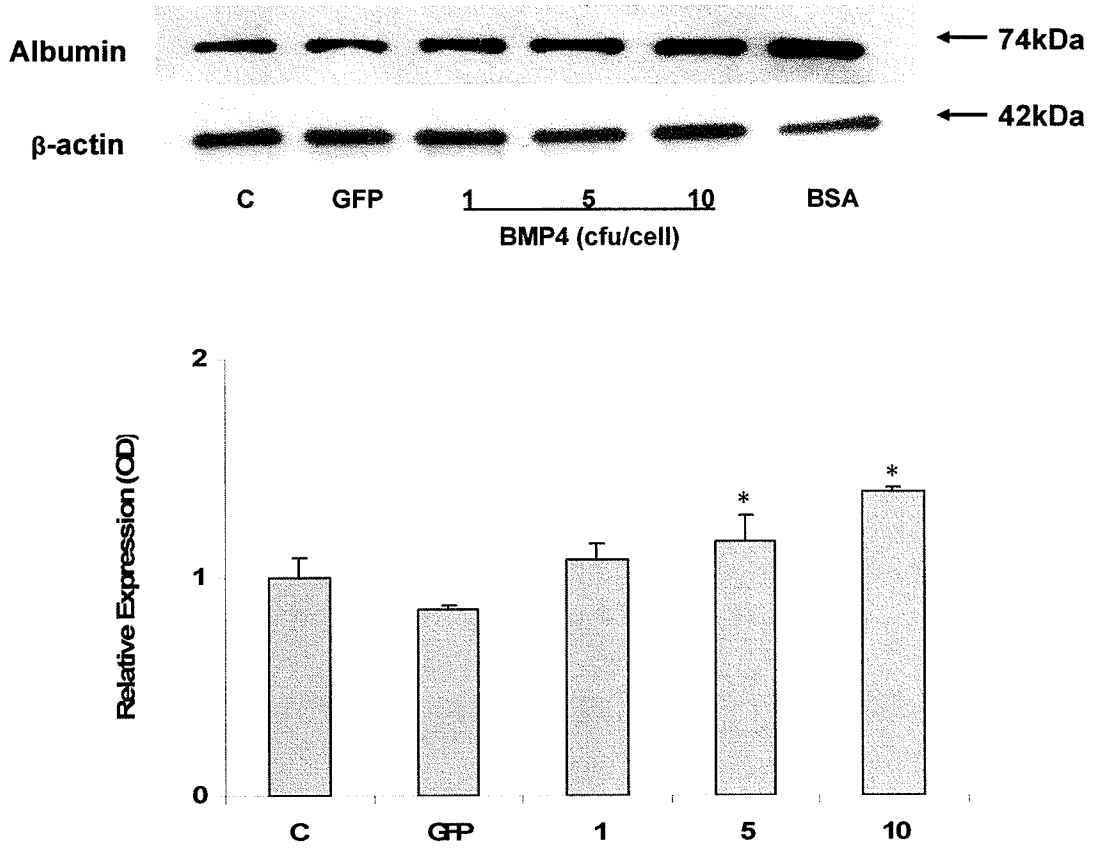

Figure 22 *Western blot analysis of albumin expression in WB-F344 cells after infection with adenovirus containing BMP4 cDNA.* Cells were infected with adenovirus for 72hrs. Western blot was performed as described in Materials and methods. The β-actin was used for loading control and bovine serum albumin was used as positive control. Ad-GFP was used as vector control. The lower part displays the density histogram data from three-separated western blot analysis (mean±SE). *indicates $P<0.05$ between Ad-GFP and Ad-BMP4 treated groups. C: control; GFP: green fluorescent protein; CFU: colony forming unit.

2.2.3 Co-culture of WB-F344 cells with hepatic stellate cells

To examine whether BMP4 released from HSCs could affect WB-F344 cells differentiation, we co-cultured HPCs and HSCs in a dish for one week. The BMP4 inhibitor Noggin was also used in some dishes. After one week, total RNA was extracted and the mRNA abundances of hepatocyte and cholangiocyte markers were examined by RT-PCR analysis. As shown in Figure 23, expression of albumin and G6Pase in both WB-F344 cells and CFSC-8B cells were seen, however a significant increase in albumin, G6Pase and TAT-1 mRNAs were observed after co-culture of these two kinds of cells. Moreover, Noggin significantly inhibited the increase in albumin, G6Pase and TAT-1 expression in the co-cultured cells.

Figure 23 *RT-PCR analysis of the expression of hepatocyte and cholangiocyte markers in WB-F344 cells, CFSC-8B cells and the co-cultured cells..* CFSC-8B cells ($1X10^3$) and WB-F344 cells ($1X10^4$) were mixed and cultured in a 35mm well in serum free MEM medium for 1 week, or they were cultured in the same medium individually for 1 week. Total RNA was extracted for RT-PCR as described in Materials and methods. The top part displays a typical agarose gel picture of different hepatocyte and cholangiocyte markers expression. GAPDH was used as loading control and liver cells were used as positive control. The lower part represents the density histogram data (mean±SE) from three separate experiments. **indicates $P<0.001$ between cocultured cells and individually cultured WB-F344 cells. ## indicates $P<0.001$ between cocultured cells and cocultured cells with treatment of Noggin. M: Marker, 1: WB-F344 cells, 2: CFSC-8B cells, 3: CFSC-8B+WB-F344 cells, 4: CFSC-8B+WB-F344 cells +Noggin (200ng/ml), 5: WB-F344+Noggin (200ng/ml), 6: Positive control, 7: Negative control.

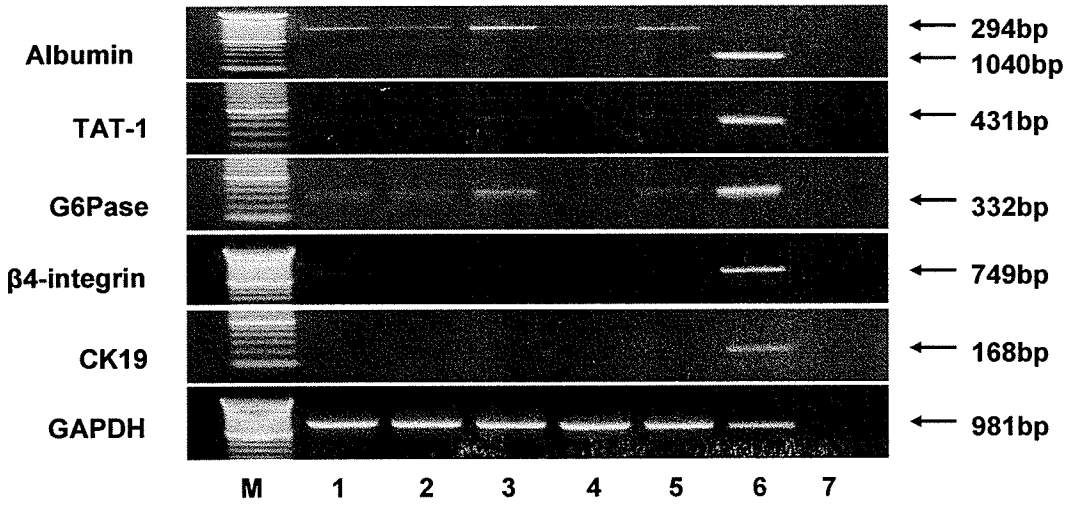
Albumin
TAT-1
G6Pase
β4-integrin
CK19
GAPDH
294bp
1040bp
431bp
332bp
749bp
168bp
981bp
M 1 2 3 4 5 6 7

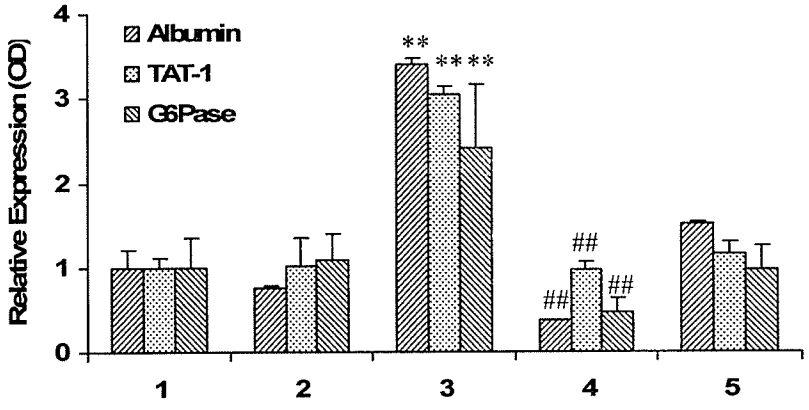
Albumin
TAT-1
G6Pase
Relative Expression (OD)
0
1
2
3
4
1 2 3 4 5
**
****
##
##
##

2.2.4 Autocrine regulation of BMP4 and intracellular signaling pathways of BMP4 in WB-F344 cells

During these experiments, an interesting phenomenon observed was that BMP4 could stimulate the expression of BMP4 gene in WB-F344 cells. When WB-F344 cells were incubated with BMP4, there was a significant increase in BMP4 mRNA abundance whereas the mRNA levels of BMP4 receptors - BMPR1A and BMPRII remained unchanged (Figure 24A). The self-up-regulation of BMP4 indicates a function of BMP4 as autocrine factor to sustain the effect of BMP4 on WB-F344 cells differentiation toward hepatocyte lineage.

It is known that in order to function as a cytokine, BMP4 needs to activate its intracellular signaling pathways. There are two well-known intracellular signaling pathways involved in BMP4 signal transduction. One is the typical Smad pathway and the other is the MAPK pathway. By employing WB-F344 cells, we examined the expression and phosphorylation of Smad1, ERK1/2, p38 and JNK1/2. As shown in Figure 24B, BMP4 led to phosphorylation of Smad1 after 5 minutes treatment, and then the phosphorylation of Smad1 was rapidly returned to its basic level. The rapidly activated Smad1 might act as an important signaling molecule to induce the hepatic marker genes expression in WB-F344 cells. Three MAPKs were examined in WB-F344 cells after BMP4 treatment. As shown in Figure 24B, BMP4 induced a phosphorylation of ERK1/2 after 15 minutes treatment and the phosphorylation of ERK1/2 was sustained up to 2 hours. In addition, BMP4 had no effect on the phosphorylation of p38 and JNK1/2 in WB-F344 cells.

A

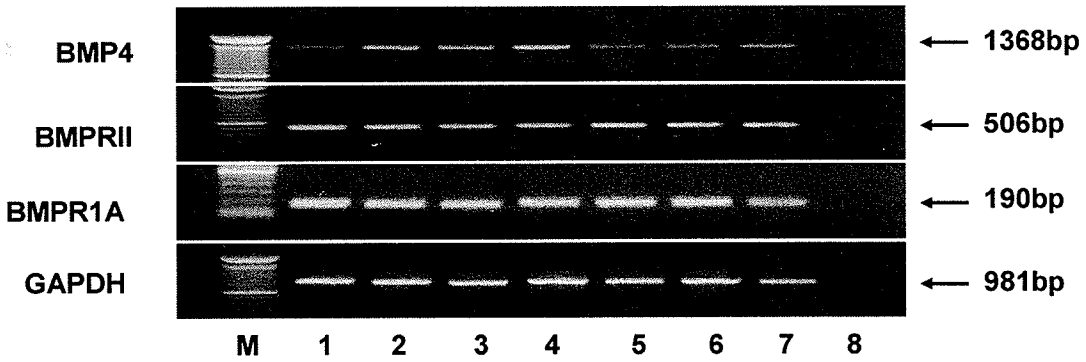
BMP4
BMPRII
BMPR1A
GAPDH
1368bp
506bp
190bp
981bp
M 1 2 3 4 5 6 7 8

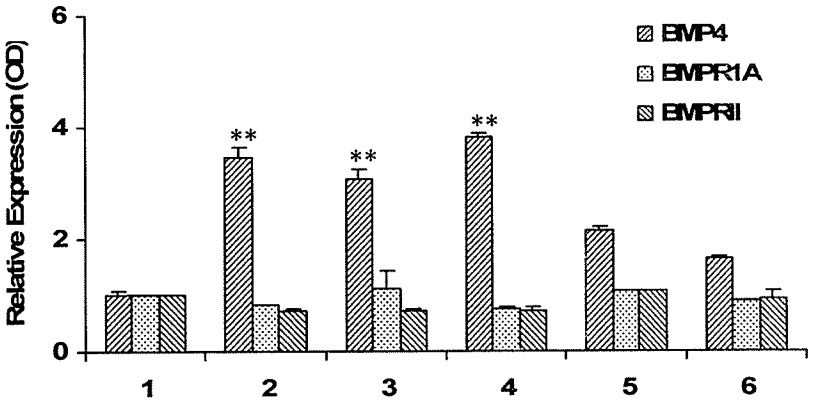
Relative Expression (OD)
BMP4
BMPR1A
BMPRII
**
**
**
0
2
4
6
1 2 3 4 5 6

B

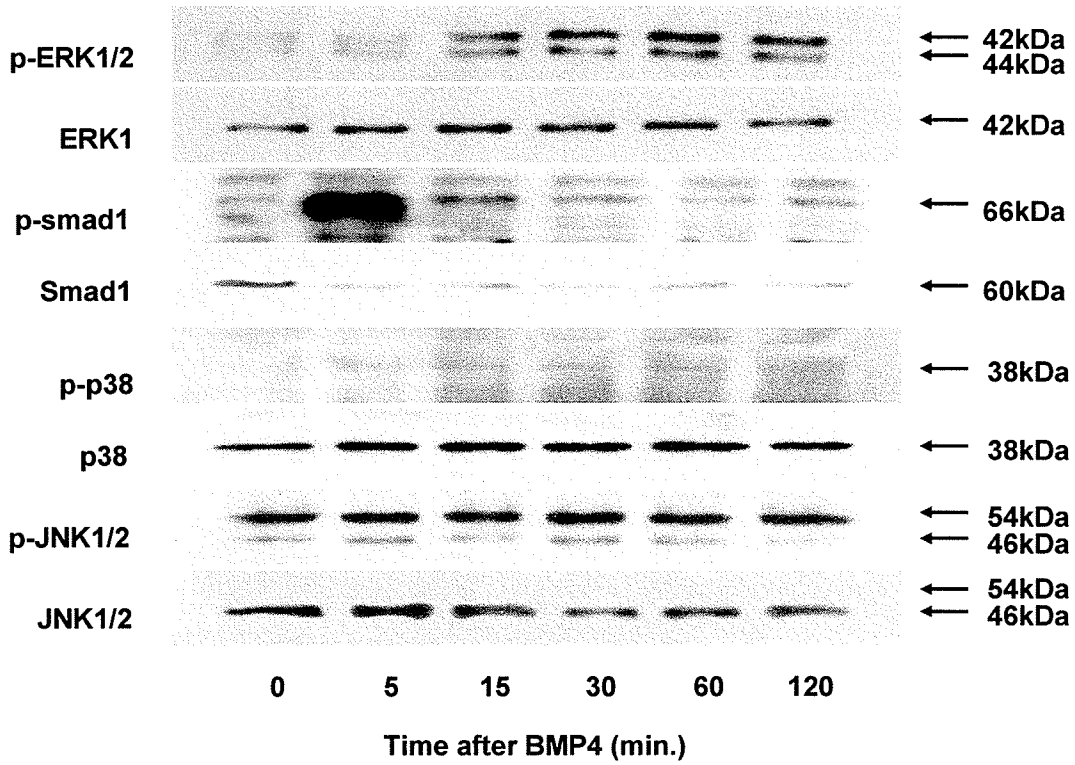
p-ERK1/2
ERK1
p-smad1
Smad1
p-p38
p38
p-JNK1/2
JNK1/2
42kDa
44kDa
42kDa
66kDa
60kDa
38kDa
38kDa
54kDa
46kDa
54kDa
46kDa
0
5
15
30
60
120
Time after BMP4 (min.)

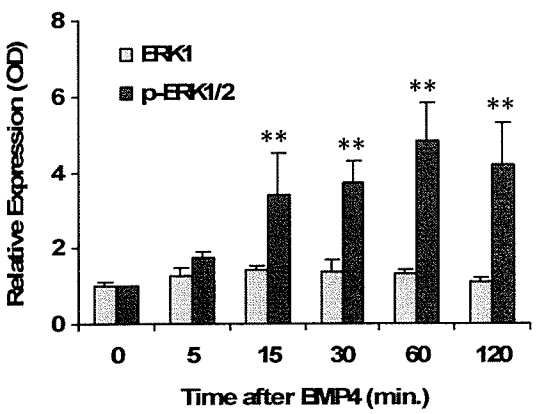
Relative Expression (OD)
ERK1
p-ERK1/2
**
**
**
**
0
5
15
30
60
120
Time after BMP4 (min.)

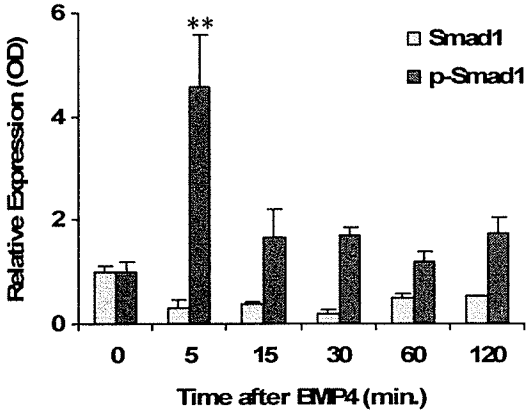
Relative Expression (OD)
Smad1
p-Smad1
**
0
5
15
30
60
120
Time after BMP4 (min.)

2.2.5 BMP4 regulation on C/EBP transcription factors expression in WB-F344 cells

CCAAT enhancer binding proteins (C/EBPs) are a family of transcription factors, which play an important role in cell differentiation (Rao, Yukawa et al., 1996). In order to understand BMP4 regulation on HPC differentiation and hepatocytes marker gene expression, we examined the effect of BMP4 on the expression of C/EBP members such as C/EBPα, C/EBPβ, C/EBPγ and C/EBPδ in WB-F344 cells by semiquantitative RT-PCR. As shown in Figure 25A, expression of C/EBPα mRNA level was not detectable in undifferentiated WB-F344 cells. After treatment with BMP4 at different time intervals, the C/EBPα mRNA level was rapidly upregulated at 24 hrs, and declined somewhat at 48 hrs. However, mRNA levels of other C/EBPs (C/EBPβ, C/EBPγ and C/EBPδ) remained unchanged after BMP4 treatment, indicating a lesser role of these C/EBPs in BMP4 regulation on WB-F344 cells differentiation. As a positive control for differentiation of HPCs toward hepatic lineage, dexamethasone also stimulated the expression of C/EBPα but not other C/EBPs. Moreover, the regulation of C/EBPα gene expression by BMP4 and dexamethasone was not mutually promoted. The protein level of C/EBPα was further examined by using western blot analysis after BMP4 treatment. As shown in Figure 25B, after treatment with BMP4 for 0, 2, 3, 4, and 5 days, there was a gradual increase in all isoforms of C/EBPα from 30 to 42 kDa in the nuclear of WB-F344 cells.

Figure 25 ***A:*** *RT-PCR analysis of mRNA levels of hepatic transcription factors, C/EBPα, C/EBPβ, C/EBPγ and C/EBPδ, in WB-F344 cells stimulated with or without BMP4 (50 ng/ml).* WB-F344 cells were treated with BMP4 (50ng/ml) and total RNA was extracted at different time points as indicated. The top part represents typical agarose gel pictures of hepatic transcription factors expressions after treatment with BMP4. The lower part displays the density histogram data from three-separated experiments (mean±SE), which represents the relative expression of C/EBPα mRNA. Liver cells were used as positive control. GAPDH was used for loading control. **indicates $P<0.001$ between treated and control groups. M: Marker, C: Control, 1: BMP4 (50ng/ml), 2: Dexamethasone (10^{-7}M), 3: BMP4+Dexamethasone, P: Positive control, N: Negative Control. **B:** *Western blot analysis of protein level of C/EBPα in WB-F344 cells stimulated with or without BMP4 (50 ng/ml).* Nuclear proteins were isolated from WB-F344 cells at different time points as indicated. Expression of C/EBPα was analyzed by Western blot as described in Materials and methods. Histone was used for loading control. The top part represents typical Western blot of C/EBPα. The lower part displays the density histogram data from three-separated Western blot analysis (mean±SE). * indicates $P<0.05$ between treated and control groups.

A

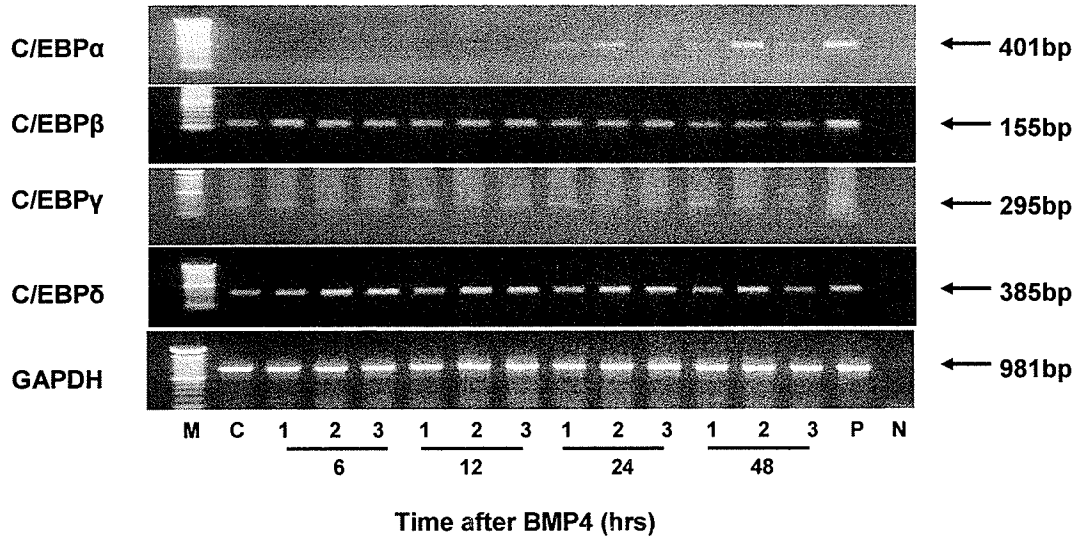
C/EBPα
C/EBPβ
C/EBPγ
C/EBPδ
GAPDH
401bp
155bp
295bp
385bp
981bp
M C 1 2 3 1 2 3 1 2 3 1 2 3 P N
6
12
24
48
Time after BMP4 (hrs)

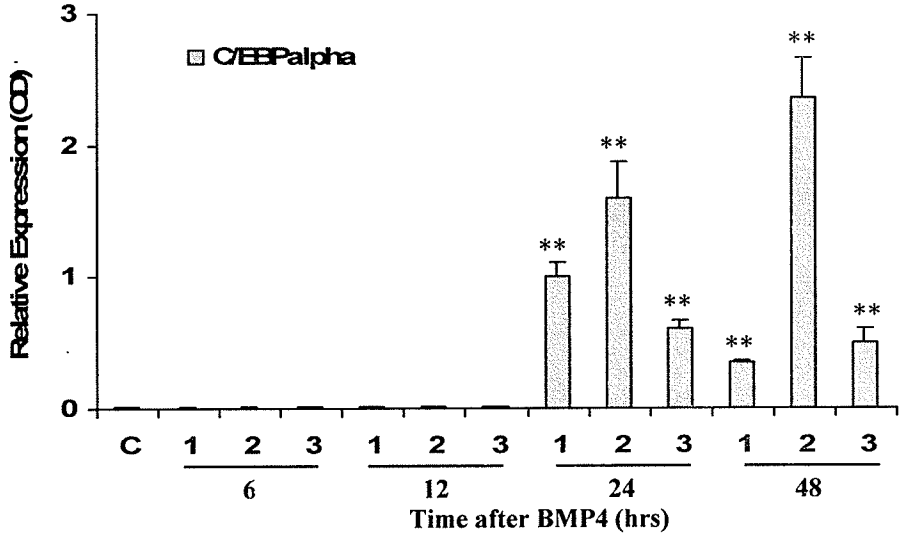
C/EBPalpha
Relative Expression (OD)
0
1
2
3
**
C 1 2 3 1 2 3 1 2 3 1 2 3
6
12
24
48
Time after BMP4 (hrs)

B

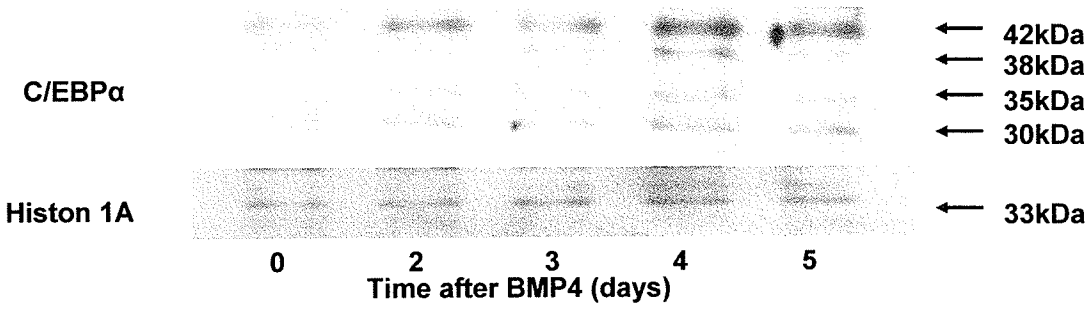
C/EBPα
Histon 1A
42kDa
38kDa
35kDa
30kDa
33kDa
0
2
3
4
5
Time after BMP4 (days)

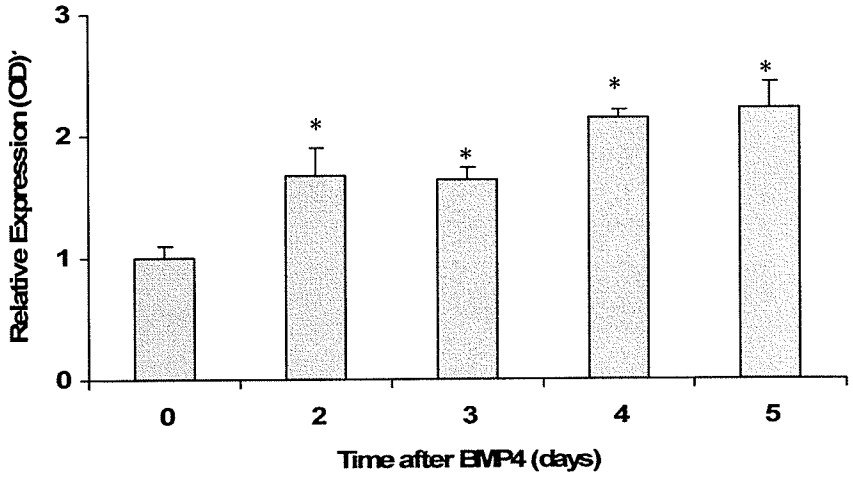
Relative Expression (OD)
3
2
1
0
*
*
*
*
0
2
3
4
5
Time after BMP4 (days)

2.2.6 Effect of BMP4 on DNA binding activity of C/EBPα in WB-F344 cells

In order to know whether BMP4 induced C/EBPα has functional activity, we examined the effect of BMP4 on DNA binding activity of C/EBPα in WB-F344 cells by electrophoretic mobility shift assay (EMSA). Consensus C/EBP responsive element and mutated C/EBP responsive element were employed in this experiment. Nuclear extracts from WB-F344 cells after treatment with BMP4 for 0, 3, 4, and 5 days were obtained and incubated with these C/EBP elements. As shown in Figure 26, several gel-shift bands were observed. However, only the top band marked as C1 was specific to C/EBPα because with cold C/EBP consensus probe and antibody, there is a significant repletion of C1 band. Moreover, the mutated cold C/EBP probe could not deplete the protein DNA binding band. However, the confirmation of C/EBPα DNA binding will be investigated in the future with help of proteomic techniques. Furthermore, other bands (C2 and C3) could be the DNA binding of other members of C/EBP family, which could be confirmed with specific antibodies against other members of C/EBP family.

Figure 26 *Effect of BMP4 treatment on DNA binding activity of C/EBPα in WB-F344 cells as measured by electrophoretic mobility shift assay (EMSA).* Nuclear proteins were isolated from WB-F344 cells after treatment with BMP4 (50ng/ml) for 3 to 5 days as described in Materials and methods. EMSA was conducted using a 22-mer oligonucleotide containing C/EBP binding site. The figure showed a representative EMSA gel of protein binding to the consensus C/EBP-binding DNA oligonucleotide. All lanes contained 8μg of nuclear extract and 0.05pmol of labeled C/EBP-binding DNA. The C/EBP proteins present in the complex were identified by supershift assay, which was carried out by incubating the nuclear extract (with BMP4 treatment for 4 days) with the polyclonal antibody (2 μg each) directed against C/EBPα, whereas competition assays were performed with unlabeled C/EBP oligonucleotide (100 or 200-fold molar excess) or unlabeled mutant C/EBP oligonucleotide (200-fold molar excess). The C/EBPs and the non-specific (NS) complexes are indicated. C1: Complex 1; C2: Complex 2; C3: Complex 3; NS: Non-specific shift band; FP: Free probe.

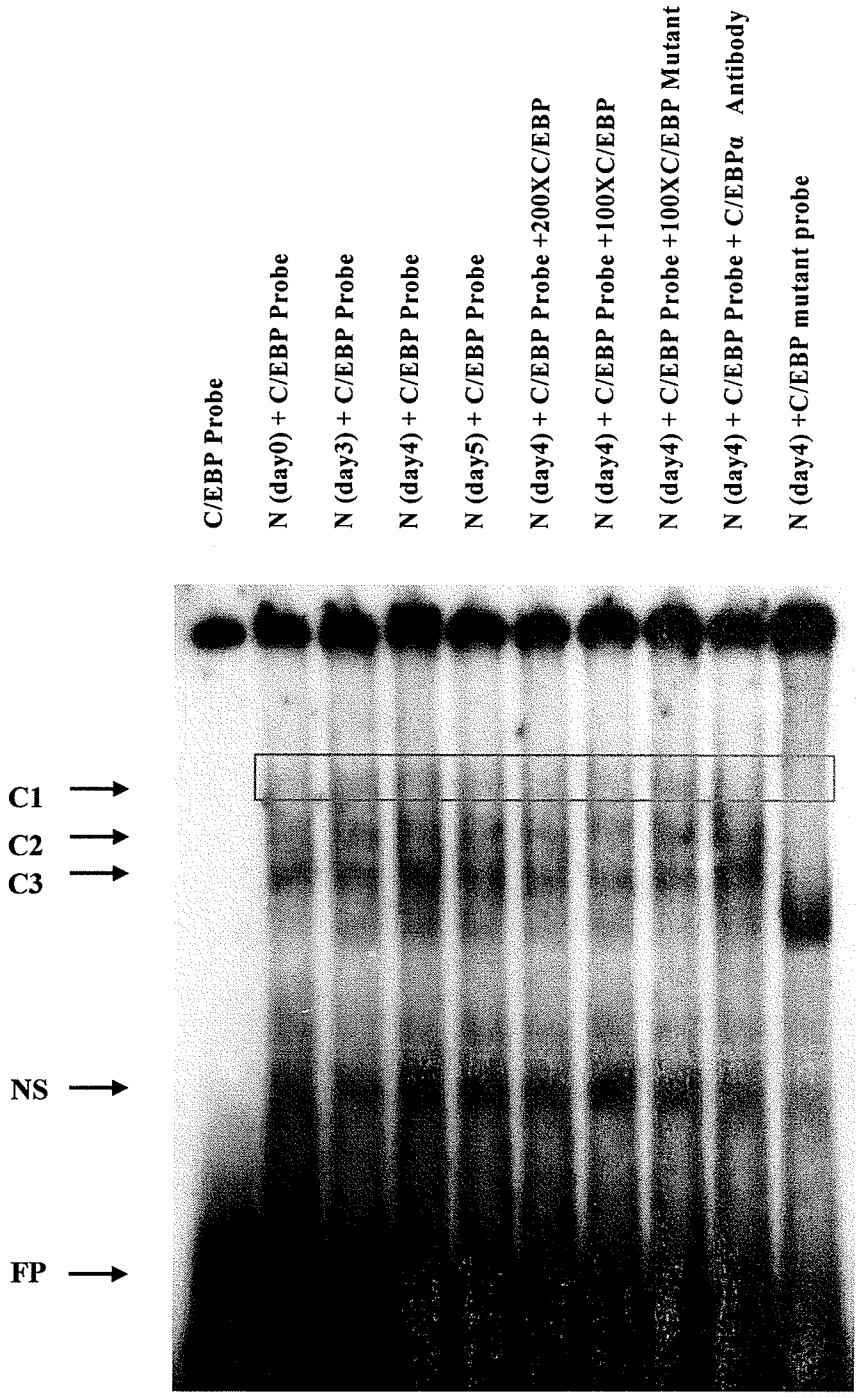
C/EBP Probe
N (day0) + C/EBP Probe
N (day3) + C/EBP Probe
N (day4) + C/EBP Probe
N (day5) + C/EBP Probe
N (day4) + C/EBP Probe +200XC/EBP
N (day4) + C/EBP Probe +100XC/EBP
N (day4) + C/EBP Probe +100XC/EBP Mutant
N (day4) + C/EBP Probe + C/EBPα Antibody
N (day4) +C/EBP mutant probe
C1
C2
C3
NS
FP

2.2.7 Effect of BMP4 on WB-F344 cell proliferation

The aforementioned studies indicated a role of BMP4 in WB-F344 cell differentiation. But what is the effect of BMP4 on WB-F344 cell proliferation. A preliminary experiment employing WST-1 proliferation reagent revealed that BMP4 could stimulate WB-F344 cell proliferation under *in vitro* culture condition (Figure 27). The effect of BMP4 on WB-F344 cell proliferation was time and dose dependent. With concentrations of 50 and 100ng/ml, BMP4 significantly stimulated WB-F344 cell proliferation after 3 and 6 days treatment while there was no stimulative effect of BMP4 on WB-F344 cell proliferation when the concentrations were at 0.5, 1.5 and 10ng/ml.

Figure 27 *Effect of BMP4 on the proliferation of WB-F344 cells.* WB-F344 cells were incubated with different concentration of BMP4 (0-100ng/ml) for 1, 3, 6 and 9 days. Cell proliferation was determined by using WST-1 reagent. The data represent mean±SE from 8 wells. *indicates $P<0.05$ between control (0ng/ml) and BMP4 treated groups.

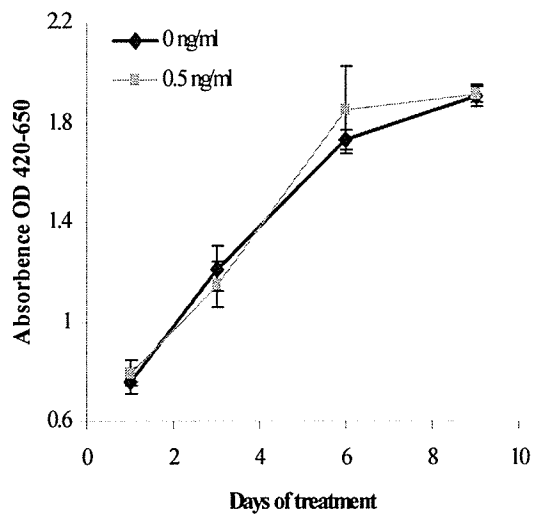
0 ng/ml
0.5 ng/ml
Absorbence OD 420-650
Days of treatment

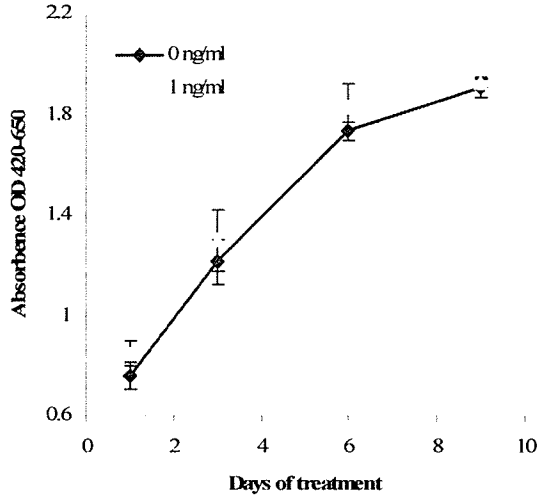
0 ng/ml
1 ng/ml
Absorbence OD 420-650
Days of treatment

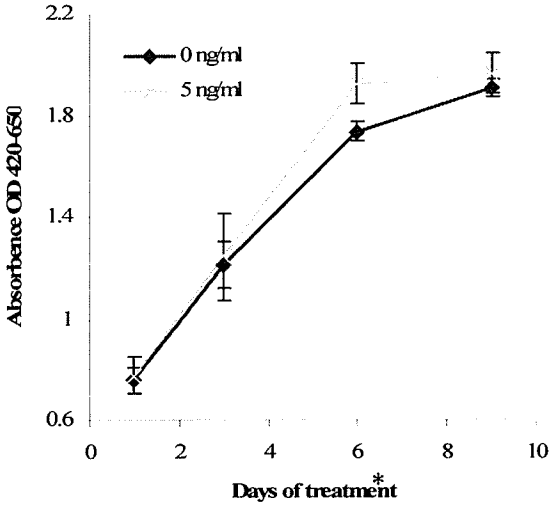
0 ng/ml
5 ng/ml
Absorbence OD 420-650
Days of treatment

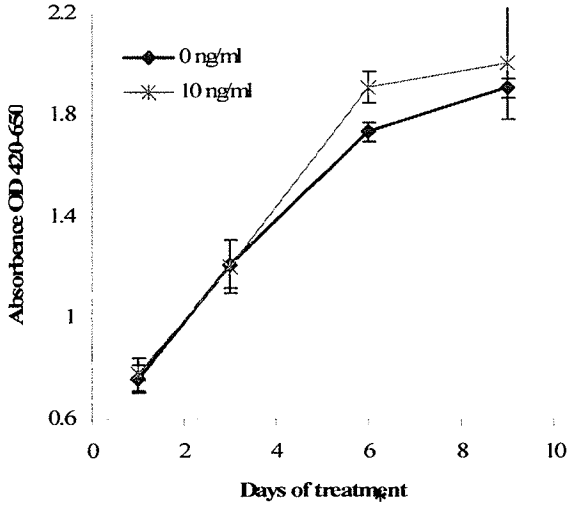
0 ng/ml
10 ng/ml
Absorbence OD 420-650
Days of treatment

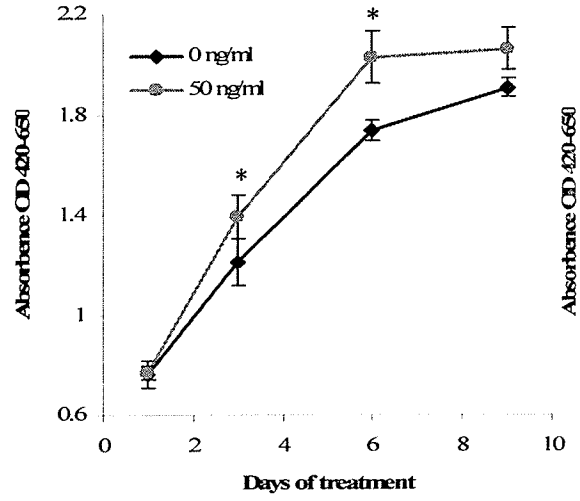
0 ng/ml
50 ng/ml
Absorbence OD 420-650
Days of treatment

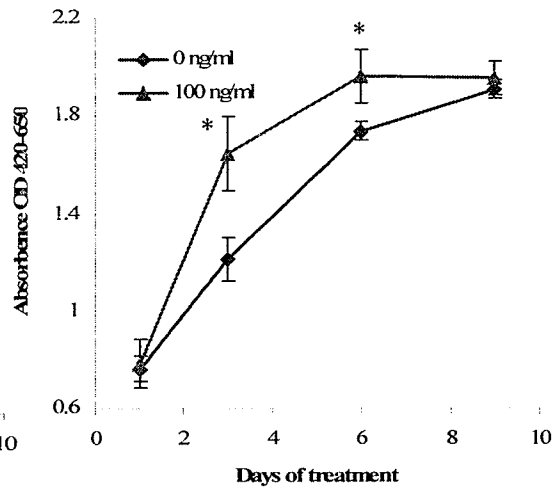
0 ng/ml
100 ng/ml
Absorbence OD 420-650
Days of treatment

2.3 Discussion

Hepatic stem cells (progenitor cells for human or oval cells for rat) are located at the end of biliary duct, the so-called the canals of Hering. According to the concept of stem cells, the areas around the canals of Hering are considered as niche, which converts the signals from these areas to hepatic stem cells and influences the self-renewal of stem cells. Self-renewal of stem cells features the controlled proliferation and differentiation of stem cells. From this point, current studies identified a very important role of BMP4 in HPCs self-renewal. BMP4 stimulates not only hepatic oval cell differentiation toward hepatocyte lineage but also cell proliferation.

Our early consideration of this project is to investigate the effect of BMP4 secreted from HSCs on HPC proliferation and differentiation. The reason that HSCs and HPCs are in close proximity to each other is that during hepatic fibrosis there is a earlier so-called "ductual response" or "oval cell response", which indicates the proliferation of hepatic oval cells in rat model of liver fibrosis (Theise, Saxena et al., 1999). However, the mechanism of oval cell response is still unknown. Since it was demonstrated that HSCs are in direct contact with the canals of Hering through small gaps of the basement membrane in the liver (Paku, Schnur et al., 2001) and the elevated BMP4 expression was found in fibrotic liver and activated HSCs, we initiated the study to investigate the role of BMP4 on HPCs and found that BMP4 could induce WB-F344 cell differentiation toward hepatocytes. This finding was confirmed by not only incubation with recombinant BMP4 but also with adenovirus-delivered BMP4. Moreover, the specificity of BMP4 in the stimulation of WB-F344 cell differentiation was confirmed by employing a specific BMP4 inhibitor – Noggin. Furthermore, we also confirmed that BMP4 secreted from

HSCs could stimulate HPC differentiation and the effect of BMP4 from HSCs could be blocked by BMP4 specific inhibitor (Noggin). In addition to BMP4 induction of hepatic stem cell differentiation, we also demonstrated that BMP4 could stimulate WB-F344 cell proliferation. This finding could have an important impact on our understanding of hepatic cancer stem cells. It is documented that hepatocellular carcinoma could be derived from the stem cells either from the bone marrow or the liver (Sell, 2004; Burkert, Wright et al., 2006). Moreover, for stem cell to become malignant phenotype, there is a need to break down normal self-renewal process in favor of un-controlled proliferation, which can be influenced by factors secreted from niche (Hagymasi, Molnar et al., 2007) . However, further research is required to confirm our hypothesis that BMP4 plays a carcinogenetic role in hepatic stem cells.

Our results indicated that BMP4 has the capability to induce differentiation of WB-F344 cells toward hepatocyte in the *in vitro* culture condition. However, there are still some issues that could not be resolved from the current study. First, the early phase gene (AFP) of hepatic differentiation could not be detected in WB-F344 cells after treatment with BMP4; Second, the expression of mid phase gene (albumin) and late phase genes (G6Pase and TAT) was remained at a relative high level after BMP4 treatment. Whether these observations indicated that BMP4 could initiate the differentiation of WB-F344 cells, and further promote the hepatic lineage progression to pass through the early phase and then went to the mid-late phase is still not clear. A controversial result was also observed in a paper published in 2004, which suggested that acidic fibroblast growth factor (aFGF) could significantly induce the expression of albumin in differentiating human embryonic stem cells, whereas basic fibroblast growth factor (bFGF), HGF and

BMP4 did not have significant effect on cell differentiation (Lavon, Yanuka et al., 2004). This different observation could be due to different differentiation stage of stem cells (embryonic stem cells versus hepatic stem cells) or different expression pattern of specific surface receptors for hepatogenic-promoting factors (Heng, Yu et al., 2005).

Dexamethasone was shown to inhibit DNA synthesis and promote hepatic stem cells differentiation through PIP3 signaling pathway (Dasgupta, Hughey et al., 2005). In current studies, dexamethasone also induced the expression of hepatic markers in WB-F344 cells and the expression of C/EBPα, which is one of transcription factors involved in regulation of albumin gene expression (Takiguchi, 1998). Although co-treatment of WB-F344 cells with both BMP4 and dexamethasone did not synergistically stimulate the expression of C/EBPα, co-treatment with BMP4 and dexamethasone did increase the mRNA abundance of hepatic markers. Possibility of the mechanisms is that BMP4 and dexamethasone may mutually stimulate the expression of hepatic markers through other transcription factors.

One interesting observation was noticed regarding the transcription of albumin in the current studies. By designing a pair of primers for RT-PCR analysis of albumin, an unexpected size of amplified band was observed. A 746 bp insert was present at mRNA sequence between exon 8 and exon 9 because the primers we designed were located at the exon 8 and exon 9. After sequencing the 746 bp insert, it revealed that the sequence completely matched the sequence of intron 8-9 of albumin and there was no mutation and deletion. An exon skipping was reported in the case where a 7-base-pair deletion at the splice donor site of intron 8-9 of the albumin gene would result in the skipping of exon 9 during RNA splicing in Nagase analbuminemic rats (Shalaby and Shafritz, 1990). To

exclude possible genomic contamination during PCR, we also designed another pair of primers located at exon 3 and exon 4. There was no genomic contamination observed. Although the exact mechanism could not be delineated, it could be that the albumin mRNA process is different in WB-F344 cells and mature hepatocytes.

Our data showed that there were expression of BMP4 and its receptors in WB-F344 cells and HSCs increased expression of BMP4 in fibrotic liver and activated HSCs. It is possible that BMP4 could be a cytokine playing autocrine and paracrine functions between HSCs and WB-F344 cells. By employing a co-culture system and BMP4 antagonist (Noggin), it was demonstrated that BMP4 from HSCs stimulated the differentiation of WB-F344 cells toward hepatocytes. A similar observation has been reported indicating that co-culture of HSCs and liver epithelial (stem-like) cells for 1 week induced liver epithelial (stem-like) cells differentiation toward hepatic lineage (Nagai, Terada et al., 2002). Although other cytokines or growth factors from HSCs could also influence the differentiation of WB-F344 cells (Nagai, Terada et al., 2002; Miura, Nagai et al., 2003), Noggin could reverse the differentiation of WB-F344 cells toward hepatocytes in co-culture system, which indicated the critical role of BMP4 in the differentiation of WB-F344 cells.

Intracellular signaling molecules play an important role in cytokine regulation of cell differentiation and proliferation. It is especially important in the case of BMP4 activity. Since there are two intracellular signaling pathways mediating BMP4 signal transduction, we investigated the role of these signaling pathways in BMP4-induced differentiation of WB-F344 cells. The first and major signaling pathway of BMP4 is the Smad pathway. It has been shown that Smad1 is involved in many stem cells differentiation. BMP4-

activated Smad1 signal pathway could promote an astrocytic cell fate in SVZ neural progenitors and participate in the differentiation process of chondrocytes into bone (Xin, Li et al., 2006). Moreover, BMP4-activated Smad1 trans-located into nucleus and recruited transcription coactivators cAMP responsive element-binding protein (CREB) and p300, which subsequently activated hepatic differentiation gene expression in hepatic stem cells (Suzuki, Raya et al., 2006). Our results demonstrated for the first time that BMP4-activated Smad1 signaling pathway is involved in the hepatic differentiation process of stem cells. The second pathway of BMP4 is the MAPK signal pathway. It has been reported that FGF-activated MAPK/ERK1/2 signaling was responsible for the initiation of hepatic gene expression in embryonic endoderm cells, whereas activation of the PI3K pathway by FGF exerted a proliferative effect on hepatic stem cells in endoderm explants (Okano, Shiota et al., 2003; Calmont, Wandzioch et al., 2006). However, the role of ERK1/2 remains to be further investigated because it has been demonstrated that ERK pathway may be complex and depend on different process of cell differentiation since ERK activated by different mitogens could exert opposite effects in the same stem cells (Bost, Aouadi et al., 2005).

In conclusion, BMP4 could be considered as an efficient candidate that induces the differentiation of WB-F344 cells toward hepatocytes. Moreover, BMP4 secreted from activated hepatic stellate cells may act as a paracrine factor to stimulate WB-F344 cell differentiation.

3. Role of Extracellular Signal-regulated Kinase (ERK) and Protein Kinase C in Heterogeneous Population of Hepatic Stellate Cells

3.1 Introduction

Regression of liver fibrosis and, possibly, cirrhosis has been reported in patients with chronic liver disease and experimental liver fibrosis animal model (Iredale, 2001; Friedman, 2003; Desmet and Roskams, 2004). Specific induction of apoptosis in HSCs may be considered as a possible realistic approach for cell targeted therapy to liver fibrosis. During the past decade, about 60 papers contributed to the study of molecular mechanism involved in HSCs apoptosis. It has been shown that HSCs undergo spontaneous apoptosis during *in vitro* culture (Saile, Matthes et al., 2001). The trans-differentiation of HSCs to myofibroblasts was paralleled by an increased sensitivity to apoptosis (Gong, Pecci et al., 1998). Moreover, some apoptotic systems have been demonstrated in HSCs (Gong, Pecci et al., 1998; Fischer, Cariers et al., 2002; Wang, Zhang et al., 2004; Chen, Wang et al., 2006). However, it is difficult to find a proper reagent, which can selectively induce the apoptosis of α-SMA positive HSCs. The reason for the difficulty is that the difference between survival and apoptotic signals in activated and quiescent HSCs has not yet been identified.

The ERK signaling pathway, also known as the p42/p44 MAP kinase pathway, is a major intracellular signaling pathway to control cell proliferation, differentiation and apoptosis. It has been demonstrated that ERK1/2 signaling generally transduces proliferative (Bridle, Li et al., 2006; Wang, Zhang et al., 2006), and profibrogenic signals in HSCs (Ceni, Crabb et al., 2006; Perez de Obanos, Lopez Zabalza et al., 2006).

However, N-acetyl-L-cysteine-activated ERK signaling provoked a cell cycle arrest in HSCs (Kim, Rhim et al., 2001). Another important intracellular signaling in HSCs is protein kinase C, which has multiple isoforms and is interactive with ERK signaling (Hu and Gereau, 2003; Hu, Glauner et al., 2003). It has been shown that angiotensin-II-induced TIMP-1 expression was mediated through PKC signaling in HSCs (Yoshiji, Kuriyama et al., 2003). Moreover, PKC activators could promote HSCs proliferation but inhibit α-SMA expression (Ramm, Li et al., 2003). The activation of PKC by acetaldehyde enhanced collagen α2(I) promoter activity in HSCs (Anania, Womack et al., 1999). Furthermore, ERK and PKC signaling were always coupled and synergically promoted HSCs activation (Pettersson, Couture et al., 2004; Ceni, Crabb et al., 2006). However, in breast cancer cells (MDA-MB-231), PKC inhibitors could stimulate ERK activation and induce cell apoptosis (Pettersson, Couture et al., 2004). Therefore, in order to understand the role of ERK and PKC signaling in apoptosis of HSCs, the current study investigated the expression of ERK and the regulation of PKC inhibitor on HSCs apoptosis in heterogeneous population of hepatic stellate cell lines including CFSC-8B, 2G, 3H and 5H.

3.2 Results

3.2.1 Morphology of CFSC-8B, 2G, 3H and 5H cells and expression of smooth muscle alpha actin in these cells.

The morphologies of CFSC-8B, 2G, 3H and 5H cells were shown in Figure 28A. CFSC-8B cells show flat and parallel to each other; CFSC-2G cells are small and star shape, whereas CFSC-3H and 5H cells look similar in a disorganized growth pattern. Moreover, CFSC-8B cells grow faster than CFSC-3H and CFSC-5H cells. The mRNA expression of α-SMA (a marker for activated HSCs) was demonstrated in Figure 28B. CFSC-8B and CFSC-2G cells have higher mRNA level of α-SMA than CFSC-3H and CFSC-5H cells. Based on the expression of α-SMA, CFSC-8B and CFSC-2G cells resemble myofibroblast-like HSCs, whereas CFSC-3H and CFSC-5H cells are more like quiescent HSCs.

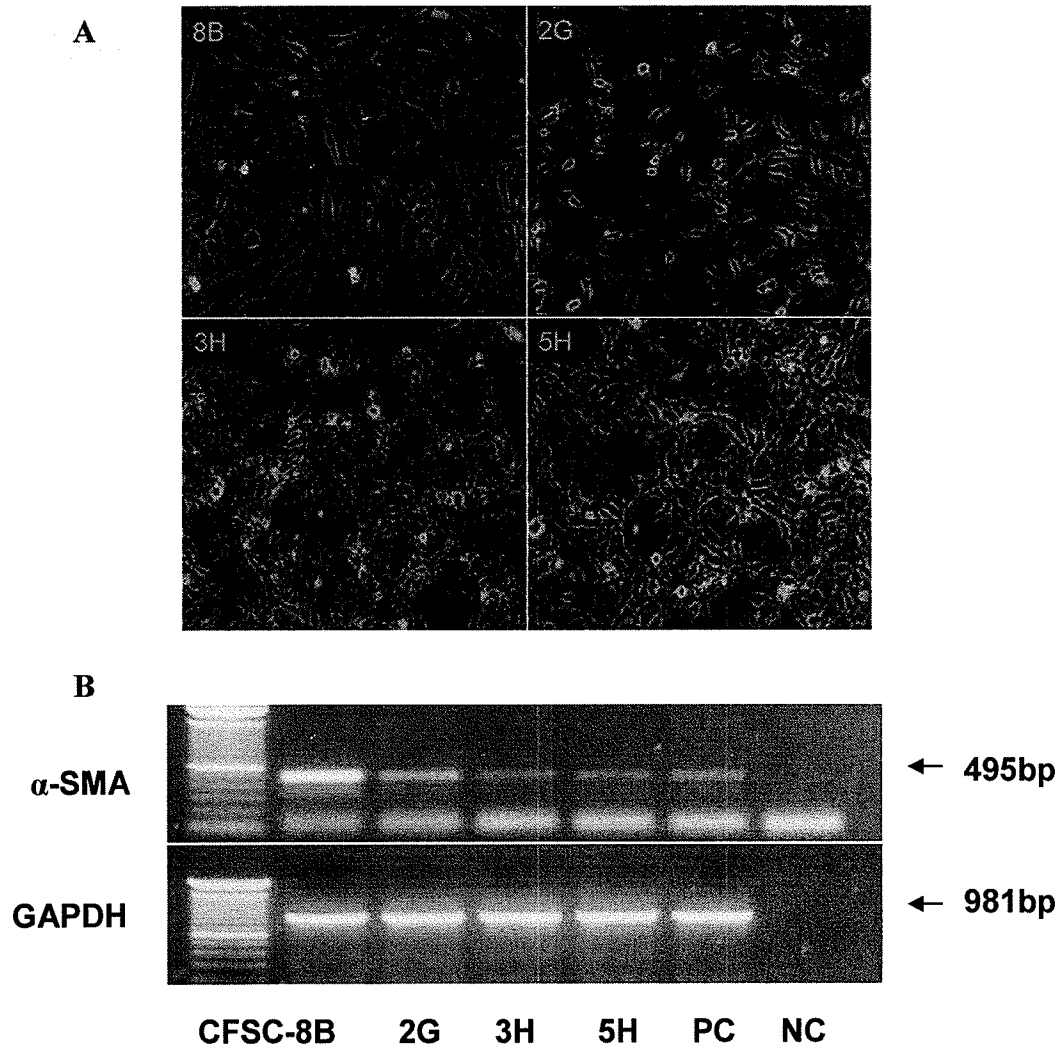

Figure 28 *Morphology of CFSC-8B, 2G, 3H and 5H cells and expression of smooth muscle alpha actin in four HSC clones.* **A:** Cell morphology of four HSC clones at day 2 after plating of cells. Cells were maintained in standard culture medium supplement with 10% FBS. **B:** Total RNA was extracted as described in Materials and methods. Representative ethidium bromide-stained gel demonstrated the abundance of mRNA for α-SMA in four HSC clones. GAPDH was used for loading control.

3.2.2 Effect of staurosporine on heterogeneous population of hepatic stellate cells apoptosis

To investigate the susceptibility of heterogeneous population of HSCs to staurosporine-induced apoptosis, CFSC-8B, CFSC-2G, CFSC-3H and CFSC-5H cells were incubated with staurosporine for different time periods as indicated, and cell apoptosis was determined by flow cytometry. As shown in Figure 29, after treatment of staurosporine for 48 hrs, the annexin V-Cy3-positive and 7-ADD-negative cell population was increased in both CFSC-8B cells (18.3%) and CFSC-2G cells (27.6%). In contrast, treatment of staurosporine for 48 hrs had no effect on apoptosis of CFSC-3H and CFSC-5H cells. Moreover, after treatment of staurosporine, there was a decrease in normal cell number with concomitant increase in the cell number of early apoptosis and late apoptosis/necrosis in CFSC-8B and 2G cells. This result indicated that CFSC-3H and CFSC-5H cells were more resistant to staurosporine-induced apoptosis than CFSC-8B and 2G cells.

Figure 29 *Flow cytometric analysis of CFSC-8B, 2G, 3H and 5H cells after treatment with staurosporine*. Cells were incubated with staurosporine (8nM) for 0, 16, 24 and 48 hrs, respectively. Then cells were stained with annexinV-Cy3 and 7-ADD as described in Materials and methods. Cell fluorescence was measured by flow cytometry. AnnexinV-Cy3 was excited with 543nm laser and detected using the green (564–606 nm) filter, while 7-ADD was excited with 488nm laser and detected using the red (653–669 nm) filter. Normal cells (annexinV-Cy3- and 7-AAD-negative, A3); cells in early apoptosis (annexinV-Cy3-positive and 7-AAD-negative, A4); cells in late apoptosis/necrosis (annexin V-Cy3- and 7-AAD-positive, A2); and cells in necrosis (annexin V-Cy3- negative and 7-AAD-positive, A1). For each measurement, 10,000 cells were counted. I: 0 hr, II: 16 hrs, III: 24 hrs, IV: 48 hrs.

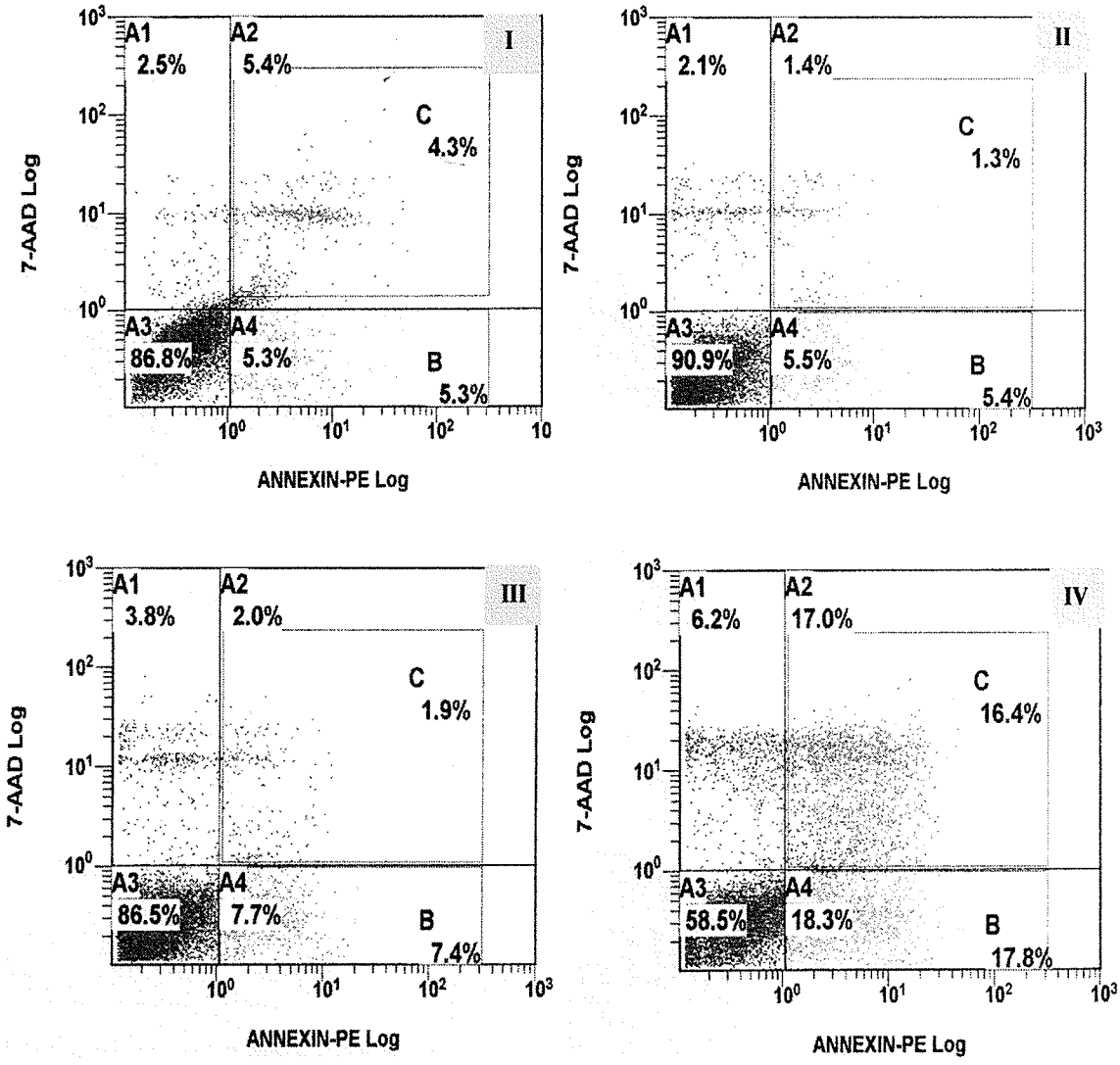
I
A1
2.5%
A2
5.4%
C
4.3%
A3
86.8%
A4
5.3%
B
5.3%
7-AAD Log
ANNEXIN-PE Log
II
A1
2.1%
A2
1.4%
C
1.3%
A3
90.9%
A4
5.5%
B
5.4%
7-AAD Log
ANNEXIN-PE Log
III
A1
3.8%
A2
2.0%
C
1.9%
A3
86.5%
A4
7.7%
B
7.4%
7-AAD Log
ANNEXIN-PE Log
IV
A1
6.2%
A2
17.0%
C
16.4%
A3
58.5%
A4
18.3%
B
17.8%
7-AAD Log
ANNEXIN-PE Log

A: CFSC-8B

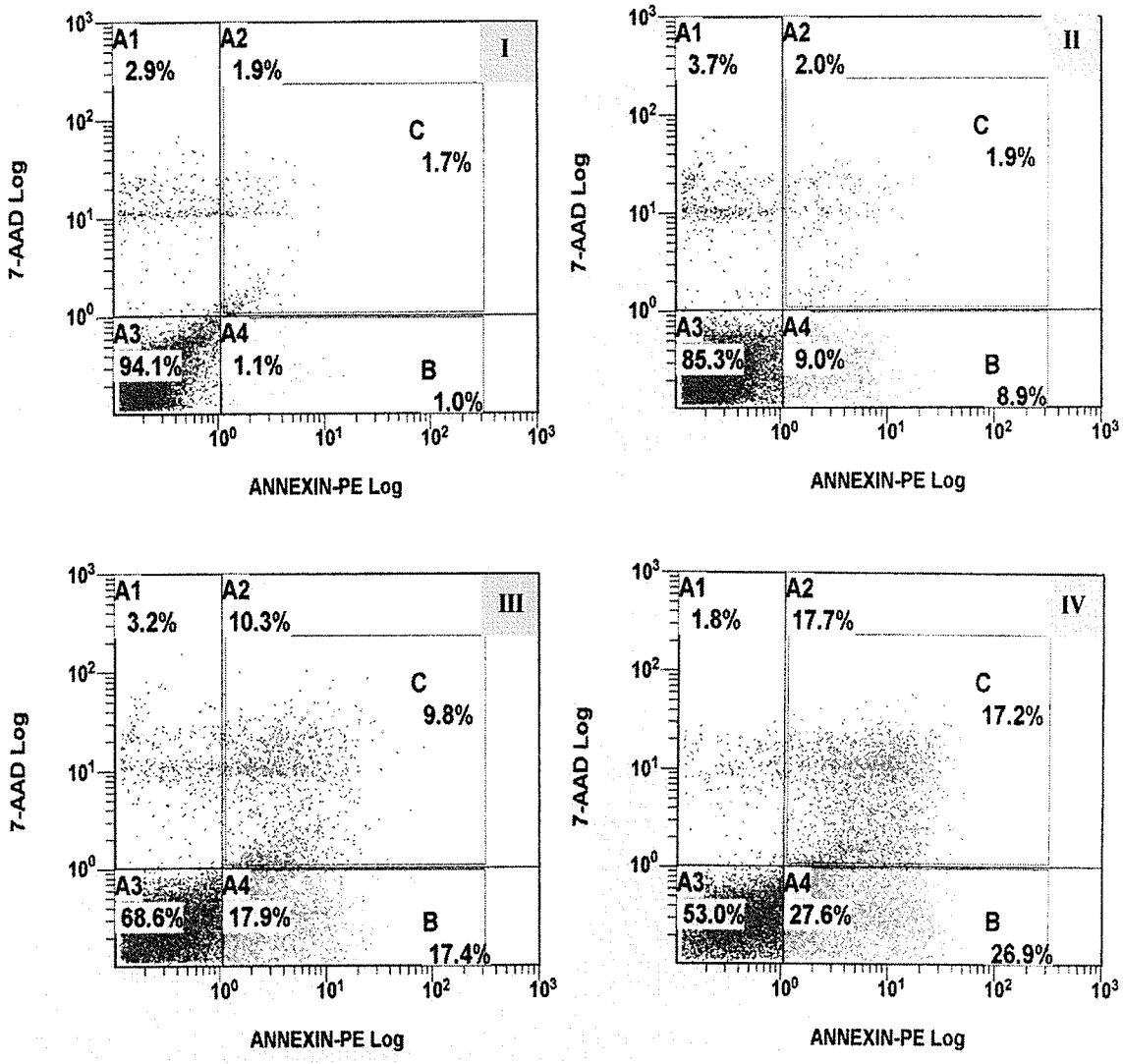
I
A1
2.9%
A2
1.9%
C
1.7%
A3
94.1%
A4
1.1%
B
1.0%
II
A1
3.7%
A2
2.0%
C
1.9%
A3
85.3%
A4
9.0%
B
8.9%
III
A1
3.2%
A2
10.3%
C
9.8%
A3
68.6%
A4
17.9%
B
17.4%
IV
A1
1.8%
A2
17.7%
C
17.2%
A3
53.0%
A4
27.6%
B
26.9%
7-AAD Log
ANNEXIN-PE Log

B: CFSC-2G

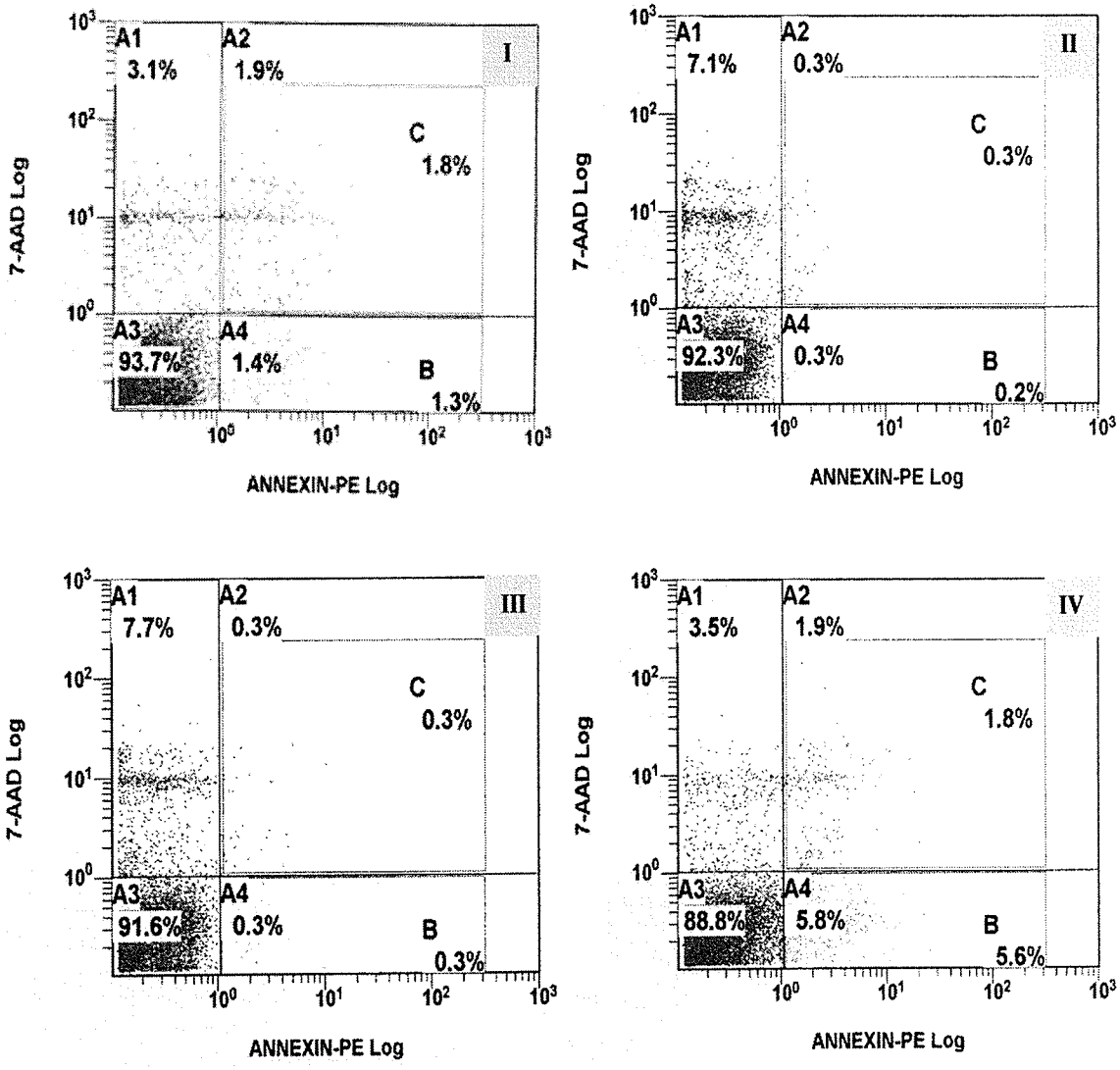
I
A1
3.1%
A2
1.9%
C
1.8%
A3
93.7%
A4
1.4%
B
1.3%
II
A1
7.1%
A2
0.3%
C
0.3%
A3
92.3%
A4
0.3%
B
0.2%
III
A1
7.7%
A2
0.3%
C
0.3%
A3
91.6%
A4
0.3%
B
0.3%
IV
A1
3.5%
A2
1.9%
C
1.8%
A3
88.8%
A4
5.8%
B
5.6%
7-AAD Log
ANNEXIN-PE Log

C: CFSC-3H

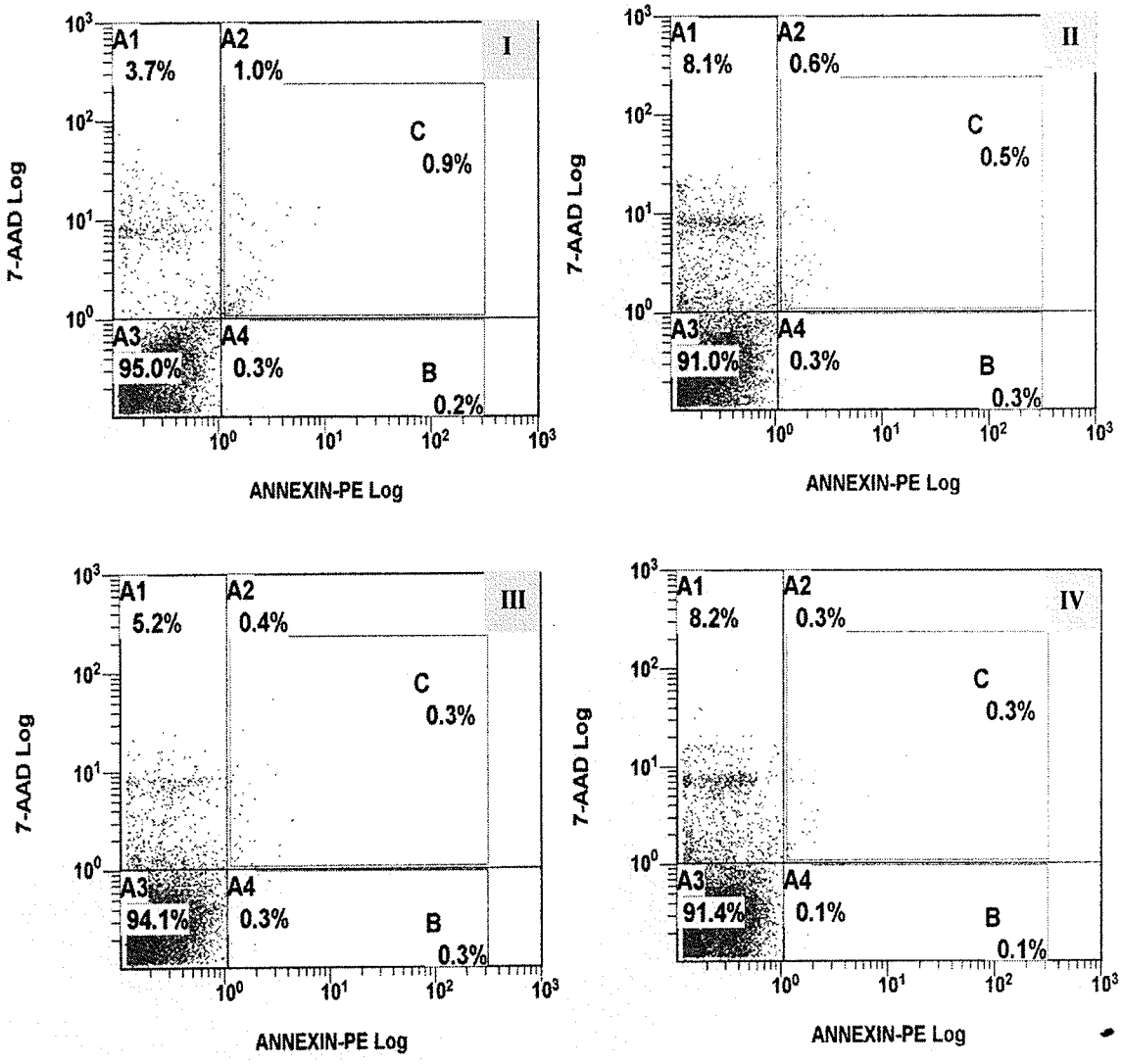
I
A1
3.7%
A2
1.0%
C
0.9%
A3
95.0%
A4
0.3%
B
0.2%
7-AAD Log
ANNEXIN-PE Log
II
A1
8.1%
A2
0.6%
C
0.5%
A3
91.0%
A4
0.3%
B
0.3%
7-AAD Log
ANNEXIN-PE Log
III
A1
5.2%
A2
0.4%
C
0.3%
A3
94.1%
A4
0.3%
B
0.3%
7-AAD Log
ANNEXIN-PE Log
IV
A1
8.2%
A2
0.3%
C
0.3%
A3
91.4%
A4
0.1%
B
0.1%
7-AAD Log
ANNEXIN-PE Log

D: CFSC-5H

3.2.3 Effect of staurosporine and U0126 on expression and phosphorylation of ERK in CFSC-8B and 5H cells.

To investigate the mechanism involved in staurosporine-induced apoptosis in different HSC lines, we examined the effect of staurosporine and U0126 on expression and phosphorylation of ERK in CFSC-8B and 5H cells by western blot analysis. U0126 is a chemically synthesized organic compound that specifically inhibits both active and inactive MEK1/2, and downstream phosphorylation of ERK1/2, in turn, is blocked. As shown in Figure 30A, the basal level of phospho-ERK1/2 was higher in CFSC-8B and 2G cells than in CFSC-3H and 5H cells. It was hardly detectable for phospho-ERK1/2 in CFSC-3H and CFSC-5H cells. Staurosporine significantly induced the phosphorylation of ERK1/2 in CFSC-8B cells after 5 minutes treatment and the phospho-ERK1/2 level was steadily increased and peaked at 2 hrs after treatment. Although the basal level of phospho-ERK1/2 in CFSC-5H cells was very low, staurosporine still induced the phosphorylation of ERK1/2 after treatment of 30 minutes (Figure 30B). Moreover, dose dependent stimulation of ERK1/2 phosphorylation by staurosporine was observed in CFSC-5H cells (Figure 30C). In addition, U0126 (40μM) completely abolished the phosphorylation of ERK1/2 in CFSC-5H cells after treatment of 5 minutes in a dose dependent manner (Figure 30D).

Figure 30 *Western blot analysis of ERK1 and phospho-ERK1/2 expression in CFSC-8B, 2G, 3H and 5H cells stimulated with or without staurosporine and U0126.* Expression of ERK and phospho-ERK1/2 were analyzed by Western blot as described in Materials and methods. A: The basal expression levels of ERK and phospho-ERK1/2 in CFSC-8B, 2G, 3H and 5H cells. B: CFSC-8B and 5H cells were treated with or without staurosporine (8nM) at different time points as indicated. C: CFSC-5H cells were treated with different concentration of staurosporine (0-32nM) for 48hr. D: CFSC-5H cells were treated with or without U0126 (40μM) at different time points as indicated. The top part represents typical Western blot of ERK and phospho-ERK1/2. The lower part displays the density histogram data from three-separated Western blot analysis (mean±SE). *indicates $P<0.05$ between control and treated groups. **indicates $P<0.001$ between control and treated groups.

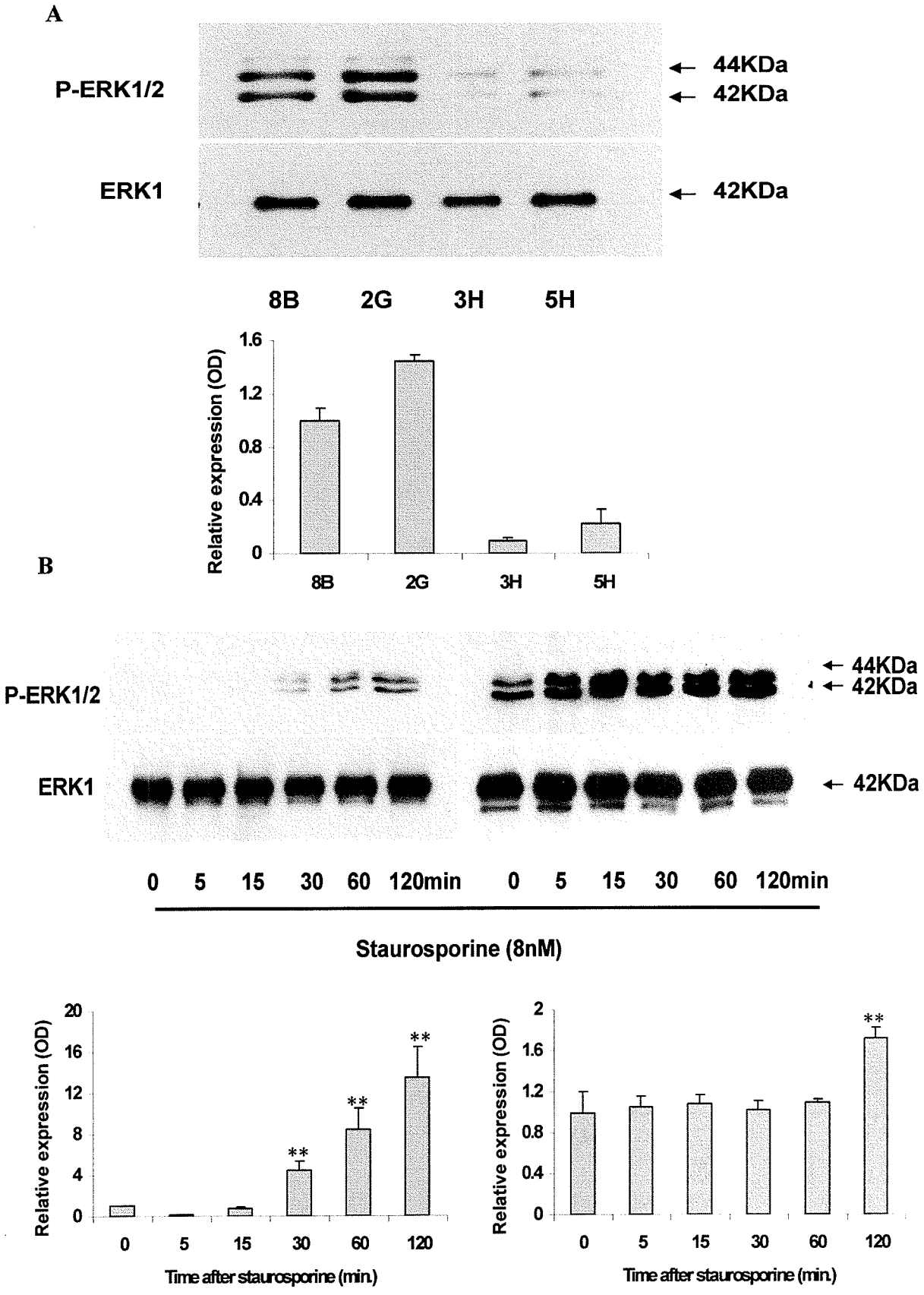
A
P-ERK1/2
ERK1
44KDa
42KDa
42KDa
8B
2G
3H
5H
Relative expression (OD)
1.6
1.2
0.8
0.4
0
8B
2G
3H
5H
B
P-ERK1/2
ERK1
44KDa
42KDa
42KDa
0 5 15 30 60 120min 0 5 15 30 60 120min
Staurosporine (8nM)
Relative expression (OD)
20
16
12
8
4
0
**
**
**
0 5 15 30 60 120
Time after staurosporine (min.)
Relative expression (OD)
2
1.6
1.2
0.8
0.4
0
**
0 5 15 30 60 120
Time after staurosporine (min.)

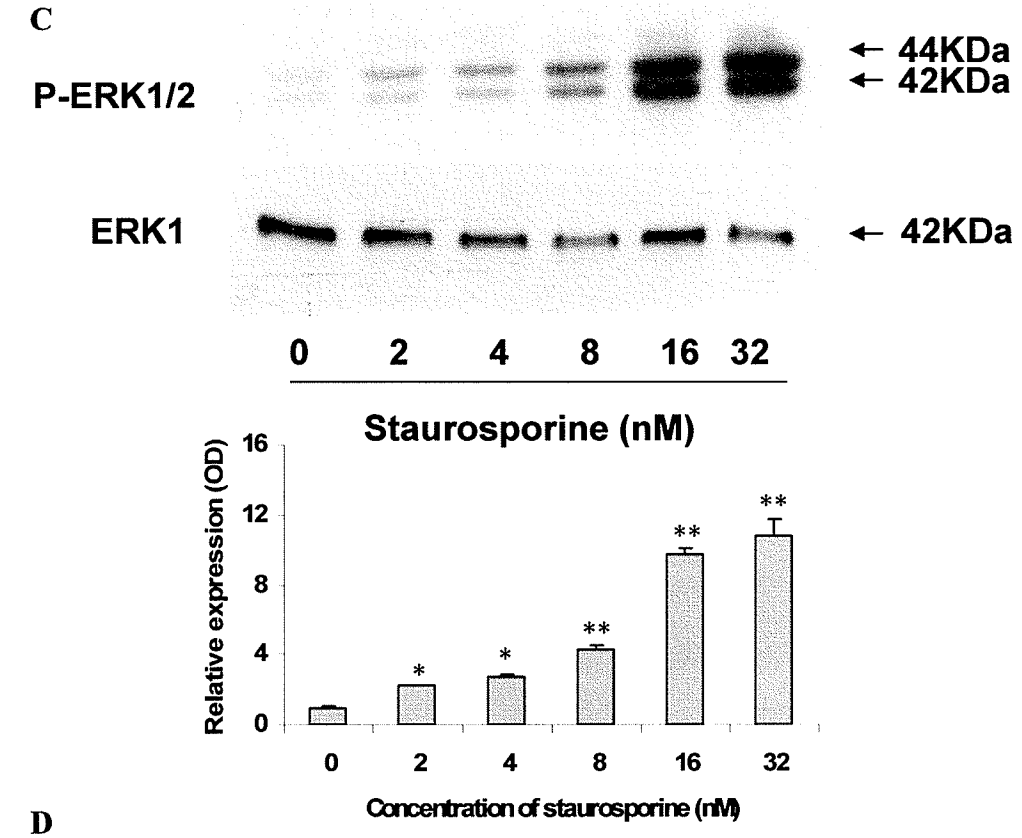
C
P-ERK1/2
ERK1
← 44KDa
← 42KDa
← 42KDa
0 2 4 8 16 32
Staurosporine (nM)
Relative expression (OD)
16
12
8
4
0
*
*
**
**
**
0 2 4 8 16 32
Concentration of staurosporine (nM)

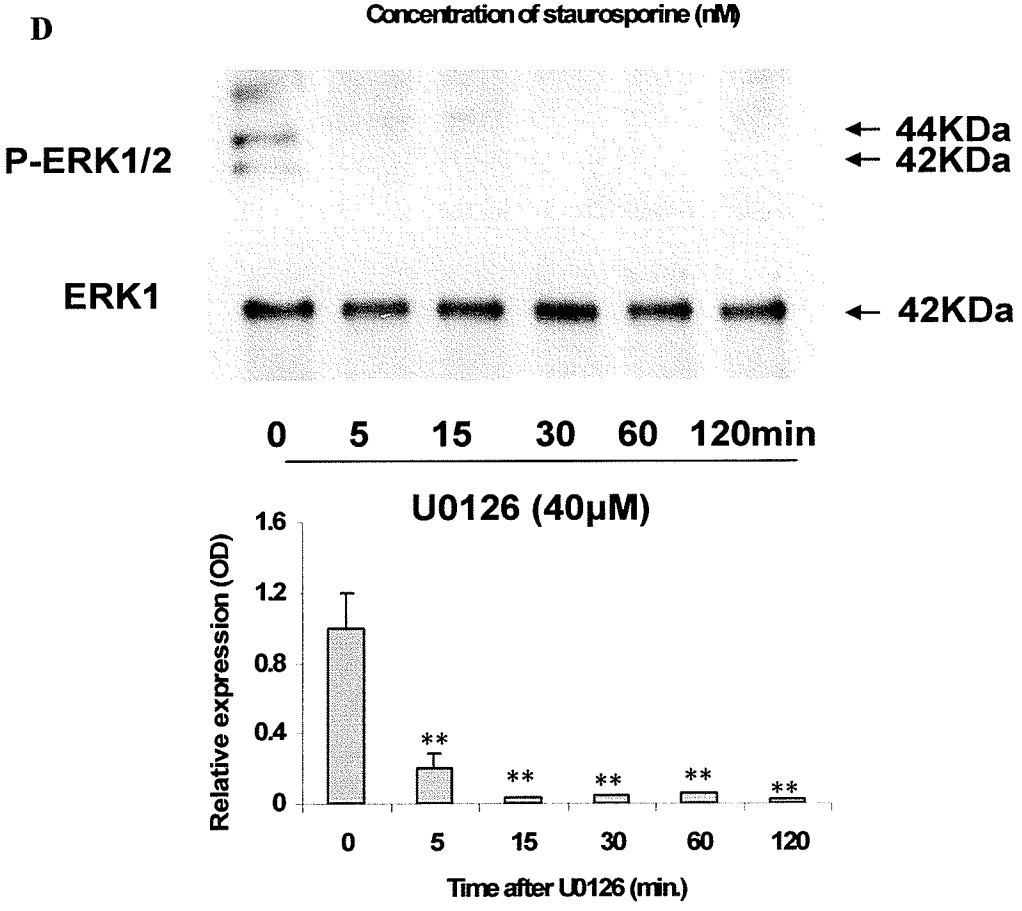
D
P-ERK1/2
ERK1
← 44KDa
← 42KDa
← 42KDa
0 5 15 30 60 120min
U0126 (40μM)
Relative expression (OD)
1.6
1.2
0.8
0.4
0
**
**
**
**
**
0 5 15 30 60 120
Time after U0126 (min.)

3.2.4 Effect of co-treatment of staurosporine and U0126 on hepatic stellate cells apoptosis

Previous experiment documented that CFSC-8B cells were more susceptible to staurosporine-induced apoptosis than CFSC-5H cells and there was higher expression of phospho-ERK1/2 in CFSC-8B cells than that in CFSC-5H cells. Whether the status of phospho-ERK1/2 contributes to the susceptibility of HSCs to staurosporine-induced apoptosis, we examined CFSC-5H apoptosis after treatment of staurosporine alone and co-treatment of staurosporine and U0126. After treatment of CFSC-5H cells with different concentrations of staurosporine (0-32nM) or co-treatment of staurosporine with U0126 (40μM) for 48 hrs, respectively, apoptosis was determined by flow cytometry. As shown in Figure 31, after treatment with different concentration of staurosporine for 48 hrs, the annexin V-Cy3-negative and 7-ADD-negative normal cell population maintained unchanged. However, after co-treatment of staurosporine with U0126 for 48 hrs, most CFSC-5H cells underwent apoptosis. The annexin V-Cy3-positive and 7-ADD-negative cells number was significantly increased from 5.9 to 62.2%.

Figure 31 *Flow cytometric analysis of CFSC-5H cells apoptosis after treatment of staurosporine alone or co-treatment of staurosporine and U0126.* Cells were incubated with different concentration of staurosporine (0-32nM) or co-treatment of U0126 (40μM) and different concentration of staurosporine (0-32nM) for 48 hrs. Then cells were stained with annexinV-Cy3 and 7-ADD as described in Materials and methods. Cell fluorescence was measured by flow cytometry. AnnexinV-Cy3 was excited with 543nm laser and detected using the green (564–606 nm) filter, while 7-ADD was excited with 488nm laser and detected using the red (653–669 nm) filter. Normal cells (annexinV-Cy3- and 7-AAD-negative, A3); cells in early apoptosis (annexinV-Cy3-positive and 7-AAD-negative, A4); cells in late apoptosis/necrosis (annexin V-Cy3- and 7-AAD-positive, A2); and cells in necrosis (annexin V-Cy3- negative and 7-AAD-positive, A1). For each measurement, 10,000 cells were counted.

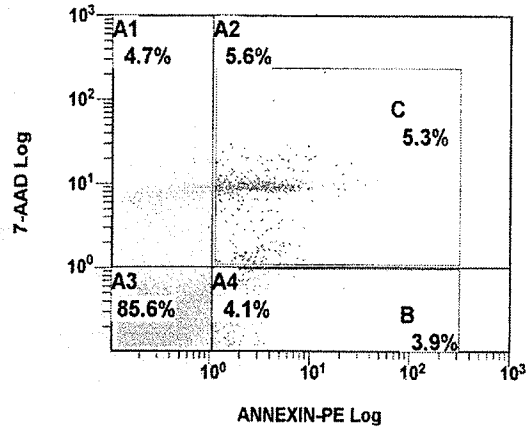

STP (0nM)

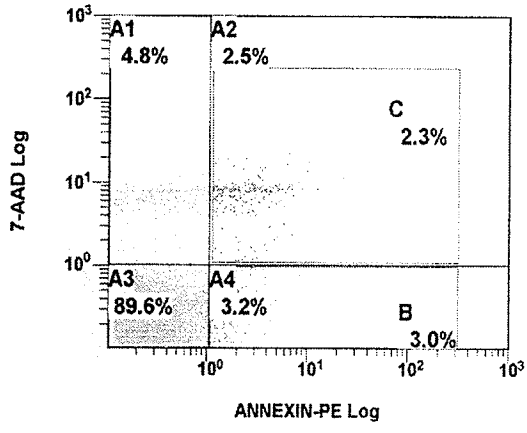

STP (4nM)

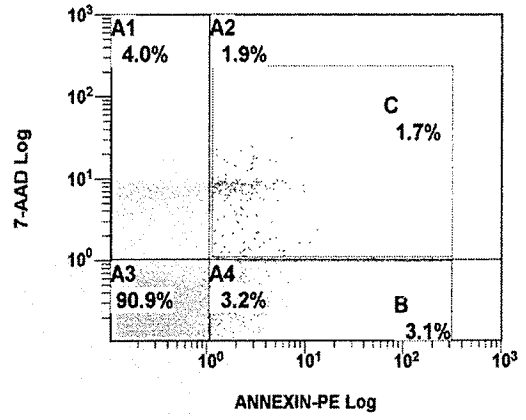

STP (16nM)

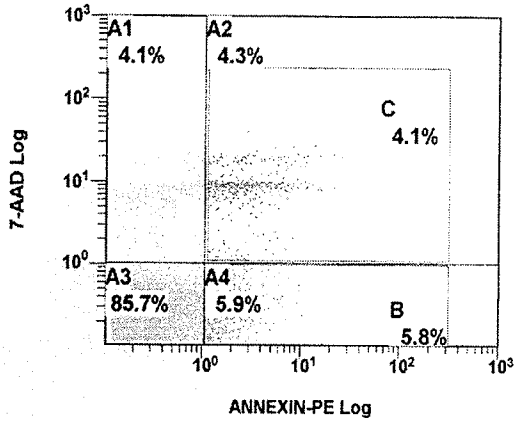

STP (32nM)

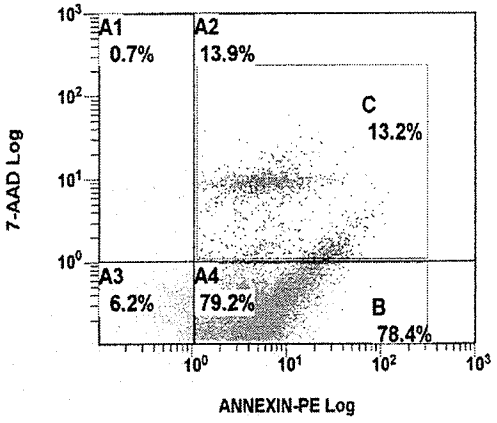

STP (0nM)+U0126 (40 μ M)

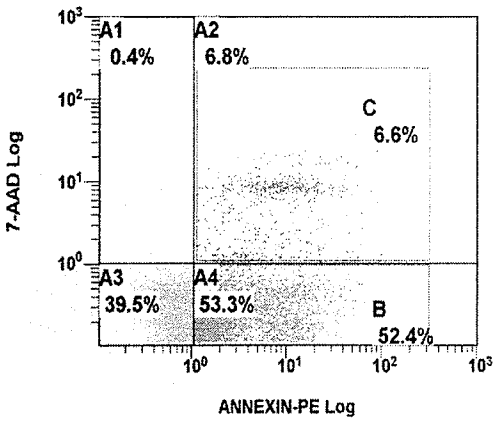

STP (4nM)+U0126 (40 μ M)

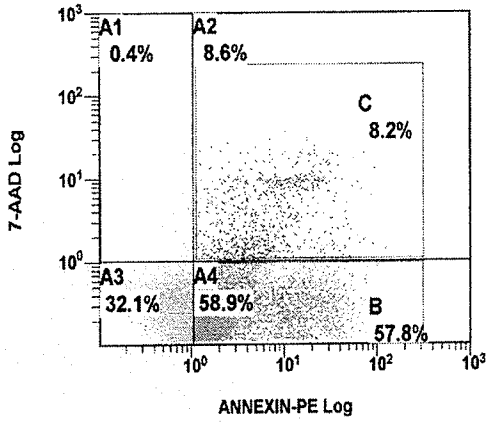

STP (16nM)+U0126 (40 μ M)

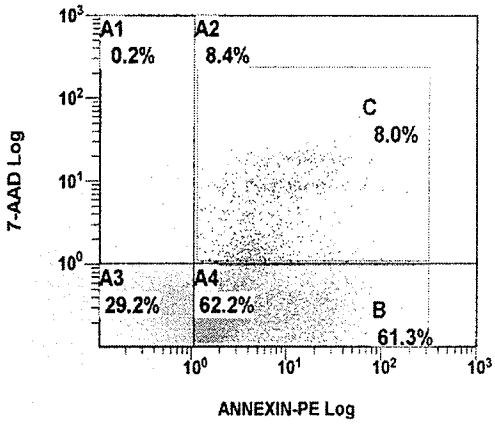

STP (32nM)+U0126 (40 μ M)

3.3 Discussion

Understanding of HSC apoptosis is becoming more and more important to develop specific target treatment for patients with liver fibrosis and cirrhosis. The fact that activated HSCs undergo an apoptotic process and expression of death receptor p75 was different in quiescent and activated HSCs indicates an important role of apoptosis in HSC biology. By employing a heterogeneous population of transformed HSC lines, we demonstrated the difference of HSC's susceptibility to staurasporine-induced apoptosis and the phosphorylation of an intracellular signaling molecule (ERK).

Staurosporine is a less selective inhibitor of PKC. It has been shown that staurosporine can suppress proliferation of HSCs (Ramm, Li et al., 2003) and induce apoptosis of HSCs (Yoshiji, Kuriyama et al., 2003). The current study indicated that susceptibility of HSCs to staurosporine-induced apoptosis may be related to the levels of α-SMA and phospho-ERK1/2. The higher levels of α-SMA and phospho-ERK1/2 HSCs had, the more susceptible to staurosporine-induced apoptosis HSCs were. Moreover, the susceptibility of HSCs to staurosporine-induced apoptosis may be also related to the proliferation rate of HSCs because CFSC-8B and CFSC-2G have higher proliferation index than CFSC-3H and 5H cells (Schaefer, Rivas-Estilla et al., 2003). This is consistent with the observations found in other cell types. The sensitivity to Fas-mediated apoptosis in leukemic cells was largely restricted in proliferating cells (Macnamara, Palucka et al., 1999).

Although there is a correlation between phospho-ERK1/2 and the susceptibility of HSCs to staurosporine-induced apoptosis, result from U0126-treated cells did not support that phospho-ERK1/2 mediates apoptosis in CFSC-5H cells. Treatment of CFSC-5H

cells with U0126 induced a significant apoptosis. Whether U0126 specifically inhibited the ERK activity in CFSC-5H cells and induced apoptosis or mediated other apoptotic signal remains to be investigated. However, it indicated that ERK1/2 signaling was an important signaling pathway to CFSC-5H cells survival. In addition, it has been demonstrated that ERK1/2 mediates IGF1 induced apoptosis in HSCs (Saile, DiRocco et al., 2004). However, it was shown that cellular responses to ERK1/2 signaling depend on the strength and duration of activated ERK signal. Usually transient activation of ERK1/2 resulted to increase in cell proliferation, whereas sustained high levels of ERK1/2 activity could cause cell apoptosis (Pettersson, Couture et al., 2004). This seems to be true in HSCs as we observed that CFSC-8B and CFSC-2G cells with higher basal level of phospho-ERK1/2 were more susceptible to staurosporine-induced apoptosis, whereas CFSC-3H and CFSC-5H cells with lower basal level of phospho-ERK1/2 were less susceptible to staurosporine-induce apoptosis. Moreover, staurosporine can induce a strong and sustained phosphorylation of ERK1/2 in CFSC-8B cells which also showed higher susceptibility to apoptosis. Whether ERK1/2 signaling could initiate the apoptosis process in CFSC-8B cells remains to be investigated.

In conclusion, CFSC-3H and 5H cells are more resistant to apoptosis induced by staurosporine than CFSC-8B and 2G cells. The different phosphorylation level of ERK1/2 and proliferation index may contribute to the susceptibility of HSCs to apoptosis.

IV. SUMMARY

This study was the first to investigate the roles of BMP4 during liver fibrogenesis. The data present here shows that BMP4 expression was significantly increased in the liver of BDL rats and during HSCs activation. We further showed that BMP4 efficiently induced the differentiation of HSCs, but had no effect on the proliferation of HSCs. Studies on the intracellular signaling initiated by BMP4 in HSCs indicated that Smad1 and p38 MAPK signaling might be involved in the differentiation of HSCs, whereas ERK MAPK was important for HSCs survival.

This study highlighted the critical roles of BMP4 on the induction of differentiation of WB-F344 cells toward hepatocytes. Autocrine and paracrine stimulation of BMP4 on WB-F344 cells in liver could be possible given there were expression of BMP4 and its receptors in WB-F344 cells. As the major cellular source of BMP4 in liver, HSCs can induce the differentiation of WB-F344 cells through the interaction of epithelial–mesenchymal cells. BMP4-activated Smad1 signal might mediate the hepatic differentiation of WB-F344 cells. Additionally, BMP4 can increase the expression and DNA binding activity of C/EBPα, which is involved in the regulation of liver-specific genes expression.

The signaling directing the survival and apoptosis in activated and quiescent HSCs was also investigated in this study. CFSC-3H and 5H cells were more resistant to apoptosis induced by staurosporine than CFSC-8B and 2G cells. The different expression level of p-ERK1/2 and different proliferative capacity may determine the susceptibility of CFSC to apoptosis.

V. CONCLUSION

It has been demonstrated that BMP4, as an inductive factor, plays a key role in cell proliferation and differentiation. BMP4 and its down-stream signaling are capable to switch on certain genes required for a particular cell type during the developmental process or in a disease situation. BMP4 signaling is important to promote the specification of early hepatocytes during liver development (Rossi, Dunn et al., 2001). Although BMP4 expression appears undetectable in normal adult liver, stable expression of BMPRs in hepatocytes, hepatic stellate cells and hepatic stem cells obviously renders these cells responsive to BMP4. In the present study, we investigated the roles of BMP4 during liver fibrogenesis, which involved hepatic stellate cell trans-differentiation.

The research that contributed to this thesis supports the hypothesis that BMP4 and its signaling play crucial roles in trans-differentiation and apoptosis of hepatic stellate cells as well as differentiation of hepatic stem cells.

Figure 32, shows an important role of BMP4 during liver fibrogenesis. In normal liver, the expression of BMP4 was rarely observed. However, high level of BMP4 was detected in fibrotic liver and activated HSCs. This may indicate that BMP4 was involved in trans-differentiation of hepatic stellate cells during fibrogenesis. Thereafter, our study demonstrated that the stimulatory effects of BMP4 on the expression of α-SMA, a marker for activated HSCs. Compared with transient increased expression of TGFβ in the activation of HSCs (Gong, Roth et al., 1998), sustained highly expressed BMP4 during fibrogenesis may serve as a more important cytokine mediating the pathological change during liver fibrogenesis.

Of interest is the fact that activated HSCs can move across the basement membrane and form direct contact with oval cells. It was reported that some chemoattractants expressed in ductal epithelium, such as PDGF, MCP-1, and IGF-1, trigger the migration of activated HSCs (Friedman, 2003; Clouston, Powell et al., 2005). It was shown that BMP4 has a distinguishable role on the onset of neural crest cell migration (Sela-Donenfeld and Kalcheim, 1999). Whether BMP4 is involved in the migration of HSCs remains unknown. Oval cells, acting as rat hepatic stem cells, are located at the canal of Hering. The canal of Hering serves as oval cells niche, and tightly regulates oval cells self-renewal and differentiation. Upon the arrival of activated HSCs to the oval cell niche, the overall balance of signals maintaining normal oval cell self-renewal is inevitably disrupted. The current studies have demonstrated that BMP4 secreted from activated HSCs plays a very important role on oval cells self-renewal and differentiation through the interaction of epithelial–mesenchymal cells. It was shown that BMP4 can stimulate not only hepatic oval cell differentiation toward hepatocyte lineage but also cell proliferation. Moreover, the self-upregulation of BMP4 in oval cells after stimulation with BMP4 may enhance its capability of inducing differentiation. Hepatic differentiation of oval cells induced by BMP4 may provide a possibility for oval cells to be the source of regenerating hepatocytes. However, it should be cautious to determine the phenotype of differentiated oval cells, since many studies have indicated that hepatocellular carcinoma could be derived from the stem cells either from the bone marrow or the liver (Sell, 2004; Alison and Lovell, 2005; Burkert, Wright et al., 2006). Moreover, BMP4 showed a certain relationship with cancer development (Alarmo, Kuukasjarvi et al., 2006; Theriault, Shepherd et al., 2007). Therefore, whether the

differentiated oval cells induced by BMP4 become mature hepatocytes or hepatocellular carcinoma need to be further investigated.

Regression of liver fibrosis and possibly cirrhosis has been reported in patients with chronic liver disease and experimental liver fibrosis animal model. Specific induction of apoptosis in HSCs may be considered as a possibly realistic approach for cell targeted therapy to liver fibrosis. By employing a heterogeneous population of transformed HSC lines, we demonstrated the differences of HSCs in susceptibility to staurasporine-induced apoptosis and expression of an intracellular signaling molecule (ERK). Our results suggested that susceptibility of HSCs to staurosporine-induced apoptosis had a positive correlation with expression of α-SMA and phosphor-ERK1/2 in HSCs. Moreover, our studies demonstrated that BMP4 could increase abundance of α-SMA and phospho-ERK1/2 in HSCs. However, it is not clear whether BMP4-increased expression of α-SMA and phosphor-ERK1/2 are directly related to susceptibility of HSCs undergoing apoptosis. It has been known that the activated HSCs appear more susceptible to apoptotic stimulation than quiescent cells (Canbay, Friedman et al., 2004). However, the role of ERK1/2 in HSCs remains controversial. Some studies showed that cellular responses to ERK1/2 signaling depend on strength and duration of activated ERK signal (Kim, Rhim et al., 2001). Transient activation of ERK1/2 usually resulted to an increase in cell proliferation, whereas sustained high levels of ERK1/2 activity could cause cell apoptosis. Our results seem to support this conclusion. Further detailed study is required to determine the exact role of ERK1/2 in HSCs.

At present, some studies have proved that Smad1 signaling was directly related to the cell differentiation. Myocyte phenotype of lung fibroblasts was induced by the

increase in BMP4 dependent Smad1 signaling (Jeffery, Upton et al., 2005). Retinoic acid stimulated chondrocyte differentiation through induction of Smad1 (Li, Schwarz et al., 2003). In addition, BMP2 signaling through Smad1 participated in chondrogenic differentiation (Ju, Hoffmann et al., 2000). Our results showed that the expression of phosphor-Smad1 was increased significantly in both HSCs and WB-F344 cells after stimulation with BMP4. Therefore, we speculate that BMP4 induced the differentiation of HSCs and hepatic stem cells through the activation of Smad1. However, what is the exact role of Smad1 in these cells remains to be further investigated.

In conclusion, BMP4 could be considered as an efficient candidate that induces both hepatic stellate cell trans-differentiation and differentiation of WB-F344 cells toward hepatocytes. BMP4 secreted from activated hepatic stellate cells may act as a paracrine factor to stimulate WB-F344 cell differentiation. The smad1 signaling initiated by BMP4 may involve in the differentiation of hepatic stellate cells and hepatic stem cells. Moreover, different phosphorylation level of ERK1/2 and proliferation index may contribute to the susceptibility of HSCs to apoptosis.

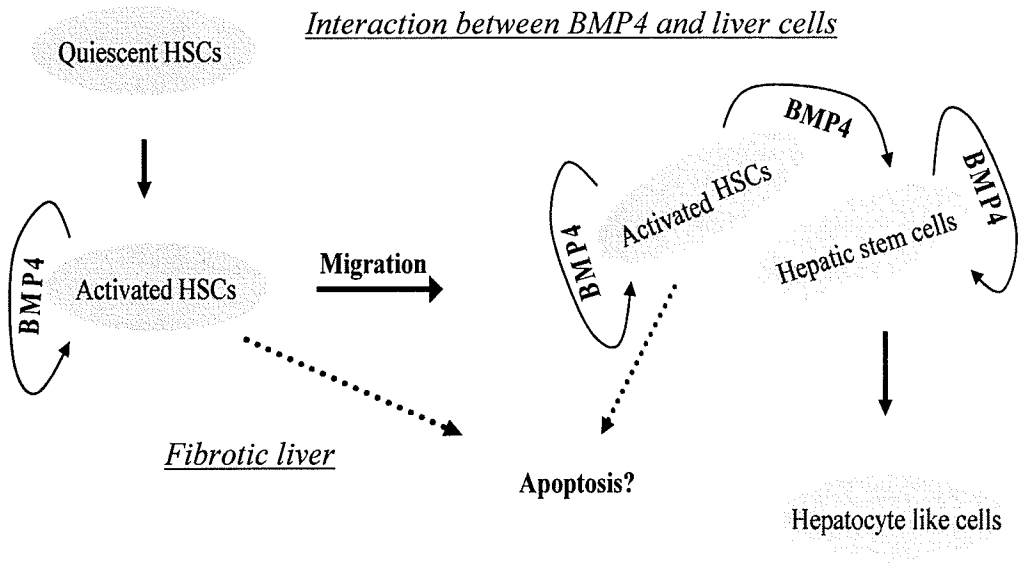

Figure 32 *Interaction of BMP4 and liver cells.* In this model, the expression of BMP4 was increased in activated HSCs. Autocrine stimulation of BMP4 stimulated the expression of α-SMA and p-ERK1/2 in activated HSCs. Susceptibility of activated HSCs to apoptosis is increased with elevated expression of α-SMA and p-ERK1/2. Activated HSCs could migrate to areas that close to hepatic stem cells. Hepatic stem cells, in turn, could be induced to differentiate toward hepatocytes through autocrine and paracrine stimulation of BMP4.

V. REFERENCES

Abe, E. (2006). "Function of BMPs and BMP antagonists in adult bone." Ann N Y Acad Sci **1068**: 41-53.

Ackerman, Z., F. Karmeli, et al. (1996). "Renal vasoactive mediator generation in portal hypertensive and bile duct ligated rats." J Hepatol **24**(4): 478-86.

Alarmo, E. L., T. Kuukasjarvi, et al. (2006). "A comprehensive expression survey of bone morphogenetic proteins in breast cancer highlights the importance of BMP4 and BMP7." Breast Cancer Res Treat.

Alison, M. R. and M. J. Lovell (2005). "Liver cancer: the role of stem cells." Cell Prolif **38**(6): 407-21.

Alison, M. R., R. Poulsom, et al. (1993). "Expression of hepatocyte growth factor mRNA during oval cell activation in the rat liver." J Pathol **171**(4): 291-9.

Anania, F. A., L. Womack, et al. (1999). "Acetaldehyde enhances murine alpha2(I) collagen promoter activity by Ca2+-independent protein kinase C activation in cultured rat hepatic stellate cells." Alcohol Clin Exp Res **23**(2): 279-84.

Arii, S. and M. Imamura (2000). "Physiological role of sinusoidal endothelial cells and Kupffer cells and their implication in the pathogenesis of liver injury." J Hepatobiliary Pancreat Surg **7**(1): 40-8.

Aubin, J., A. Davy, et al. (2004). "In vivo convergence of BMP and MAPK signaling pathways: impact of differential Smad1 phosphorylation on development and homeostasis." Genes Dev **18**(12): 1482-94.

Avsian-Kretchmer, O. and A. J. Hsueh (2004). "Comparative genomic analysis of the eight-membered ring cystine knot-containing bone morphogenetic protein antagonists." Mol Endocrinol **18**(1): 1-12.

Baliga, B. C. and S. Kumar (2002). "Role of Bcl-2 family of proteins in malignancy." Hematol Oncol **20**(2): 63-74.

Bataller, R. and D. A. Brenner (2005). "Liver fibrosis." J Clin Invest **115**(2): 209-18.

Beck, H. N., K. Drahushuk, et al. (2001). "Bone morphogenetic protein-5 (BMP-5) promotes dendritic growth in cultured sympathetic neurons." BMC Neurosci **2**: 12.

Bedossa, P. and V. Paradis (1995). "Transforming growth factor-beta (TGF-beta): a key-role in liver fibrogenesis." J Hepatol **22**(2 Suppl): 37-42.

Bell, E., I. Munoz-Sanjuan, et al. (2003). "Cell fate specification and competence by Coco, a maternal BMP, TGFbeta and Wnt inhibitor." Development **130**(7): 1381-9.

Bertrand-Philippe, M., R. G. Ruddell, et al. (2004). "Regulation of tissue inhibitor of metalloproteinase 1 gene transcription by RUNX1 and RUNX2." J Biol Chem **279**(23): 24530-9.

Bisgaard, H. C., D. C. Parmelee, et al. (1993). "Keratin 14 protein in cultured nonparenchymal rat hepatic epithelial cells: characterization of keratin 14 and keratin 19 as antigens for the commonly used mouse monoclonal antibody OV-6." Mol Carcinog **7**(1): 60-6.

Boise, L. H., M. Gonzalez-Garcia, et al. (1993). "bcl-x, a bcl-2-related gene that functions as a dominant regulator of apoptotic cell death." Cell **74**(4): 597-608.

Bost, F., M. Aouadi, et al. (2005). "The role of MAPKs in adipocyte differentiation and obesity." Biochimie **87**(1): 51-6.

Botchkarev, V. A. and A. A. Sharov (2004). "BMP signaling in the control of skin development and hair follicle growth." Differentiation **72**(9-10): 512-26.

Bridle, K. R., L. Li, et al. (2006). "Coordinate activation of intracellular signaling pathways by insulin-like growth factor-1 and platelet-derived growth factor in rat hepatic stellate cells." J Lab Clin Med **147**(5): 234-41.

Buckley, S., W. Shi, et al. (2004). "BMP4 signaling induces senescence and modulates the oncogenic phenotype of A549 lung adenocarcinoma cells." Am J Physiol Lung Cell Mol Physiol **286**(1): L81-6.

Bugianesi, E., R. Marzocchi, et al. (2004). "Non-alcoholic fatty liver disease/non-alcoholic steatohepatitis (NAFLD/NASH): treatment." Best Pract Res Clin Gastroenterol **18**(6): 1105-16.

Burkert, J., N. A. Wright, et al. (2006). "Stem cells and cancer: an intimate relationship." J Pathol **209**(3): 287-97.

Burt, A. D. (1999). "Pathobiology of hepatic stellate cells." J Gastroenterol **34**(3): 299-304.

Calmont, A., E. Wandzioch, et al. (2006). "An FGF response pathway that mediates hepatic gene induction in embryonic endoderm cells." Dev Cell **11**(3): 339-48.

Canbay, A., S. Friedman, et al. (2004). "Apoptosis: the nexus of liver injury and fibrosis." Hepatology **39**(2): 273-8.

Ceni, E., D. W. Crabb, et al. (2006). "Acetaldehyde inhibits PPARgamma via H2O2-mediated c-Abl activation in human hepatic stellate cells." Gastroenterology **131**(4): 1235-52.

Chen, X., Y. Z. Wang, et al. (2006). "[The effects of nerve growth factor-induced apoptosis on hepatic stellate cells of fibrotic rat liver]." Zhonghua Yi Xue Za Zhi **86**(28): 1985-8.

Clouston, A. D., E. E. Powell, et al. (2005). "Fibrosis correlates with a ductular reaction in hepatitis C: roles of impaired replication, progenitor cells and steatosis." Hepatology **41**(4): 809-18.

Craig, C. E., A. Quaglia, et al. (2004). "The histopathology of regeneration in massive hepatic necrosis." Semin Liver Dis **24**(1): 49-64.

Crosby, H. A., S. G. Hubscher, et al. (1998). "Immunolocalization of OV-6, a putative progenitor cell marker in human fetal and diseased pediatric liver." Hepatology **28**(4): 980-5.

Csiszar, A., M. Ahmad, et al. (2006). "Bone morphogenetic protein-2 induces proinflammatory endothelial phenotype." Am J Pathol **168**(2): 629-38.

Dai, J., J. Keller, et al. (2005). "Bone morphogenetic protein-6 promotes osteoblastic prostate cancer bone metastases through a dual mechanism." Cancer Res **65**(18): 8274-85.

Dal-Pra, S., M. Furthauer, et al. (2006). "Noggin1 and Follistatin-like2 function redundantly to Chordin to antagonize BMP activity." Dev Biol **298**(2): 514-26.

Dasgupta, A., R. Hughey, et al. (2005). "E-cadherin synergistically induces hepatospecific phenotype and maturation of embryonic stem cells in conjunction with hepatotrophic factors." Biotechnol Bioeng **92**(3): 257-66.

Degli-Esposti, M. (1999). "To die or not to die--the quest of the TRAIL receptors." J Leukoc Biol **65**(5): 535-42.

Deng, H., R. Makizumi, et al. (2007). "Bone morphogenetic protein-4 is overexpressed in colonic adenocarcinomas and promotes migration and invasion of HCT116 cells." Exp Cell Res **313**(5): 1033-44.

Desmet, V. J. and T. Roskams (2004). "Cirrhosis reversal: a duel between dogma and myth." J Hepatol **40**(5): 860-7.

Diehl, A. M. (2002). "Liver disease in alcohol abusers: clinical perspective." Alcohol **27**(1): 7-11.

Dooley, S., B. Delvoux, et al. (2001). "Transforming growth factor beta signal transduction in hepatic stellate cells via Smad2/3 phosphorylation, a pathway that is abrogated during in vitro progression to myofibroblasts. TGFbeta signal transduction during transdifferentiation of hepatic stellate cells." FEBS Lett **502**(1-2): 4-10.

Dunsford, H. A., R. Maset, et al. (1985). "Connection of ductlike structures induced by a chemical hepatocarcinogen to portal bile ducts in the rat liver detected by injection of bile ducts with a pigmented barium gelatin medium." Am J Pathol **118**(2): 218-24.

Dunsford, H. A. and S. Sell (1989). "Production of monoclonal antibodies to preneoplastic liver cell populations induced by chemical carcinogens in rats and to transplantable Morris hepatomas." Cancer Res **49**(17): 4887-93.

Ebara, S. and K. Nakayama (2002). "Mechanism for the action of bone morphogenetic proteins and regulation of their activity." Spine **27**(16 Suppl 1): S10-5.

Eckes, B., D. Kessler, et al. (1999). "Interactions of fibroblasts with the extracellular matrix: implications for the understanding of fibrosis." Springer Semin Immunopathol **21**(4): 415-29.

Enomoto, K., Y. Nishikawa, et al. (2004). "Cell biology and pathology of liver sinusoidal endothelial cells." Med Electron Microsc **37**(4): 208-15.

Estes, B. T., A. W. Wu, et al. (2006). "Potent induction of chondrocytic differentiation of human adipose-derived adult stem cells by bone morphogenetic protein 6." Arthritis Rheum **54**(4): 1222-32.

Evarts, R. P., Z. Hu, et al. (1996). "Precursor-product relationship between oval cells and hepatocytes: comparison between tritiated thymidine and bromodeoxyuridine as tracers." Carcinogenesis **17**(10): 2143-51.

Fan, J., H. Shen, et al. (2006). "Bone morphogenetic protein 4 mediates bile duct ligation induced liver fibrosis through activation of Smad1 and ERK1/2 in rat hepatic stellate cells." J Cell Physiol **207**(2): 499-505.

Farber, E. (1956). "Similarities in the sequence of early histological changes induced in the liver of the rat by ethionine, 2-acetylamino-fluorene, and 3'-methyl-4-dimethylaminoazobenzene." Cancer Res **16**(2): 142-8.

Farrell, G. C. and C. Z. Larter (2006). "Nonalcoholic fatty liver disease: from steatosis to cirrhosis." Hepatology **43**(2 Suppl 1): S99-S112.

Faure, C., A. Chalazonitis, et al. (2007). "Gangliogenesis in the enteric nervous system: Roles of the polysialylation of the neural cell adhesion molecule and its regulation by bone morphogenetic protein-4." Dev Dyn **236**(1): spc1.

Feng, J. Q., D. Chen, et al. (1995). "The mouse bone morphogenetic protein-4 gene. Analysis of promoter utilization in fetal rat calvarial osteoblasts and regulation by COUP-TFI orphan receptor." J Biol Chem **270**(47): 28364-73.

Fischer, R., A. Cariers, et al. (2002). "Caspase 9-dependent killing of hepatic stellate cells by activated Kupffer cells." Gastroenterology **123**(3): 845-61.

Frank, D. B., A. Abtahi, et al. (2005). "Bone morphogenetic protein 4 promotes pulmonary vascular remodeling in hypoxic pulmonary hypertension." Circ Res **97**(5): 496-504.

Friedman, M. S., M. W. Long, et al. (2006). "Osteogenic differentiation of human mesenchymal stem cells is regulated by bone morphogenetic protein-6." J Cell Biochem **98**(3): 538-54.

Friedman, S. L. (1993). "Seminars in medicine of the Beth Israel Hospital, Boston. The cellular basis of hepatic fibrosis. Mechanisms and treatment strategies." N Engl J Med **328**(25): 1828-35.

Friedman, S. L. (2003). "Liver fibrosis -- from bench to bedside." J Hepatol **38 Suppl 1**: S38-53.

Fuchshofer, R., A. H. Yu, et al. (2007). "Bone morphogenetic protein-7 is an antagonist of transforming growth factor-beta2 in human trabecular meshwork cells." Invest Ophthalmol Vis Sci **48**(2): 715-26.

Gabele, E., D. A. Brenner, et al. (2003). "Liver fibrosis: signals leading to the amplification of the fibrogenic hepatic stellate cell." Front Biosci **8**: d69-77.

Gazzerro, E. and E. Canalis (2006). "Bone morphogenetic proteins and their antagonists." Rev Endocr Metab Disord **7**(1-2): 51-65.

Germain, L., M. Noel, et al. (1988). "Promotion of growth and differentiation of rat ductular oval cells in primary culture." Cancer Res **48**(2): 368-78.

Giacomini, D., M. Paez-Pereda, et al. (2006). "Bone morphogenetic protein-4 inhibits corticotroph tumor cells: involvement in the retinoic acid inhibitory action." Endocrinology **147**(1): 247-56.

Golding, M., C. E. Sarraf, et al. (1995). "Oval cell differentiation into hepatocytes in the acetylaminofluorene-treated regenerating rat liver." Hepatology **22**(4 Pt 1): 1243-53.

Goldman, D. C., R. Hackenmiller, et al. (2006). "Mutation of an upstream cleavage site in the BMP4 prodomain leads to tissue-specific loss of activity." Development **133**(10): 1933-42.

Gong, W., A. Pecci, et al. (1998). "Transformation-dependent susceptibility of rat hepatic stellate cells to apoptosis induced by soluble Fas ligand." Hepatology **28**(2): 492-502.

Gong, W., S. Roth, et al. (1998). "Isoforms and splice variant of transforming growth factor beta-binding protein in rat hepatic stellate cells." Gastroenterology **114**(2): 352-63.

Gong, Y., S. Deng, et al. (2002). "A cyclin-dependent kinase inhibitor (p21(WAF1/CIP1)) affects thymidine incorporation in human liver cancer cells." Br J Cancer **86**(4): 625-9.

Gouon-Evans, V., L. Boussemart, et al. (2006). "BMP-4 is required for hepatic specification of mouse embryonic stem cell-derived definitive endoderm." Nat Biotechnol **24**(11): 1402-11.

Graham, F. L., J. Smiley, et al. (1977). "Characteristics of a human cell line transformed by DNA from human adenovirus type 5." J Gen Virol **36**(1): 59-74.

Gratacos, E., N. Gavalda, et al. (2002). "Bone morphogenetic protein-6 is a neurotrophic factor for calbindin-positive striatal neurons." J Neurosci Res **70**(5): 638-44.

Greenwel, P., J. Rubin, et al. (1993). "Liver fat-storing cell clones obtained from a CCl4-cirrhotic rat are heterogeneous with regard to proliferation, expression of extracellular matrix components, interleukin-6, and connexin 43." Lab Invest **69**(2): 210-6.

Gressner, A. M. (1996). "Transdifferentiation of hepatic stellate cells (Ito cells) to myofibroblasts: a key event in hepatic fibrogenesis." Kidney Int Suppl **54**: S39-45.

Gressner, A. M. and R. Weiskirchen (2006). "Modern pathogenetic concepts of liver fibrosis suggest stellate cells and TGF-beta as major players and therapeutic targets." J Cell Mol Med **10**(1): 76-99.

Gressner, A. M., R. Weiskirchen, et al. (2002). "Roles of TGF-beta in hepatic fibrosis." Front Biosci **7**: d793-807.

Grigoriadis, A. E., J. N. Heersche, et al. (1990). "Continuously growing bipotential and monopotential myogenic, adipogenic, and chondrogenic subclones isolated from the multipotential RCJ 3.1 clonal cell line." Dev Biol **142**(2): 313-8.

Gross, A., J. M. McDonnell, et al. (1999). "BCL-2 family members and the mitochondria in apoptosis." Genes Dev **13**(15): 1899-911.

Hagymasi, K., B. Molnar, et al. (2007). "[Stem cell theory of colorectal cancer and its connection with molecularbiological data.]." Orv Hetil **148**(17): 779-85.

Harrison, T., F. Graham, et al. (1977). "Host-range mutants of adenovirus type 5 defective for growth in HeLa cells." Virology **77**(1): 319-29.

Hase, T. and J. Brim (1966). "Observation on the microcirculatory architecture of the rat liver." Anat Rec **156**(2): 157-73.

He, X. L. and K. C. Garcia (2004). "Structure of nerve growth factor complexed with the shared neurotrophin receptor p75." Science **304**(5672): 870-5.

Heckman, J. D., W. Ehler, et al. (1999). "Bone morphogenetic protein but not transforming growth factor-beta enhances bone formation in canine diaphyseal nonunions implanted with a biodegradable composite polymer." J Bone Joint Surg Am **81**(12): 1717-29.

Hellerbrand, C., B. Stefanovic, et al. (1999). "The role of TGFbeta1 in initiating hepatic stellate cell activation in vivo." J Hepatol **30**(1): 77-87.

Heng, B. C., H. Yu, et al. (2005). "Factors influencing stem cell differentiation into the hepatic lineage in vitro." J Gastroenterol Hepatol **20**(7): 975-87.

Hockenbery, D., G. Nunez, et al. (1990). "Bcl-2 is an inner mitochondrial membrane protein that blocks programmed cell death." Nature **348**(6299): 334-6.

Hsieh, P. C., R. D. Kenagy, et al. (2006). "Bone morphogenetic protein 4: potential regulator of shear stress-induced graft neointimal atrophy." J Vasc Surg **43**(1): 150-8.

Hsu, Y. L., J. K. Chang, et al. (2007). "Myricetin induces human osteoblast differentiation through bone morphogenetic protein-2/p38 mitogen-activated protein kinase pathway." Biochem Pharmacol **73**(4): 504-14.

Hu, H. J. and R. W. t. Gereau (2003). "ERK integrates PKA and PKC signaling in superficial dorsal horn neurons. II. Modulation of neuronal excitability." J Neurophysiol **90**(3): 1680-8.

Hu, H. J., K. S. Glauner, et al. (2003). "ERK integrates PKA and PKC signaling in superficial dorsal horn neurons. I. Modulation of A-type K+ currents." J Neurophysiol **90**(3): 1671-9.

Iredale, J. P. (2001). "Hepatic stellate cell behavior during resolution of liver injury." Semin Liver Dis **21**(3): 427-36.

Israsena, N. and J. A. Kessler (2002). "Msx2 and p21(CIP1/WAF1) mediate the proapoptotic effects of bone morphogenetic protein-4 on ventricular zone progenitor cells." J Neurosci Res **69**(6): 803-9.

Ito, T. and S. Shibasaki (1968). "Electron microscopic study on the hepatic sinusoidal wall and the fat-storing cells in the normal human liver." Arch Histol Jpn **29**(2): 137-92.

Itoh, K., H. Kataoka, et al. (2006). "Bone morphogenetic protein 2 induced differentiation toward superficial epithelial cells in the gastric mucosa." J Gastroenterol **41**(11): 1064-75.

Jeffery, T. K., P. D. Upton, et al. (2005). "BMP4 inhibits proliferation and promotes myocyte differentiation of lung fibroblasts via Smad1 and JNK pathways." Am J Physiol Lung Cell Mol Physiol **288**(2): L370-8.

Jiang, F., C. J. Parsons, et al. (2006). "Gene expression profile of quiescent and activated rat hepatic stellate cells implicates Wnt signaling pathway in activation." J Hepatol **45**(3): 401-9.

Jiang, X., S. A. Gittens, et al. (2006). "The use of tissue-engineered bone with human bone morphogenetic protein-4-modified bone-marrow stromal cells in repairing mandibular defects in rabbits." Int J Oral Maxillofac Surg **35**(12): 1133-9.

Ju, W., A. Hoffmann, et al. (2000). "The bone morphogenetic protein 2 signaling mediator Smad1 participates predominantly in osteogenic and not in chondrogenic

differentiation in mesenchymal progenitors C3H10T1/2." J Bone Miner Res **15**(10): 1889-99.

Kaivo-oja, N., L. A. Jeffery, et al. (2006). "Smad signalling in the ovary." Reprod Biol Endocrinol **4**: 21.

Kaplan, D. R. and F. D. Miller (2004). "Neurobiology: a move to sort life from death." Nature **427**(6977): 798-9.

Kavurma, M. M. and L. M. Khachigian (2003). "Signaling and transcriptional control of Fas ligand gene expression." Cell Death Differ **10**(1): 36-44.

Kawai, S., H. Enzan, et al. (2003). "Vinculin: a novel marker for quiescent and activated hepatic stellate cells in human and rat livers." Virchows Arch **443**(1): 78-86.

Kim, J. S., H. Crooks, et al. (2002). "Oncogenic beta-catenin is required for bone morphogenetic protein 4 expression in human cancer cells." Cancer Res **62**(10): 2744-8.

Kim, K. Y., T. Rhim, et al. (2001). "N-acetylcysteine induces cell cycle arrest in hepatic stellate cells through its reducing activity." J Biol Chem **276**(44): 40591-8.

Kinnman, N., O. Goria, et al. (2001). "Hepatic stellate cell proliferation is an early platelet-derived growth factor-mediated cellular event in rat cholestatic liver injury." Lab Invest **81**(12): 1709-16.

Kinoshita, K., Y. Iimuro, et al. (2007). "Adenovirus-mediated expression of BMP-7 suppresses the development of liver fibrosis in rats." Gut **56**(5): 706-14.

Kiyono, M. and M. Shibuya (2003). "Bone morphogenetic protein 4 mediates apoptosis of capillary endothelial cells during rat pupillary membrane regression." Mol Cell Biol **23**(13): 4627-36.

Knittel, T., P. Fellmer, et al. (1997). "Bone morphogenetic protein-6 is expressed in nonparenchymal liver cells and upregulated by transforming growth factor-beta 1." Exp Cell Res **232**(2): 263-9.

Krajewski, S., S. Tanaka, et al. (1993). "Investigation of the subcellular distribution of the bcl-2 oncoprotein: residence in the nuclear envelope, endoplasmic reticulum, and outer mitochondrial membranes." Cancer Res **53**(19): 4701-14.

Kretzschmar, M., J. Doody, et al. (1997). "Opposing BMP and EGF signalling pathways converge on the TGF-beta family mediator Smad1." Nature **389**(6651): 618-22.

Kruglov, E. A., P. R. Correa, et al. (2007). "Molecular basis for calcium signaling in hepatic stellate cells." Am J Physiol Gastrointest Liver Physiol **292**(4): G975-82.

Kugimiya, F., H. Kawaguchi, et al. (2005). "Involvement of endogenous bone morphogenetic protein (BMP) 2 and BMP6 in bone formation." J Biol Chem **280**(42): 35704-12.

Kumagai, T., T. Shimizu, et al. (2006). "Bone morphogenetic protein-2 suppresses invasiveness of TSU-Pr1 cells with the inhibition of MMP-9 secretion." Anticancer Res **26**(1A): 293-8.

Kusu, N., J. Laurikkala, et al. (2003). "Sclerostin is a novel secreted osteoclast-derived bone morphogenetic protein antagonist with unique ligand specificity." J Biol Chem **278**(26): 24113-7.

Lake-Bakaar, G. (2003). "Current and future therapy for chronic hepatitis C virus liver disease." Curr Drug Targets Infect Disord **3**(3): 247-53.

Laurent, J. J., K. M. Webb, et al. (2004). "The use of bone morphogenetic protein-6 gene therapy for percutaneous spinal fusion in rabbits." J Neurosurg Spine **1**(1): 90-4.

Lavanchy, D. (2005). "Worldwide epidemiology of HBV infection, disease burden, and vaccine prevention." J Clin Virol **34 Suppl 1**: S1-3.

Lavon, N., O. Yanuka, et al. (2004). "Differentiation and isolation of hepatic-like cells from human embryonic stem cells." Differentiation **72**(5): 230-8.

Lechuga, C. G., Z. H. Hernandez-Nazara, et al. (2004). "TGF-beta1 modulates matrix metalloproteinase-13 expression in hepatic stellate cells by complex mechanisms involving p38MAPK, PI3-kinase, AKT, and p70S6k." Am J Physiol Gastrointest Liver Physiol **287**(5): G974-87.

Leite, A. R., M. L. Correa-Giannella, et al. (2007). "Fibronectin and laminin induce expression of islet cell markers in hepatic oval cells in culture." Cell Tissue Res **327**(3): 529-37.

Lewis, T. S., P. S. Shapiro, et al. (1998). "Signal transduction through MAP kinase cascades." Adv Cancer Res **74**: 49-139.

Li, X., E. M. Schwarz, et al. (2003). "Retinoic acid stimulates chondrocyte differentiation and enhances bone morphogenetic protein effects through induction of Smad1 and Smad5." Endocrinology **144**(6): 2514-23.

Lin, S. J., T. F. Lerch, et al. (2006). "The structural basis of TGF-beta, bone morphogenetic protein, and activin ligand binding." Reproduction **132**(2): 179-90.

Lindert, S., L. Wickert, et al. (2005). "Transdifferentiation-dependent expression of alpha-SMA in hepatic stellate cells does not involve TGF-beta pathways leading to coinduction of collagen type I and thrombospondin-2." Matrix Biol **24**(3): 198-207.

Lowes, K. N., B. A. Brennan, et al. (1999). "Oval cell numbers in human chronic liver diseases are directly related to disease severity." Am J Pathol **154**(2): 537-41.

Luckey, S. W. and D. R. Petersen (2001). "Activation of Kupffer cells during the course of carbon tetrachloride-induced liver injury and fibrosis in rats." Exp Mol Pathol **71**(3): 226-40.

Ma, L. and H. Y. Wang (2006). "Suppression of cyclic GMP-dependent protein kinase is essential to the Wnt/cGMP/Ca2+ pathway." J Biol Chem **281**(41): 30990-1001.

Macnamara, B., K. A. Palucka, et al. (1999). "Balance between proliferation and apoptosis in leukemic cell lines resistant to cytostatics." Leuk Lymphoma **36**(1-2): 179-89.

Massague, J. (2003). "Integration of Smad and MAPK pathways: a link and a linker revisited." Genes Dev **17**(24): 2993-7.

Massague, J., J. Seoane, et al. (2005). "Smad transcription factors." Genes Dev **19**(23): 2783-810.

Matthews, S. J. (2005). "Biological activity of bone morphogenetic proteins (BMP's)." Injury **36 Suppl 3**: S34-7.

McCaughan, G. W. and J. George (2004). "Fibrosis progression in chronic hepatitis C virus infection." Gut **53**(3): 318-21.

McGee, J. O. and R. S. Patrick (1972). "The role of perisinusoidal cells in experimental hepatic fibrogenesis." J Pathol **106**(1): Pvi.

Merino, R., J. Rodriguez-Leon, et al. (1999). "The BMP antagonist Gremlin regulates outgrowth, chondrogenesis and programmed cell death in the developing limb." Development **126**(23): 5515-22.

Miller, A. F., S. A. Harvey, et al. (2000). "Bone morphogenetic protein-9. An autocrine/paracrine cytokine in the liver." J Biol Chem **275**(24): 17937-45.

Miura, K., H. Nagai, et al. (2003). "Epimorphin is involved in differentiation of rat hepatic stem-like cells through cell-cell contact." Biochem Biophys Res Commun **311**(2): 415-23.

Miyazono, K., K. Kusanagi, et al. (2001). "Divergence and convergence of TGF-beta/BMP signaling." J Cell Physiol **187**(3): 265-76.

Montesano, R. (2007). "Bone morphogenetic protein-4 abrogates lumen formation by mammary epithelial cells and promotes invasive growth." Biochem Biophys Res Commun **353**(3): 817-22.

Murakami, G., T. Watabe, et al. (2003). "Cooperative inhibition of bone morphogenetic protein signaling by Smurf1 and inhibitory Smads." Mol Biol Cell **14**(7): 2809-17.

Nagai, H., K. Terada, et al. (2002). "Differentiation of liver epithelial (stem-like) cells into hepatocytes induced by coculture with hepatic stellate cells." Biochem Biophys Res Commun **293**(5): 1420-5.

Nakajima, Y., T. Yamagishi, et al. (2002). "Significance of bone morphogenetic protein-4 function in the initial myofibrillogenesis of chick cardiogenesis." Dev Biol **245**(2): 291-303.

Nakajima, Y., T. Yamagishi, et al. (2000). "Mechanisms involved in valvuloseptal endocardial cushion formation in early cardiogenesis: roles of transforming growth factor (TGF)-beta and bone morphogenetic protein (BMP)." Anat Rec **258**(2): 119-27.

Nakatani, K., K. Kaneda, et al. (2004). "Pit cells as liver-associated natural killer cells: morphology and function." Med Electron Microsc **37**(1): 29-36.

Nishanian, T. G., J. S. Kim, et al. (2004). "Suppression of tumorigenesis and activation of Wnt signaling by bone morphogenetic protein 4 in human cancer cells." Cancer Biol Ther **3**(7): 667-75.

Oakley, F., N. Trim, et al. (2003). "Hepatocytes express nerve growth factor during liver injury: evidence for paracrine regulation of hepatic stellate cell apoptosis." Am J Pathol **163**(5): 1849-58.

Ohata, M., M. Lin, et al. (1997). "Diminished retinoic acid signaling in hepatic stellate cells in cholestatic liver fibrosis." Am J Physiol **272**(3 Pt 1): G589-96.

Okano, J., G. Shiota, et al. (2003). "Hepatocyte growth factor exerts a proliferative effect on oval cells through the PI3K/AKT signaling pathway." Biochem Biophys Res Commun **309**(2): 298-304.

Okaya, A., J. Kitanaka, et al. (2005). "Oncostatin M inhibits proliferation of rat oval cells, OC15-5, inducing differentiation into hepatocytes." Am J Pathol **166**(3): 709-19.

Otani, H., F. Otsuka, et al. (2007). "Antagonistic effects of bone morphogenetic protein-4 and -7 on renal mesangial cell proliferation induced by aldosterone through MAPK activation." Am J Physiol Renal Physiol.

Paez-Pereda, M., D. Giacomini, et al. (2003). "Involvement of bone morphogenetic protein 4 (BMP-4) in pituitary prolactinoma pathogenesis through a Smad/estrogen receptor crosstalk." Proc Natl Acad Sci U S A **100**(3): 1034-9.

Paku, S., J. Schnur, et al. (2001). "Origin and structural evolution of the early proliferating oval cells in rat liver." Am J Pathol **158**(4): 1313-23.

Pearson, G., F. Robinson, et al. (2001). "Mitogen-activated protein (MAP) kinase pathways: regulation and physiological functions." Endocr Rev **22**(2): 153-83.

Perez de Obanos, M. P., M. J. Lopez Zabalza, et al. (2006). "Leucine stimulates procollagen alpha1(I) translation on hepatic stellate cells through ERK and PI3K/Akt/mTOR activation." J Cell Physiol **209**(2): 580-6.

Petersen, B. E. (2001). "Hepatic "stem" cells: coming full circle." Blood Cells Mol Dis **27**(3): 590-600.

Pettersson, F., M. C. Couture, et al. (2004). "Enhanced retinoid-induced apoptosis of MDA-MB-231 breast cancer cells by PKC inhibitors involves activation of ERK." Oncogene **23**(42): 7053-66.

Pierre, A., C. Pisselet, et al. (2005). "Bone morphogenetic protein 5 expression in the rat ovary: biological effects on granulosa cell proliferation and steroidogenesis." Biol Reprod **73**(6): 1102-8.

Pierre, A., C. Pisselet, et al. (2005). "Testing the antagonistic effect of follistatin on BMP family members in ovine granulosa cells." Reprod Nutr Dev **45**(4): 419-25.

Pinzani, M., A. Gentilini, et al. (1995). "Transforming growth factor-beta 1 regulates platelet-derived growth factor receptor beta subunit in human liver fat-storing cells." Hepatology **21**(1): 232-9.

Pinzani, M. and K. Rombouts (2004). "Liver fibrosis: from the bench to clinical targets." Dig Liver Dis **36**(4): 231-42.

Potten, C. S. and M. Loeffler (1990). "Stem cells: attributes, cycles, spirals, pitfalls and uncertainties. Lessons for and from the crypt." Development **110**(4): 1001-20.

Purohit, V. and D. A. Brenner (2006). "Mechanisms of alcohol-induced hepatic fibrosis: a summary of the Ron Thurman Symposium." Hepatology **43**(4): 872-8.

Raida, M., A. C. Heymann, et al. (2006). "Role of bone morphogenetic protein 2 in the crosstalk between endothelial progenitor cells and mesenchymal stem cells." Int J Mol Med **18**(4): 735-9.

Ramm, G. A., L. Li, et al. (2003). "Effect of protein kinase C activation and inhibition on rat hepatic stellate cell activation." Dig Dis Sci **48**(4): 790-6.

Rao, M. S., M. Yukawa, et al. (1996). "Expression of transcription factors and stem cell factor precedes hepatocyte differentiation in rat pancreas." Gene Expr **6**(1): 15-22.

Reddi, A. H. (2001). "Interplay between bone morphogenetic proteins and cognate binding proteins in bone and cartilage development: noggin, chordin and DAN." Arthritis Res **3**(1): 1-5.

Reeves, H. L. and S. L. Friedman (2002). "Activation of hepatic stellate cells--a key issue in liver fibrosis." Front Biosci **7**: d808-26.

Rengachary, S. S. (2002). "Bone morphogenetic proteins: basic concepts." Neurosurg Focus **13**(6): e2.

Revel, J. P., S. B. Yancey, et al. (1981). "Cellular architecture and intercellular communication in rat liver." Jama **245**(9): 958-9.

Ro, T. B., R. U. Holt, et al. (2004). "Bone morphogenetic protein-5, -6 and -7 inhibit growth and induce apoptosis in human myeloma cells." Oncogene **23**(17): 3024-32.

Rockey, D. C. and J. J. Chung (1996). "Regulation of inducible nitric oxide synthase in hepatic sinusoidal endothelial cells." Am J Physiol **271**(2 Pt 1): G260-7.

Rojkind, M. and P. Greenwel (1993). "Animal models of liver fibrosis." Adv Vet Sci Comp Med **37**: 333-55.

Rossi, J. M., N. R. Dunn, et al. (2001). "Distinct mesodermal signals, including BMPs from the septum transversum mesenchyme, are required in combination for hepatogenesis from the endoderm." Genes Dev **15**(15): 1998-2009.

Safadi, R. and S. L. Friedman (2002). "Hepatic fibrosis--role of hepatic stellate cell activation." MedGenMed **4**(3): 27.

Saile, B., P. DiRocco, et al. (2004). "IGF-I induces DNA synthesis and apoptosis in rat liver hepatic stellate cells (HSC) but DNA synthesis and proliferation in rat liver myofibroblasts (rMF)." Lab Invest **84**(8): 1037-49.

Saile, B., T. Knittel, et al. (1997). "CD95/CD95L-mediated apoptosis of the hepatic stellate cell. A mechanism terminating uncontroiled hepatic stellate cell proliferation during hepatic tissue repair." Am J Pathol **151**(5): 1265-72.

Saile, B., N. Matthes, et al. (2001). "The bcl, NFkappaB and p53/p21WAF1 systems are involved in spontaneous apoptosis and in the anti-apoptotic effect of TGF-beta or TNF-alpha on activated hepatic stellate cells." Eur J Cell Biol **80**(8): 554-61.

Saile, B., N. Matthes, et al. (2002). "Rat liver myofibroblasts and hepatic stellate cells differ in CD95-mediated apoptosis and response to TNF-alpha." Am J Physiol Gastrointest Liver Physiol **283**(2): G435-44.

Sakou, T. (1998). "Bone morphogenetic proteins: from basic studies to clinical approaches." Bone **22**(6): 591-603.

Sato, M., S. Suzuki, et al. (2003). "Hepatic stellate cells: unique characteristics in cell biology and phenotype." Cell Struct Funct **28**(2): 105-12.

Saxena, N. K., M. A. Titus, et al. (2004). "Leptin as a novel profibrogenic cytokine in hepatic stellate cells: mitogenesis and inhibition of apoptosis mediated by

extracellular regulated kinase (Erk) and Akt phosphorylation." Faseb J **18**(13): 1612-4.

Schaefer, B., A. M. Rivas-Estilla, et al. (2003). "Reciprocal modulation of matrix metalloproteinase-13 and type I collagen genes in rat hepatic stellate cells." Am J Pathol **162**(6): 1771-80.

Schnabl, B., C. A. Bradham, et al. (2001). "TAK1/JNK and p38 have opposite effects on rat hepatic stellate cells." Hepatology **34**(5): 953-63.

Schuppan, D., A. Krebs, et al. (2003). "Hepatitis C and liver fibrosis." Cell Death Differ **10 Suppl 1**: S59-67.

Sela-Donenfeld, D. and C. Kalcheim (1999). "Regulation of the onset of neural crest migration by coordinated activity of BMP4 and Noggin in the dorsal neural tube." Development **126**(21): 4749-62.

Sell, S. (2004). "Stem cell origin of cancer and differentiation therapy." Crit Rev Oncol Hematol **51**(1): 1-28.

Senoo, H. (2004). "Structure and function of hepatic stellate cells." Med Electron Microsc **37**(1): 3-15.

Shalaby, F. and D. A. Shafritz (1990). "Exon skipping during splicing of albumin mRNA precursors in Nagase analbuminemic rats." Proc Natl Acad Sci U S A **87**(7): 2652-6.

Shalhoub, V., D. Conlon, et al. (1992). "Glucocorticoids promote development of the osteoblast phenotype by selectively modulating expression of cell growth and differentiation associated genes." J Cell Biochem **50**(4): 425-40.

Shen, H., G. J. Huang, et al. (2003). "Effect of transforming growth factor beta and bone morphogenetic proteins on rat hepatic stellate cell proliferation and trans-differentiation." World J Gastroenterol **9**(4): 784-7.

Shen, H., M. Zhang, et al. (2002). "Different effects of rat interferon alpha, beta and gamma on rat hepatic stellate cell proliferation and activation." BMC Cell Biol **3**: 9.

Shibuya, H., H. Iwata, et al. (1998). "Role of TAK1 and TAB1 in BMP signaling in early Xenopus development." Embo J **17**(4): 1019-28.

Shields, L. B., G. H. Raque, et al. (2006). "Adverse effects associated with high-dose recombinant human bone morphogenetic protein-2 use in anterior cervical spine fusion." Spine **31**(5): 542-7.

Shore, E. M., M. Xu, et al. (1998). "The human bone morphogenetic protein 4 (BMP-4) gene: molecular structure and transcriptional regulation." Calcif Tissue Int **63**(3): 221-9.

Simic, P., J. B. Culej, et al. (2006). "Systemically administered bone morphogenetic protein-6 restores bone in aged ovariectomized rats by increasing bone formation and suppressing bone resorption." J Biol Chem **281**(35): 25509-21.

Sokol, R. J. (2002). "Liver cell injury and fibrosis." J Pediatr Gastroenterol Nutr **35 Suppl 1**: S7-10.

Solt, D. B., A. Medline, et al. (1977). "Rapid emergence of carcinogen-induced hyperplastic lesions in a new model for the sequential analysis of liver carcinogenesis." Am J Pathol **88**(3): 595-618.

Song, J. J., A. J. Celeste, et al. (1995). "Bone morphogenetic protein-9 binds to liver cells and stimulates proliferation." Endocrinology **136**(10): 4293-7.

Spradling, A., D. Drummond-Barbosa, et al. (2001). "Stem cells find their niche." Nature **414**(6859): 98-104.

Suzuki, A., A. Iwama, et al. (2003). "Role for growth factors and extracellular matrix in controlling differentiation of prospectively isolated hepatic stem cells." Development **130**(11): 2513-24.

Suzuki, A., A. Raya, et al. (2006). "Nanog binds to Smad1 and blocks bone morphogenetic protein-induced differentiation of embryonic stem cells." Proc Natl Acad Sci U S A **103**(27): 10294-9.

Sykaras, N. and L. A. Opperman (2003). "Bone morphogenetic proteins (BMPs): how do they function and what can they offer the clinician?" J Oral Sci **45**(2): 57-73.

Taha, M. F., M. R. Valojerdi, et al. (2006). "Effect of bone morphogenetic protein-4 (BMP-4) on adipocyte differentiation from mouse embryonic stem cells." Anat Histol Embryol **35**(4): 271-8.

Taimr, P., H. Higuchi, et al. (2003). "Activated stellate cells express the TRAIL receptor-2/death receptor-5 and undergo TRAIL-mediated apoptosis." Hepatology **37**(1): 87-95.

Takahashi, K. (2000). "[Bone morphogenetic protein (BMP): from basic studies to clinical approaches]." Nippon Yakurigaku Zasshi **116**(4): 232-40.

Takahashi, T. (1970). "Lobular structure of the human liver from the viewpoint of hepatic vascular architecture." Tohoku J Exp Med **101**(2): 119-40.

Takiguchi, M. (1998). "The C/EBP family of transcription factors in the liver and other organs." Int J Exp Pathol **79**(6): 369-91.

Tanaka, H., C. L. Murphy, et al. (2004). "Chondrogenic differentiation of murine embryonic stem cells: effects of culture conditions and dexamethasone." J Cell Biochem **93**(3): 454-62.

Tee, L. B., Y. Kirilak, et al. (1994). "Differentiation of oval cells into duct-like cells in preneoplastic liver of rats placed on a choline-deficient diet supplemented with ethionine." Carcinogenesis **15**(12): 2747-56.

ten Dijke, P., O. Korchynskyi, et al. (2003). "Controlling cell fate by bone morphogenetic protein receptors." Mol Cell Endocrinol **211**(1-2): 105-13.

Theise, N. D. (2006). "Gastrointestinal stem cells. III. Emergent themes of liver stem cell biology: niche, quiescence, self-renewal, and plasticity." Am J Physiol Gastrointest Liver Physiol **290**(2): G189-93.

Theise, N. D., R. Saxena, et al. (1999). "The canals of Hering and hepatic stem cells in humans." Hepatology **30**(6): 1425-33.

Theriault, B. L., T. G. Shepherd, et al. (2007). "BMP4 induces EMT and Rho GTPase activation in human ovarian cancer cells." Carcinogenesis.

Tieche, S., A. De Gottardi, et al. (2001). "Overexpression of endothelin-1 in bile duct ligated rats: correlation with activation of hepatic stellate cells and portal pressure." J Hepatol **34**(1): 38-45.

Trim, N., S. Morgan, et al. (2000). "Hepatic stellate cells express the low affinity nerve growth factor receptor p75 and undergo apoptosis in response to nerve growth factor stimulation." Am J Pathol **156**(4): 1235-43.

Tsukada, S., C. J. Parsons, et al. (2006). "Mechanisms of liver fibrosis." Clin Chim Acta **364**(1-2): 33-60.

Tsukada, S., J. K. Westwick, et al. (2005). "SMAD and p38 MAPK signaling pathways independently regulate alpha1(I) collagen gene expression in unstimulated and transforming growth factor-beta-stimulated hepatic stellate cells." J Biol Chem **280**(11): 10055-64.

Tsukamoto, H., M. Matsuoka, et al. (1990). "Experimental models of hepatic fibrosis: a review." Semin Liver Dis **10**(1): 56-65.

Uemura, M., E. S. Swenson, et al. (2005). "Smad2 and Smad3 play different roles in rat hepatic stellate cell function and alpha-smooth muscle actin organization." Mol Biol Cell **16**(9): 4214-24.

Urist, M. R. (1965). "Bone: formation by autoinduction." Science **150**(698): 893-9.

Urist, M. R. (2002). "Bone: formation by autoinduction. 1965." Clin Orthop Relat Res(395): 4-10.

Urmanov, M. I. (1973). "[Architecture of the portal triad in relation to the general anatomy of the liver in man and in certain animals]." Arkh Anat Gistol Embriol **65**(11): 81-8.

Varela-Rey, M., C. Montiel-Duarte, et al. (2002). "p38 MAPK mediates the regulation of alpha1(I) procollagen mRNA levels by TNF-alpha and TGF-beta in a cell line of rat hepatic stellate cells(1)." FEBS Lett **528**(1-3): 133-8.

Vessey, C. J. and P. M. de la Hall (2001). "Hepatic stem cells: a review." Pathology **33**(2): 130-41.

Vogt, R. R., R. Unda, et al. (2006). "Bone morphogenetic protein-4 enhances vascular endothelial growth factor secretion by human retinal pigment epithelial cells." J Cell Biochem **98**(5): 1196-202.

Wang, X. Z., S. J. Zhang, et al. (2004). "Effects of platelet-derived growth factor and interleukin-10 on Fas/Fas-ligand and Bcl-2/Bax mRNA expression in rat hepatic stellate cells in vitro." World J Gastroenterol **10**(18): 2706-10.

Wang, Y., J. S. Zhang, et al. (2006). "Adrenomedullin regulates expressions of transforming growth factor-beta1 and beta1-induced matrix metalloproteinase-2 in hepatic stellate cells." Int J Exp Pathol **87**(3): 177-84.

Wang, Y. L., D. Z. Wang, et al. (2007). "The role of bone morphogenetic protein-2 in vivo in regeneration of peripheral nerves." Br J Oral Maxillofac Surg **45**(3): 197-202.

Wilkinson, L., G. Kolle, et al. (2003). "CRIM1 regulates the rate of processing and delivery of bone morphogenetic proteins to the cell surface." J Biol Chem **278**(36): 34181-8.

Williams, G. M. and M. J. Iatropoulos (2002). "Alteration of liver cell function and proliferation: differentiation between adaptation and toxicity." Toxicol Pathol **30**(1): 41-53.

Wise, G. E. and S. Yao (2006). "Regional differences of expression of bone morphogenetic protein-2 and RANKL in the rat dental follicle." Eur J Oral Sci **114**(6): 512-6.

Wozney, J. M. (2002). "Overview of bone morphogenetic proteins." Spine **27**(16 Suppl 1): S2-8.

Wu, J. and P. A. Norton (1996). "Animal models of liver fibrosis." Scand J Gastroenterol **31**(12): 1137-43.

Xia, J. L., C. Dai, et al. (2006). "Hepatocyte growth factor attenuates liver fibrosis induced by bile duct ligation." Am J Pathol **168**(5): 1500-12.

Xin, H., Y. Li, et al. (2006). "Bone marrow stromal cells induce BMP2/4 production in oxygen-glucose-deprived astrocytes, which promotes an astrocytic phenotype in adult subventricular progenitor cells." J Neurosci Res **83**(8): 1485-93.

Xu, C. P., W. M. Ji, et al. (2006). "Bone morphogenetic protein-2 is a negative regulator of hepatocyte proliferation downregulated in the regenerating liver." World J Gastroenterol **12**(47): 7621-5.

Xu, R. H., Z. Dong, et al. (1996). "Involvement of Ras/Raf/AP-1 in BMP-4 signaling during Xenopus embryonic development." Proc Natl Acad Sci U S A **93**(2): 834-8.

Yaar, M., C. Wu, et al. (2006). "Bone morphogenetic protein-4, a novel modulator of melanogenesis." J Biol Chem **281**(35): 25307-14.

Yamaguchi, K., S. Nagai, et al. (1999). "XIAP, a cellular member of the inhibitor of apoptosis protein family, links the receptors to TAB1-TAK1 in the BMP signaling pathway." Embo J **18**(1): 179-87.

Yamashita, H., P. Ten Dijke, et al. (1996). "Bone morphogenetic protein receptors." Bone **19**(6): 569-74.

Yanagita, M. (2005). "BMP antagonists: their roles in development and involvement in pathophysiology." Cytokine Growth Factor Rev **16**(3): 309-17.

Yanagita, M., M. Oka, et al. (2004). "USAG-1: a bone morphogenetic protein antagonist abundantly expressed in the kidney." Biochem Biophys Res Commun **316**(2): 490-500.

Yavrom, S., L. Chen, et al. (2005). "Peroxisome proliferator-activated receptor gamma suppresses proximal alpha1(I) collagen promoter via inhibition of p300-facilitated NF-I binding to DNA in hepatic stellate cells." J Biol Chem **280**(49): 40650-9.

Yoshida, Y., S. Tanaka, et al. (2000). "Negative regulation of BMP/Smad signaling by Tob in osteoblasts." Cell **103**(7): 1085-97.

Yoshiji, H., S. Kuriyama, et al. (2003). "Angiotensin-II induces the tissue inhibitor of metalloproteinases-1 through the protein kinase-C signaling pathway in rat liver fibrosis development." Hepatol Res **27**(1): 51-56.

Zeisberg, M. and R. Kalluri (2004). "Experimental strategies to reverse chronic renal disease." Blood Purif **22**(5): 440-5.